5.2. Permafrost, periglacial and paleo-environmental studies on New Siberian Islands

Lutz Schirrmeister, Guido Grosse, Viktor Kunitsky, Hanno Meyer, Alexander Derivyagin and Tatyana Kuznetsova

5.2.1 Introduction

5.2.1.1 General topics

The study of permafrost sequences in coastal sections of the New Siberian Archipelago and of the Yana-Indigirka-Interfluve deliver information on Quaternary environmental changes of this poorly studied Arctic area. The combined studies of frozen sediments and ground ice in selected sections were carried out in close co-operation with the "coastal erosion" team (see chapter 5.3). The main objectives of our investigations were the overview of the geomorphologic, geological, and geocryological situation in various locations of islands and mainland's coasts and the reconnaissance of scientific as well as logistically favourable sites for future detailed surveys.

Special topics of the "permafrost" team were

- The extension of the studying area for the investigations of permafrost paleo-environmental archives, concerning geocryology, ground ice isotopic composition and hydrochemistry, paleontology and geochronology;
- Studies of frozen middle to late Quaternary marine deposits in coastal sections;
- Continuation of field studies of periglacial surface phenomenons (s. chapter 4.2) using field observation and remote sensing data;
- Sedimentological and geochronological studies regarding the origin of Bunge Land.

In contrast to former expeditions we daily changed the study sites by the hydrographical research vessel "Pavel Bashmakov" and therefore the studies were mostly exemplary. Our "permafrost"-team consisted of three Russian and three German scientists and was supported for the first time by a field laboratory and a technician, in order to realize first hydrochemical and geocryological analyses and to preserve all samples for the transport.

Twelve locations were studied between Muostakh Island near Tiksi in the south and Cape Anisy at the north coast of Kotel'ny Island; between Derevyannye Gory (Novaya Sibir Island) and Oyogos Yar (Laptev Strait south coast) in the East and Bel'kovsky Island and Stolbovoy Island in the West (Fig. 5.2.1-1).

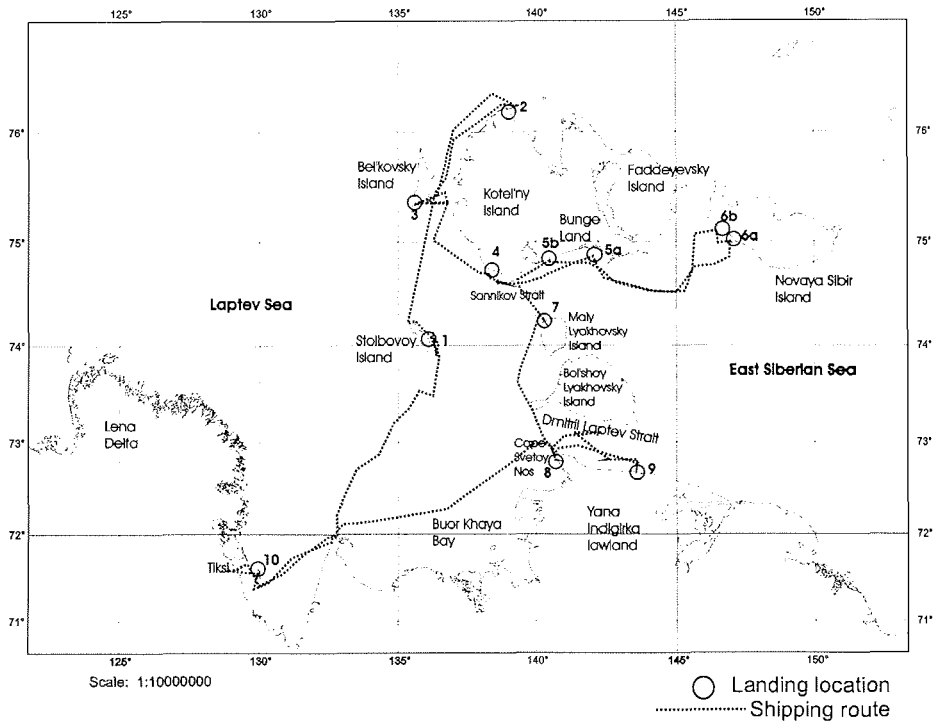

Figure 5.2.1-1: Schematic map of the study area in the eastern Laptev Sea and western East Siberian Sea with ship route and the study locations: 1 - Stolbovoy Island; 2 - Bel'kovsky Island; 3 - Kotel'ny Island (Cape Anisy); 4 - Kotel'ny Island (Khomurgannakh River mouth); 5a - Bunge Land (High terrace); 5b - Bunge Land (Low terrace); 6a - Novaya Sibir Island (Derevyannye Gory); 6b - Novaya Sibir Island (Location Hedenstrom); 7 - Maly Lyakhovsky Island; 8 - Cape Svyatoy Nos; 9 - Oyogos Yar; 10 - Muostakh Island.

5.2.1.2 General geological background

The area of the eastern Laptev Sea and the western part of East Siberian Sea belongs to the Verkhoyansk-Kolymsk Fault Region and consists of a syncline-anticline system formed on the western margin of the North American Plate. The position at the inactive plate margin has determined the accumulation of thick Palaeozoic and Mesozoic carbonate and clastic complexes, which were folded and thrusted during the Early Cretaceous (Drachev et al. 1998). Two main structures of the study area were formed during this period. The first is the northern part of the New Siberian-Chukchi Fold Belt, exposed on Kotel'ny and Bel'kovsky Islands. It consists of a 6 to 10 km thick sequence of Ordovician to Lower Cretaceous deposits (Kos'ko et al. 1990). In general, the anticlines there contain Paleozoic weakly metamorphic marine and terrigene limestones, sandstones and slates with tuffite, gypsum and anhydrite interlayers (Krasny 1981, Spektor 1981). In synclines, Mesozoic and Cenozoic deposits cover such sequences. The second is the South Anyuy-Lyakhov Ophiolitic Suture, exposed

on Cape Svyatoy Nos and Bol'shoy Lyakhovsky Island, which separates this fold belt from the Verkhoyansky fold belt (Parfenov 2000). Typical rocks are Late Paleozoic ophiolites, Late Jurassic to Early Cretaceous islands arc volcanic rocks and Cretaceous granodiorites and granites (Drachev 1998). Deformation stages occurred during Neocomian and Late Aptian.

The geological and tectonical situation of the Cenozoic is characterized by rifting processes at the plate margin. Therefore, the Laptev Sea Rift system consists of several rifts and uplifts (Ust-Lena-rift, East Laptev horst, Stolbovoy horst, Anisy rift, Kotel'ny uplift, Bel'kovsky-Svyatonosski rift, New Siberian or Faddeevsky rift and Tastakhsky rift). This is the reason for the existence of some graben and horst structures in the eastern Laptev Sea (Fig. 5.2.1-2).

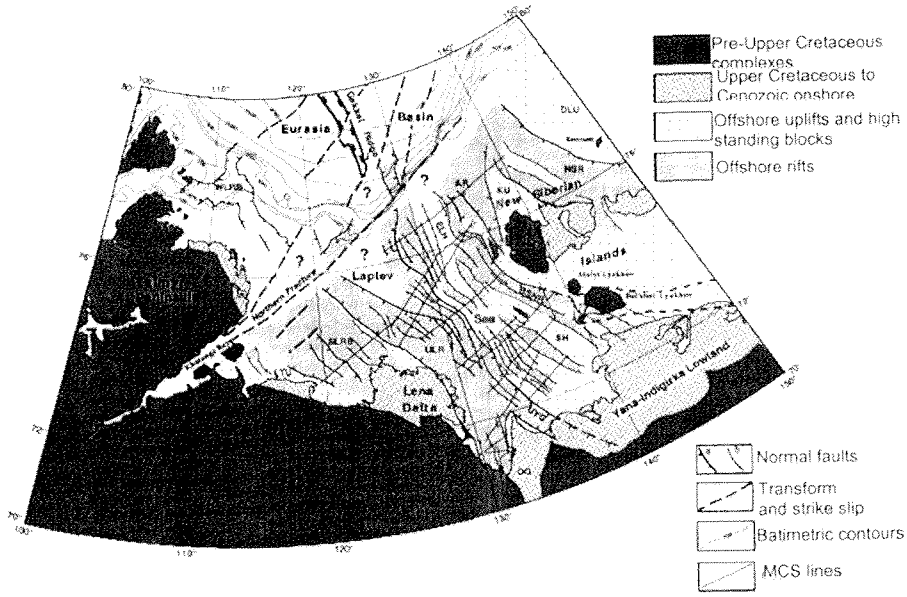

Figure 5.2.1-2: The main structural elements of the Laptev Shelf (Drachev et al. 1998): WLRB - West Laptev rift basin; LTU - Lena-Taimyr uplift; SLRB - South Laptev basin; ULR - Ust' Lena rift; UYG - Ust' Yana graben; OG - Omoloy graben; ELH - East Lena horst; AR - Anisy rift; BSNR - Bel'kov-Svyatoy Nos rift; SH - Stolbovoy horst; KU - Kotel'ny uplift; NSR - New Siberian rift; DLU - De Long uplift.

While seismic studies from Drachev et al. (1998) and Franke et al. (2000) show generally NNW-SSE oriented tectonic and geologic structures (Fig. 5.2.1-2), the map of Spektor (1981) shows a NE-SW orientation of tectonical elements. These are the Svyatoy Nos segment, the Lyakhovsky segment, the Kotel'ny segment and the Henrietta segment (Fig. 5.2.1-3). Fracture zones parallel to the general orientation of the coasts and marine straits are the boundaries of each segment. According to Spektor (1981), a fracture zone forms the northern rim of the Svyatoy Nos segment parallel to the mainland's coast along the Dmitrii Laptev Strait.

Folded terrigene Jurassic sediment (sandstones, aleurolite and tuffs) are discordantly covered by volcanites (andesite, basalts) and intruded by granodiorites. According to K-Ar-dating the basalts are formed before 148 to 159 Ma and the granodiorite before 95 to 115 Ma (Prokhorova & Ivanov, 1973, Parfenov, 2001).

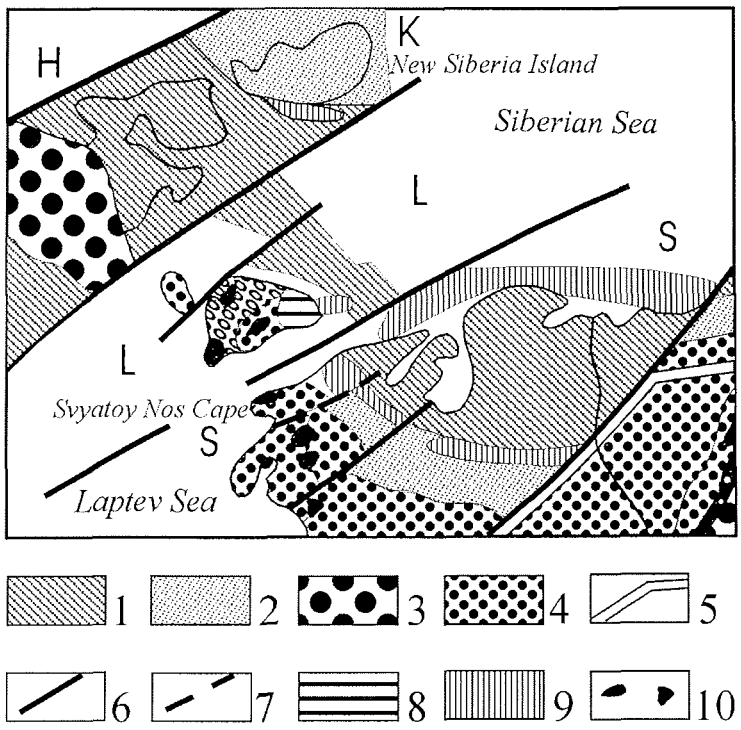

Figure 5.2.1-3: Part of schematic map of the tectonic order of the western New Sibirian-Chukchi-Fold System (according to Spektor et al. 1981): 1 - Inner zone; 2 - Transition step; 3 - Mesozoic outer depressions; 4 - Palaeozoic central depressions; 5 - Faults bounding the New Sibirian-Chukchi-Fold System; 6 - Faults between segments; 7 - Faults within segments; 8 - Gabbro, resp. ultramafic rocks, exposed at the surface; 9 - Gabbro, resp. ultramafic rock, suspected according to geophysical data; 10- Granitoids; S - Svyatoy Nos segment; L - Lyakhovsky segment; K - Kotel'ny segment; H - Henrietta segment

The northern boundary of the Lyakhovsky segment is a fault zone parallel to the Sannikov Strait between both the Lyakhovsky Islands and Kotel'ny Island. Within this segment there occur fragments of the central uplift zone of the New Siberian-Chukchi fold system with Proterozoic crystalline slates and amphibolites as well as fragments of the outer zone with granite massifs. Higher in the profile the complex of terrigene Permian deposits contain diabase and ultramafic rocks. The outer zone of the fold system here is characterized by weakly disturbed Cretaceous deposits and stronger disturbed Jurasic deposits

both folded and in places intruded by granitoids, which had been formed before 92 to 114 Ma. According to Spector (1981) the northern boundary of the Kotel'ny segment is a fault zone parallel to 76° latitude and the north coast of Kotel'ny Island. Palaeozoic carbonate sediments of the central uplift zone are folded and outcropped together with concordantly disturbed Triassic argillites on Kotel'ny Island. In the Kotel'ny segment the inner zone (Bunge Land, Faddeyevsky Island) and the transition step of the fold system are filled with Cenozoic terrigene and effusive-terrigene layers and the Cenozoic sediments of the transition step (Novaya Sibir Island) are folded as well.

The Cenozoic unit is subdivided in the Neogene and Quaternary deposits at the Svyatoy Nos segment, in Paleogene, Neogene to Quaternary and Quaternary deposits at the Lyakhovsky segment and in Paleogene, Paleogene to Neogene, Neogene, Pliocene to Quaternary and Quaternary deposits. Quaternary deposits are dated to a lesser amount and have mostly local stratigraphical orders. Therefore, a generalized Quaternary stratigraphy of the New Siberian Islands and the adjoining Yana-Indigirka Lowland is not available yet. The current knowledge of the Quaternary will be represented describing each study location.

5.2.1.3 Methodical approach

The main topics mentioned in chapter 5.2.1.1 were realized in close co-operation with the other study disciplines. Numerous sediment sub-profiles were studied at coastal cliffs and thermokarst mounds in close connection with ground ice investigations. Cryostructures and sediment structures were observed as well as sediment colour, grain size and the content of fossil plant material was described. Permafrost deposits were mostly sampled in frozen stage using small axes and hammers. Samples of 0.5 to 1 kg were taken and then packed into plastic bags. Separate samples were taken for gravimetric ice content determination in aluminum boxes. The field laboratory and the support by the lab technician on the research vessel "Pavel Bashmakov" was very helpful for sample preparation and the first measurements. We want to express especially thanks to our colleague Antje Eulenburg for her excellent work in the lab almost around the clock.

For ice content determination, the sediment samples were first weighed in frozen state and then again after drying. The gravimetric ice content was calculated as the ratio of mass of the ice in a sample to the mass of dry sample, what the common method in geocryology studies (v. Everdingen 1998). The weight determination by electronic balance was only possible on land because of strong ship movements. Besides of frozen/thawed sediment samples, some pebbles and boulders were sampled in order to determine the rocks and to examine their origin. In addition, single samples of wood remains were taken for radiocarbon age determination. A special sampling was carried out for sandy sediments on Bunge-Land, which will be dated by Infrared Optical Stimulated Luminescence (IR-OSL). These samples were taken with a hand-drilling

machine (HILTI) and a special drilling head with opaque plastic cylinders. The samples, which had to be protected from sunlight, were stored and transported in the cylinders and additional black plastic bags. Finally, each sediment sample was well-wrapped in the laboratory for the transport to Germany.

Ice wedges were studied in close connection with sediment profiles. The study conception for ice wedges (stable isotopes and hydrochemistry) is briefly described in chapter 3.11 and presented in more detail in former field reports (Rachold et al. 1999; 2000). A special emphasis was put on the sampling of recent ice veins and precipitation on New Siberian Islands. The precipitation was continuously sampled by a rain-water sampling device (type Hellmann) onboard the ship. Additionally, samples were taken from snow patches, to study in detail the connection between recent ice wedges and precipitation. During the sampling of ice-rich sediment, the segregated ice is melting. This supernatant water was extracted with a plastic syringe for the determination of the stable isotope composition and hydrochemistry of segregated ice. In addition, samples were taken from surface waters (lakes, rivers brooks, polygonal ponds), seawater and sea ice in order to get an overview of the hydrological situation of the whole region.

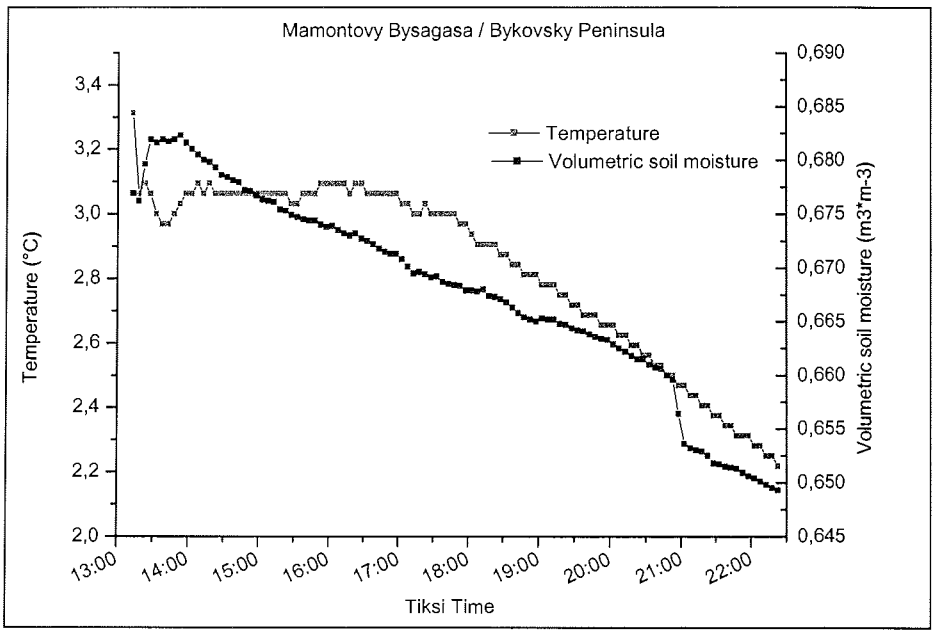

Figure 5.2.1-4: Exemplary surface data of soil temperature and soil moisture, measured with a transportable soil probe on Bykovsky Peninsula and on New Siberian Islands (alas depression Mamontovy Bysagasa, 04.09.2003)

In order to characterize the surface conditions for the interpretation of remote sensing date a transportable soil probe (TSP) was placed at each landing site for the whole time of the stay. The soil probe measured the soil temperature and soil tension voltage, which can be transfer into volumetric soil moisture

(Figure 5.3.1-4). The measurement was done for the entire stay at a typical tundra site near the landing location. Every site was chosen by its characteristic surface properties: relief, surface sediment, vegetation, and homogeneity. Altogether 10 sites were described, all of them different in their characteristics. Depending on the stay, soil temperature and soil moisture were permanently (5 min interval) measured for 2-8 hours. In Appendix 5.2-4 the sites are listed with their coordinates and their average, minimum and maximum value for temperature and volumetric soil moisture for the measurement interval.

The sizes of typical relief forms, like thermokarst mounds and ice wedge polygons were studied by measuring tape. By comparing the morphometry of recent polygonal nets from different relief positions with remains of former polygonal nets (thermokarst mounds) we want to draw conclusions on the characteristics for the Ice Complex paleo-landscape. Further, thermokarst mounds mark sites, where ice-rich deposits had existed earlier. The size and shape, hence the stage of development, of thermokarstic and erosional structures (especially valleys) were also measured. A comparison of lateral distribution over the New Siberian Islands and the adjacent coasts may detect latitudinal or longitudinal gradients in thermokarst or thermo-erosion effects. Therefore they can give hints on the effectiveness of environmental changes in the area.

5.2.2 Stolbovoy Island (15.08.)

Stolbovoy Island is the highest part of the Stolbovoy tectonical Horst (Drachev et al. 1998) and the westernmost part of Verkhoyansk-Kolymsk Fold Region within the study area. Its basement consists of Jurassic and Cretaceous sedimentary rocks, often exposed at the island's coast as well as in higher hill positions. Two ridges of about 140-220 m a.s.l. in the southern part and of 100-140 m in the northern part form the "spine" of this island. The lower relief down to the beach is dominated by a step-like morphology of cryoplanation terraces on various levels (140 m, 120 m, 60-80 m, 50 m, 25-30 m, Figure 5.2.2-1). The lowest terrace is covered by Ice Complex deposits, which were studied there on August 15.

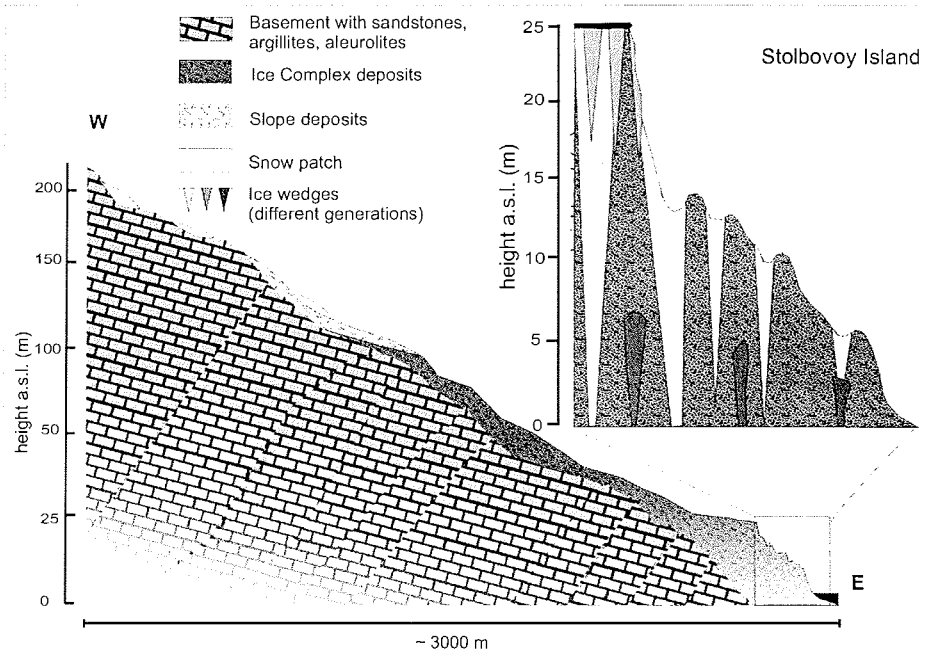

Figure 5.2.2-1: Scheme of the frequently observed geomorphological situation at the Stolbovoy Island coast with steps of cryoplanation terraces

Our study site was situated at the east coast of Stolbovoy Island 3.5 km north of the Stolbovaya River mouth (Figure 5.2.2.-2). Ice Complex deposits cover the surface of the lowest (30 m) terrace and thermo-erosional valleys occur. Four sub-profiles were sampled in various levels of the coast (Figure 5.2.2.-3 and -4).

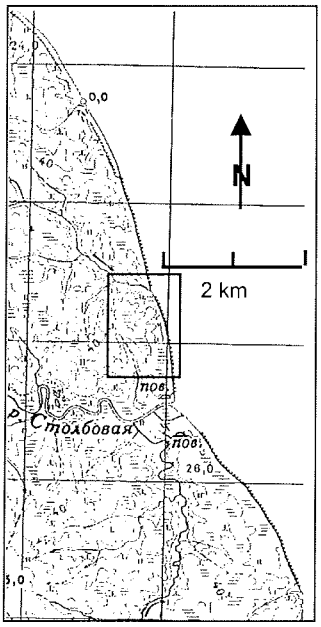

Figure 5.2.2-2: Study site at the east coast of Stolbovoy Island in August 15

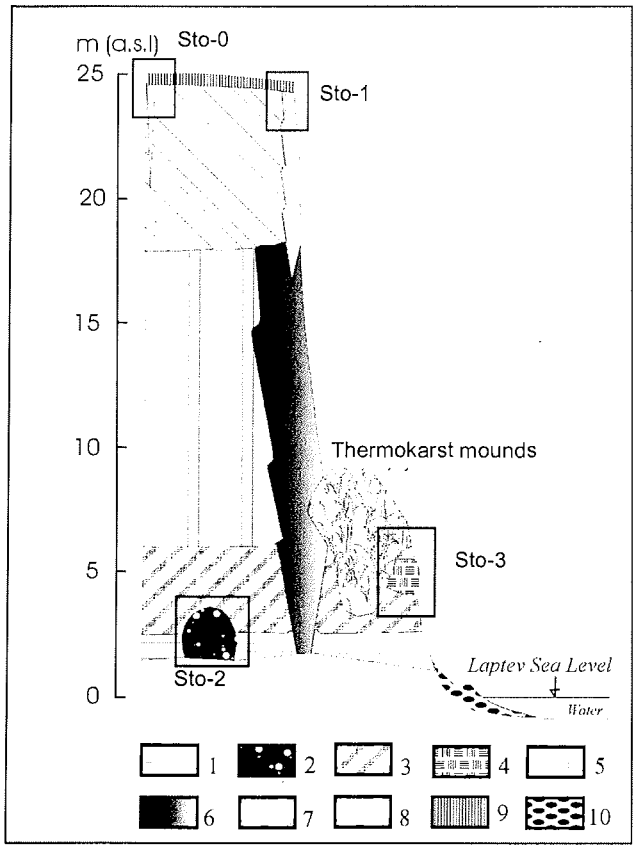

Figure 5.2.2-3:
General scheme of the studied Ice Complex section
1 - Silty sand brownish, layered, frozen, including shrub twigs and grass roots, massive;
2 - Buried, Ice wedge (Polosatic);
3 - Silty sand dark-grey, layered, with peat nests and grass roots, ice belts, massive;
4 - Moss-peat, brownish, with lenses of clear injection ice
5 - Silty sand, dark grey, layered, grass roots, ice belts
6 - Ice wedge, light-grey, 4 to 5 m wide, compact;
7 - Silty sand, grey, layered, frequent small peat lenses, grass roots, ice belts;
8 - Ice wedge, white, small (1.5 m), less compact;
9 - Active layer;
10 - Beach pebbles.

At the study site the coast is very steep and Ice Complex deposits about 25 m thick with large and small ice wedges are exposed there. In the lower part a special phenomenon was visible - a buried ice wedge with rounded head, which had deformed the covering layers above (Figure 5.2.2-4A STO 2). The sediment consists of grey silty sand (aleurit), containing some vertical grass roots *in situ.* A massive cryostructure and a gravimetric ice content of 51-60 wt-% was observed.

The ice wedge (Stb-IW-2) with round (thawing) head was striped in the baydzherakh at the height about 3 m a.s.l.. The width of ice wedge is about 1-1,2 m, and the visible thickness is about 2 m. The ice wedge ice is very dirty and has numerous mineral particles and looks like "polosatic" ice wedge, founded and described at Bol'shoy Lyakhovsky Island 1999. The thickness of vertical oriented mineral stripes is about 0.7-1 cm, the thickness of vertical oriented ice stripes is about 0,5-0,7 cm. The cryogenic construction of the ice wedge as well as of the enclosed sediments (with ice belts, ice shoulders and peat nests and pockets) may be an evidence for syngenetic evolution of this ice wedge. The general construction of the section suggests that the head of the ice wedge was thaw-treated and then buried under the sediments. 5 samples of ice wedge ice (25 cm distance) were collected.

A big peat lens of about 1-2 m thickness and 150 m length was exposed in several thermokarst mounds at the height of 5-7 m a.s.l. (Figure 5.2.2-4B STO3). This moss peat was imbedded by greyish-brown silty fine sand with grass roots, small peat nests containing ice belts and a fine lens-like cryostructure (gravimetric ice content about 56 wt-%). Large lenses of transparent injection ice were observed and sampled within this peat lens. The gravimetric ice content of the peat changes between 70 to 270 wt-%. Ice wedges of this level are 4-5 m wide, grey and compact, showing vertical striation and edgewise shoulders.

An additional ice wedge (Figure 5.2.2-4D, Sto-IW-5) was sampled at the height about of 15 m a.s.l. in the instable middle part of the outcrop. The thawed "head" of ice wedge had a width of about 3 m and the visible was about 1.5 m. The ice was turbid, and dirty and contains numerous vertical oriented mineral particles ("Polosatic") and air bubbles. Ice shoulders at the contact between ice wedge and sediment are typical feature of syngenetic ice wedges. In total 9 samples of ice wedge ice were collected in a distance of 30-35 cm.

Sediment and an ice wedge of the upper part of the outcrop were studied below the terrace surface at about 22 m a.s.l. (Figure 5.2.2-4E, STO 1). The ice wedge there consisted of yellowish-grey to milky-white transparent ice containing a lot of small gas bubbles (< 1mm) and sediment streaks. Gas bubbles were randomly distributed and not orientated. A dark-light striation was visible but single ice veins are badly recognisable. Such ice veins are 2-6 mm wide. In total, 16 samples were taken from this 1.6 m wide ice wedge (STO-IW-1). The ice wedge belongs to a series of narrow and 5-6 m high ice wedges at the top of the Ice Complex. These ice wedges are connected with the underlying wider "normal" Ice Complex ice wedges. Therefore, the question has

be solved, whether the small ice wedges still belong to the Ice Complex or whether they were formed after the deposition of the Ice Complex and what may have limited the growth of the narrow ice wedges. Grey silty fine sand with small grass roots and low ice content (gravimetric ice content 38-59 wt-%) and a massive cryostructure composed the Ice Complex deposits beneath this ice wedge near the top. The polygons at the surface point to the inactive character of ice wedge growth. They are 8-10 m in diameter and characterised by an apex, being 0.5 m lower than the elevated polygon centre. The vegetation cover is sparse and the active layer depth about 40-50 cm.

About 250 m further to the NW, a younger generation of ice wedges, possibly of Holocene age, was sampled (Figure 5.2.2-4F, STO 4). The ice wedge STO-IW-4 is composed of white and milky ice with a lot of small gas bubbles. 2-4 mm wide elementary ice veins were easily recognised. From this 0.8 m wide ice wedge, five samples were taken. Additionally, a 4 cm wide complex of three single recent ice veins, which were found at the bottom of the (still frozen) active layer, was sampled for isotope and tritium analyses. The cryogenic structure was irregular-reticulate with a low content of ice in the silty-sandy "loess-like" sediment. The polygons are again 8-10 m in diameter, with little vegetation and characterised by an apex 0.5 m lower than the centre.

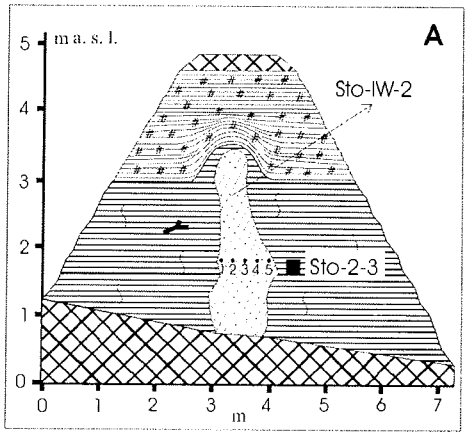

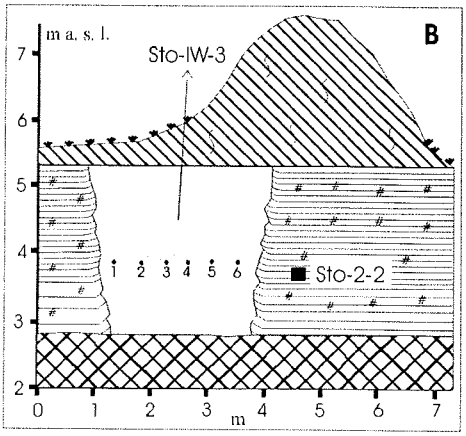

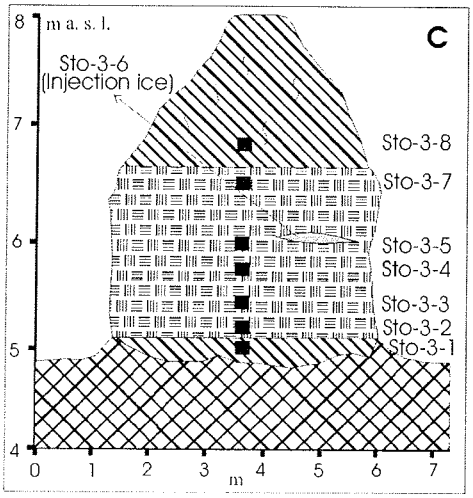

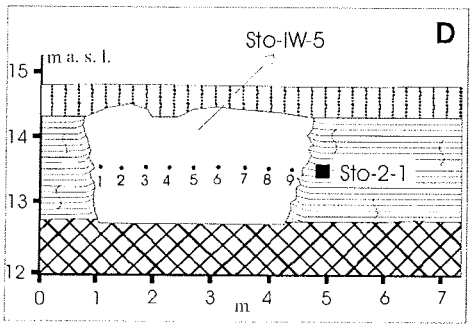

Legend:

- dark-grey silt;
- peat;
- grey silt;
- blue-grey silt with peat lenses and pockets;
- slump;
- ice wedge with numerous silt inclusions (polosatic);
- ice wedge
- lens of injection ice;
- grass roots;
- wood remains;
- bones;
- tundra plant cover;
- sample points and number of ice samples;
- sample points and number of samples of sediments;

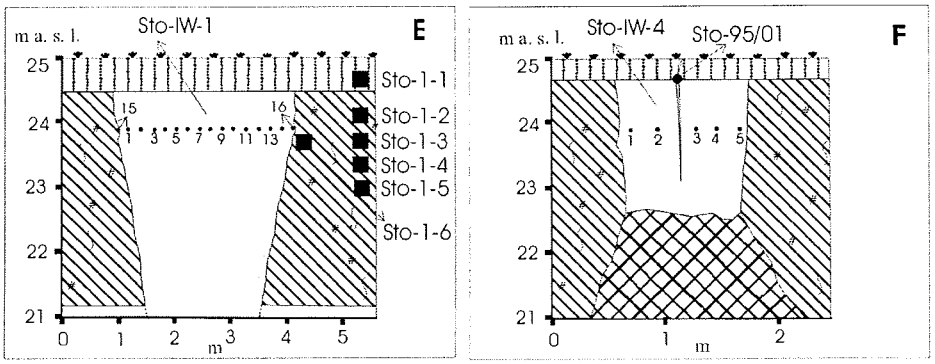

Figure 5.2.2-4: Schematic sketches of the studied sub-profiles of Stolbovoy Island.
A: Sub-profile Sto-2 – Buried ice wedge IW-2 ("Polozatic") near the beach;
B: Sampled larger ice wedge IW-3 at the beach, extending below sea level;
C: Sub-profile Sto-2 – A thermokarst mound exposes a large peat lens within Ice Complex deposits;
D: Samples of ice wedge IW-5 in the middle part of the coastal section;
E: Sub-profile Sto-1 – Ice wedge and Ice Complex deposits below the top of the coastal cliff;
F: Sub-profile Sto-0 – A recent ice wedge penetrates through an older one below the top of the coastal cliff.

Wide thermokarst valleys with flat floors are formed within a thermokarst depression north of the studied section. Very impressive polygonal nets, forming flat thermokarst mounds occurred at the slopes of these valleys (Figure 5.2.2-5). A Holocene peat cover, grown within such valley, was sampled at a small pit of a flat thermokarst mound at about 10 m a.s.l. (samples Sto 4-1 to 4-4). The distance of thermokarst mound centres were measured from one top to the other top in two locations in order to reconstruct size and shape of former polygonal nets. The distances at the top of the Ice Complex elevation (Yedoma) varied between 8 m and 20.5 m. Therefore, a more irregular shape of the ice wedge polygons is suspected. In a slope position near the beach, the distances between thermokarst mounds were smaller between 5 m and 12.5 m. A scarce vegetation of grass and moss covered the dry and sandy surface of the Ice Complex elevation as well as the slopes of thermokarst valleys. Only on the more wet valley floors a denser grass vegetation was growing.

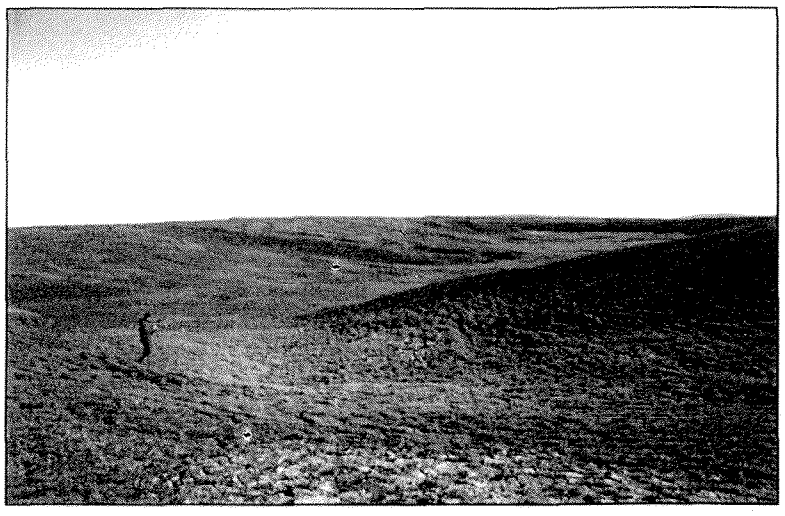

Figure 5.2.2-5: Themokarst valley with thermokarst mounds at the slope of Ice Complex elevations (Yedoma), east coast of Stolbovoy Island

At the east coast of the Stolbovoy Island at 2–4 km north from the Stolbovaya River mouth we found only 13 bones but the main part of these bones was collected at the exposure. Probably two of them (NS-Stl-O1, NS-Stl-O2) belong to an individual of musk-ox and other three bones (NS-Stl-O3, NS-Stl-O4, NS-Stl-O5) belong to an individual of horse. On the shore M. Grigor'ev found a good fragment of skull of Bison priscus with horn.

5.2.3 Kotel'ny Island – Cape Anisy (16.08.)

The northernmost station of our expedition was the coast of Kotel'ny Island near Cape Anisy (Figure 5.2.3-1). The Palaeozoic basement with Ordovician limestone (Lopatin 1998) is exposed at the beach. The relief near the NE coast of Kote'ny Island is formed by cryoplanation terraces, which extend from the hills (about 100 m a.s.l.) to the sea. Numerous snowfields were observed from a remote location at the steep edges of such cryoplanation terraces. The lowest terrace is a 5 km wide plain between 7-13 m a.s.l. covered by Ice Complex deposits.

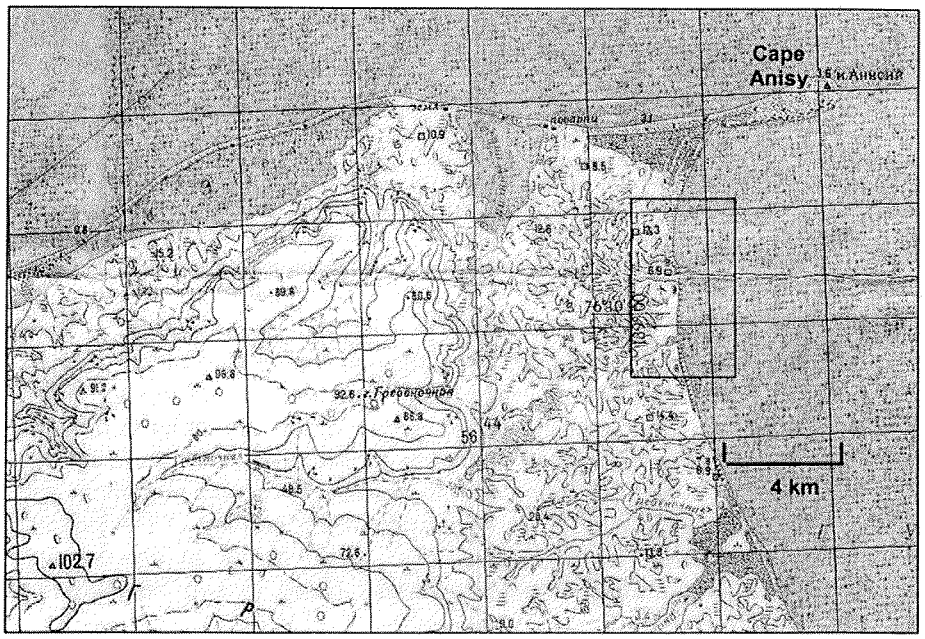

Figure 5.2.3-1: Study area near Cape Anisy with typical relief of cryoplanation terraces

Thermokarst mounds at the surface indicate the occurrence of this ice-rich permafrost deposit. The thermokarst mounds are about 1.5 m high and up to 6 m in diameter. The distances between thermokarst mounds amount to 8.5-18 m and on average are 13 m (Figure 5.2.3-2). Shallow thermokarst valleys (3–5 m deep) with wide (20-30 m) and plain floors cut the surface of the lowest terrace. Shallow brooks flow through the valley floors, where dense grass vegetation grows. The Ice Complex surface is scarcely covered by moss, grass and lichens. Numerous frost boils occur there containing fragments of basement rocks. The maximum thickness of the Ice Complex deposits seems to be 5-10 meters, as concluded from the visible basement outcrop on the beach, the shallow thermokarst valleys and the occurrence of basement rock fragments in frost boils and at valley floors.

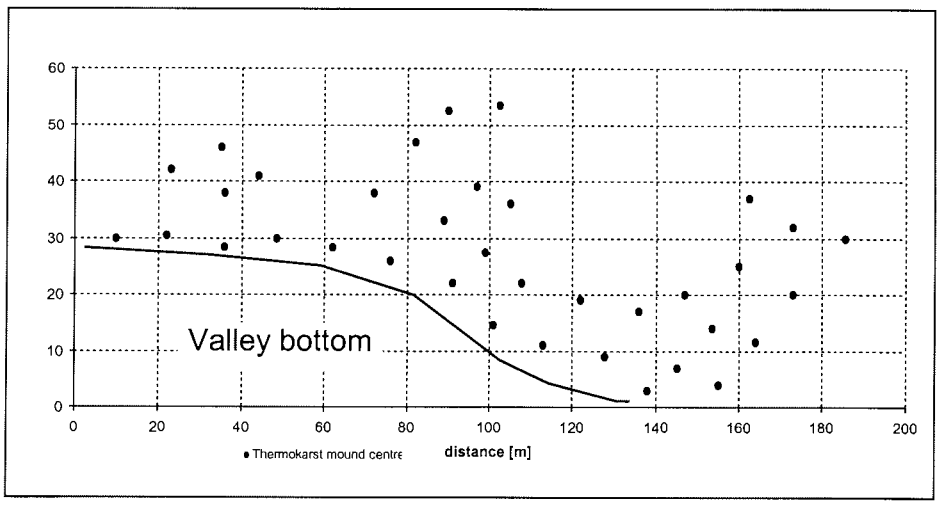

Figure 5.2.3-2: Example of mapping thermokarst mounds on Cape Anisy, N-Kotel'ny. The distances are measured by tape from the centres of thermokarst mounds to neighbouring mounds using a triangulation method. These mounds were situated along the slope of a thermokarst valley within ice-rich permafrost deposits.

Paleontological collection from Cape Anisy does not contain so much samples (49 bones and their fragments) but the most bones were found *in situ*. These bones (31) were collected from the frozen sediments of thermokarst mounds (baydzherakhs) at about 10 m a.s.l., because in this area does not exist any outcrops. We suppose that we found partial skeletons of woolly mammoth and horse. Not only *in situ* bones but also bones from the surface of thermokarst mounds probably belong to these skeletons. Large bones of anterior and posterior legs of *Mammuthus primigenius* were found in two neighbouring thermokarst mounds.

6 bones (NS-KAn-O13 a-f) were found *in situ*, two of them in natural conjunction. Probably two additional bones were moved by frost heaving to the surface of these thermokarst mounds and they belong also to this woolly mammoth' skeleton (Appendix 5.2-3). Vertebras (thorax and cervical), ribs and their fragments mainly belong to a partial horse skeleton(NS-KAn-O30 a-z). All these bones were found *in situ* in one thermokarst mound, which was named "Horse Baydzherakh" (Figure 5.2.3-3). The preservation of bones is very good. We also found two cartilage parts of a rib. Because of the plain area the transport of bones on the tundra surface is insignificant. Some bones, which were found on tundra surface probably belong to an other skeleton - for example, horse's bones (samples NS-Kan-O16 to O20) (Appendix 5.2-3).

As no large profile of Ice Complex deposits was exposed in this area, a pit was dug on the side of a thermokarst mound for geocryological studies (Figure 5.2.3-3). In the same thermokarst mound many horse bones were found. The small profile of 1.5 m thickness consists of greyish-brown cryoturbated silty to

sandy soil with fine lens-like cryostructure and contains a lot of twig fragments. The sediment was relatively poor in ice. An ice wedge (MYA-IW-1) was excavated beneath the frost mound. Three samples were taken from this ice wedge. The ice was grey and milky with numerous small gas bubbles, and it consists of 2-4 mm thick elementary ice veins.

Two additional samples were taken from a peat horizon, which covered a thermokarst mound about 1 km west of the location mentioned above (Mya-peat-1, -2).

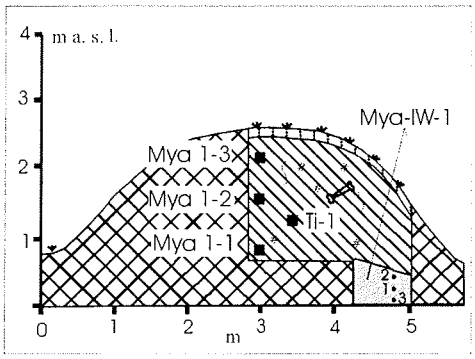

Figure 5.2.3-3: Thermokarst mound ("Horse Baydzherakh") with the sediment profile Mya-1 and the sampled ice wedge MYA-IW-1.

5.2.4 Bel'kovsky Island, Cape Skalisty (Cape Rocks) (17.08.)

A similar relief situation like that on Stolbovoy and Cape Anisy was noted at the south coast of Bel'kovsky Island, which is the westernmost island of New Siberian Archipelago (Figure 5.2.4-2). At least three steps of cryoplanation terraces were observed at about 80 m, 60-40 m and 25 m a.s.l.. According to the geological map, the basement consists of Devonian sedimentary rocks, with faults in NW-SE orientation (Lopatin 1998). The coast consists of alternations of rocky cliffs, Ice Complex fragments and thermokarst as well as thermo-erosion forms. The surface relief of the study area is shaped like a depression, which is bordered by cliffs of the exposed basement in the E and the W. The occurrence of thermokarst mounds directly above the exposed basement rocks indicates, that ice-rich permafrost deposits cover the basement (Figure 5.2.4-1).

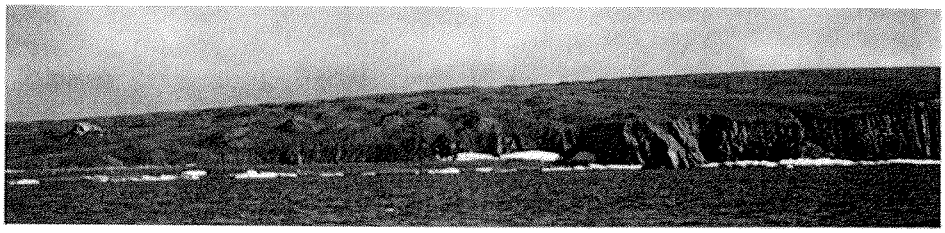

Figure 5.2.4-1: South coast of Bel'kovsky Island, Ice Complex deposits with thermokarst mounds cover basement rocks at the eastern slope of a depression, Cape Skalisty.

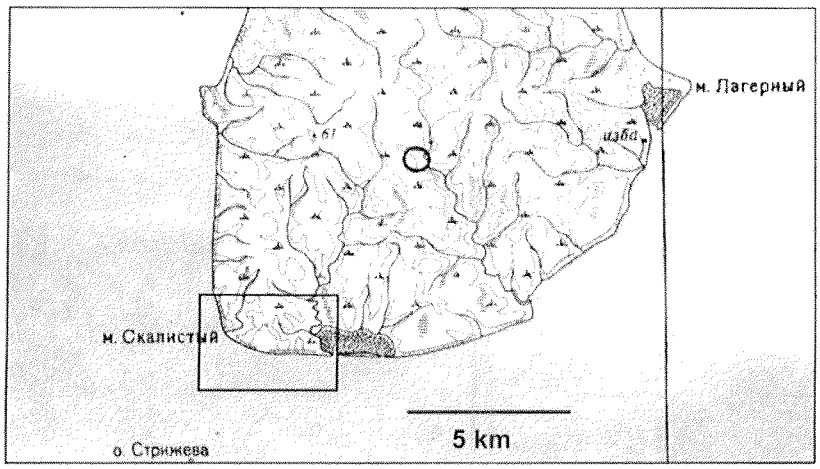

Figure 5.2.4-2 Study area near Cape Skalisty, south coast of Bel'kovsky Island

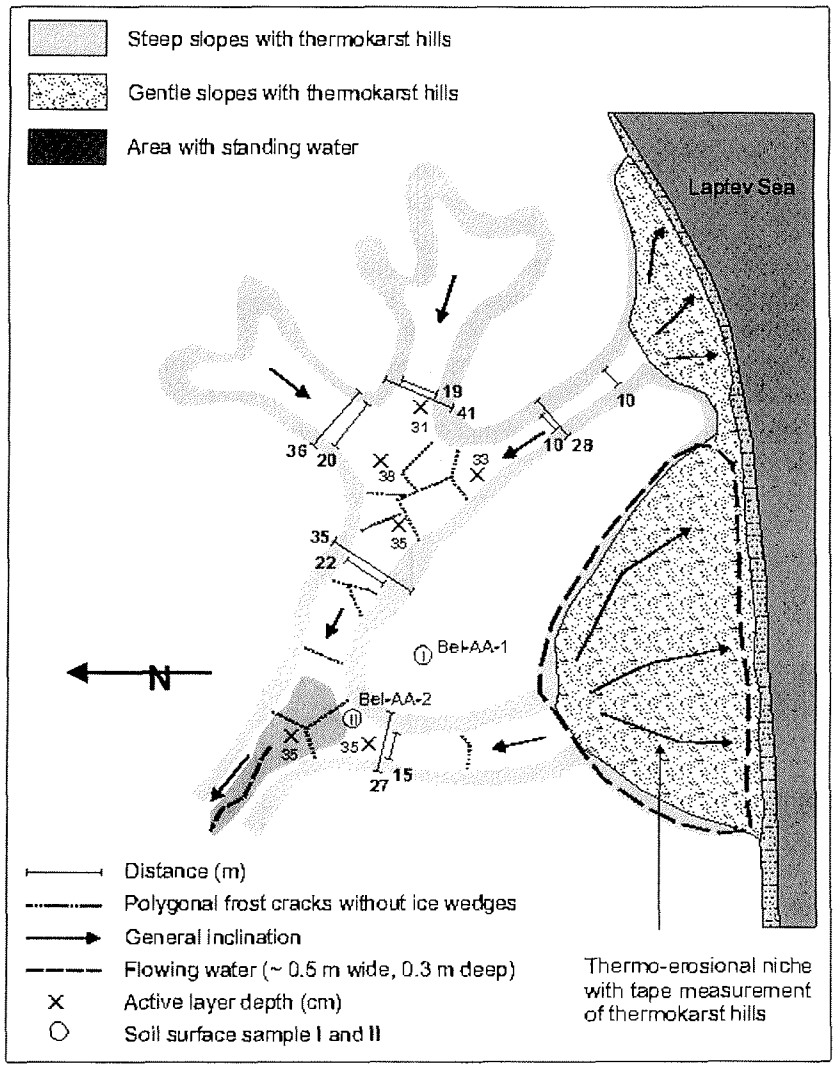

Figure 5.2.4-3: Studied thermokarst valley system at the south coast of Bel'kovsky Island.

Today this depression looks like a thermokarst depression (alas), but it may also be a result of tectonical activities. Several thermokarst valleys cross the alas floor. The valleys are 30 to 40 m wide at the top and 15 to 22 m at the bottom (Figure 5.2.4-3). The valleys are wet and boggy and densely covered by grass. Recent ice wedges could not be sampled, because of the wetness of the active layer. Nevertheless, in these depressions a lot of recent frost cracks were observed forming ideal hexagonal polygons with angles of 120° between the cracks. The active layer there is 31 to 38 cm thick. The general inclination and orientation of one studied valley system is to the northwest, towards the depression centre in the hinterland, instead of towards the sea. Hence, the

valleys were formed during thermokarst formation and their drainage is not influenced by coastal erosion. At the slope of a thermo-erosional niche near the beach (Figure 5.2.4-3) distances between thermokarst mounds were measured by measurement tape. The distances are between 3.5 and 18.5 m with an average value of 11.5 m.

In general, two different types of formations were studied. First, the exposed Ice Complex deposits with 3 to 4 m broad ice wedges. Ice wedges were exposed in a lower beach cliff (0-10 m a.s.l.) and in an upper cliff (15-25 m a.s.l.). Thermokarst mounds covered the central part of the section. The base of the Ice Complex is possibly situated below sea level because of large ice wedges near the sea level (Figure 5.2.4-4). This horizon consists of greyish silty sand containing thin grass roots and shows a banded cryostructure. Further, profiles of alas deposits with fine-laminated lacustrine sediments were studied (Figure 5.2.4-5). They contain shells, small ice wedges in the upper part and ice wedge casts at the base.

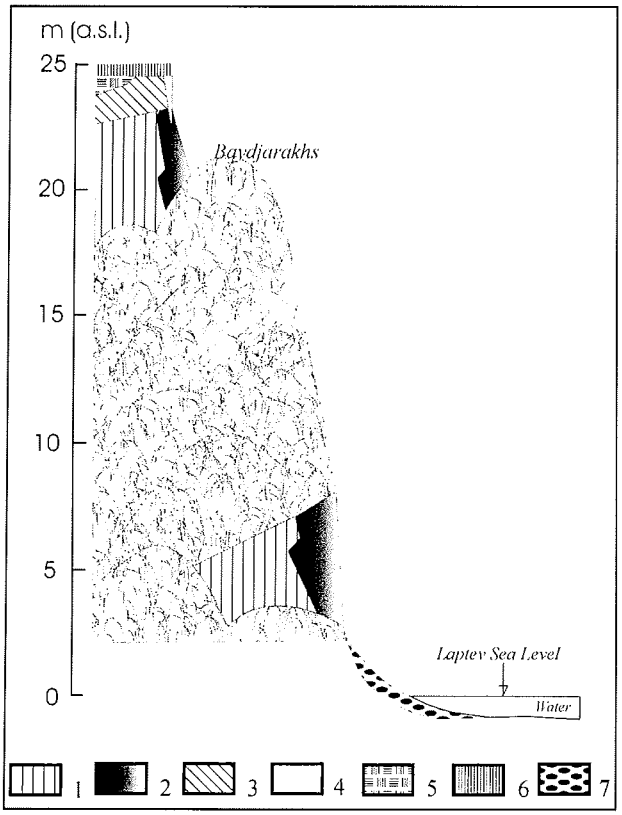

Figure 5.2.4-4:
Schematic profile of a Ice Complex fragment of the 25 m cryoplanation terrace, south coast of Bel'kovsky Island

1 – Silty sand (aleurite), light-grey, layered, with grass roots and ice belts;
2 - Ice wedge, grey, 3-4 m wide, dense, rarely with small sediment veins;
3 – Silty sand with small peat nests and shrub roots and twigs, lens-like cryostructure;
4 – Ice wedge, white, less dense,
1 m wide;
5 – Moss peat, brown, with lenses of silty sand and with shrub roots, ice-rich, supersaturated
6 – Active layer;
7 – Strand pebbles

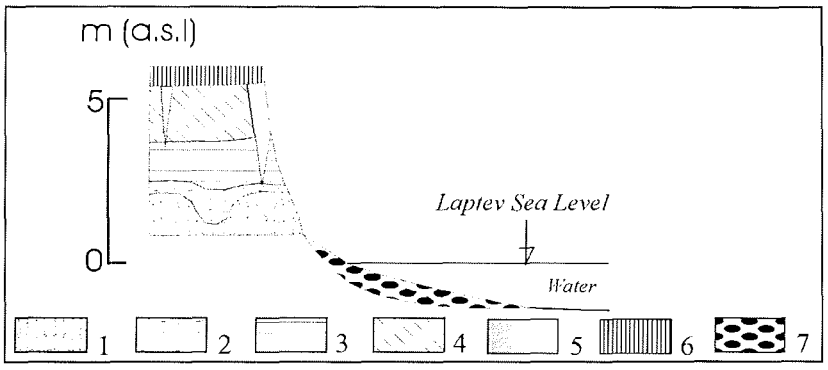

Figure 5.2.4-5: Schematic profile of an alas sequence.
1 – Silty sand, bluish-grey, deformed, loamy, skew lattice-like or lens-like cryostructure; 2 – Silty sand grey to bluish-grey, alternating with laminas of plant detritus, within ice wedge casts, lens-like cryostructure; 3 – Silty sand, grey, fine- laminated, skew or horizontal lens-like bedded cryostructure; 4 – Silty sand, dark-grey, with peat nests and grass roots, lens-like reticulated cryostructure; 5 – Ice wedge, white, small (1.2 m wide), less dense; 6 – Active layer; 7 – Strand pebbles.

All together a coastal section of about 1 km extension was studied in seven sub-profiles representing different stages of the landscape history (Figure 5.2.4-6A to J).

The easternmost section was the sub-profile Bel-3, where the Ice Complex horizon was exposed at about 3.5 to 5 m a.s.l. (Figure 5.2.4-6B). An ice wedge (BEL-IW-1) exposed about 2.5 m in width and 1.5 m in height was sampled here. In total, 21 samples were taken in 10 cm intervals with an ice screw from the right to the left. The height of the horizontal sampling transect was estimated to be at 4 m a.s.l. The ice wedge consists of grey, transparent, most likely Pleistocene ice and was estimated to be part of the Ice Complex. Many gas bubbles, which were small (<1 mm) and spherical, and not elongated were noticed in the ice. Additionally, numerous subvertical structures were observed such as 2-4 mm wide elementary ice veins and few elongated sediment veins of several decimetres in length. Hence, the ice wedge was relatively rich in sediment. The subvertical structures were cut by cracks without filling extending from the upper left to the lower right side of the ice wedge. These cracks did not seem to be related to regular frost cracking activity rather to other mechanical tensions in the permafrost. The ice wedge seemed to be subject to sublimation, which leads to a weathered appearance of the crust of the ice wedge. Therefore, this outer crust was discarded from sampling. In addition, three samples of Ice Complex deposits were exemplarily taken there. It was the typical grey silty sand with grass roots and fine lens-like reticulated cryostructure (gravimetric ice content 41 wt %)

In a distance of about 105 m to the West a 0.2 m wide and 0.7 m high ice wedge was exposed in the small sub-profile Bel-4 at about 2.5 m a.s.l. (Figure 5.2.4-6F). This ice wedge is composed of very clear, transparent ice with a lot of gas bubbles interrupted by yellowish sediment veins. This clear vertically-

striped alternation of ice and sediment veins (tiger-striped ice), so-called "Polosatic ice" (Kunitsky 1998), points to relatively dry winter conditions and high sediment supply. This may lead to the competition of the frost crack filling either by snow melt-water or by sediment. The single ice veins are 2-8 mm wide and very easily recognisable. Narrower veins are observed in the middle part and wider veins near the edge of the ice wedge. The sediment streaks are 1-3 mm wide. The sediment beneath the ice wedge is the same material as described above.

The sub-profile Bel-2 was situated 180 m west of the first profile. This was a thermokarst mound with Ice Complex deposits covered by a 0.5 to 0.8 m thick peaty soil (Figure 5.2.4-6A), which was observed in flanking mounds, too. In the lower part the silty sand is brownish coloured cryoturbated and has a lens-like cryostructure. No ice bands occurred. This cryosol is overlain by grey silty sand with fine lens-like reticulated cryostructure with ice bands. The gravimetric ice content of this frozen material is between 70 and 90-wt %. This part does not contain any large plant remains. Finally a peaty cryosol with large peat nests and shrub roots closed this profile.

About 560 m West of the first point Bel-3 the upper part of alas deposits were exposed in the sub-profile Bel-5 (Figure 5.2.4-6C). In a 20 m wide and 1.6 m high outcrop, the top being 5 m height a.s.l., Six sediment samples were taken in different positions of the outcrop. One sample was recovered from the brownish peaty soil of a 25 cm thick active layer. Second one origins from a transition horizon, which was characterised by brownish-grey, peat- and ice-rich silty sand with some clay and regular-reticulate cryostructure. The other samples were retrieved from deposits with brownish-grey ice-rich silty sand and a coarse irregular-reticulate cryostructure. Four different Holocene ice wedge generations were sampled in alas deposits. The ice wedge BEL-IW-3 is 2.3 m wide and consists of white, milky and very clean ice with big ice crystals and contains a few organic remains (mainly moss fragments). The right part of the ice wèdge belongs to a second small ice wedge connected with the main ice wedge. A number of 12 samples were retrieved from this double ice wedge by means of an ice screw in a horizontal sampling transect at ca. 4.1 m a.s.l. Elementary ice veins are relatively difficult to differentiate, in general between 2-5 mm wide and rich in small bubbles of about 1 mm in diameter.

A recent ice wedge (BEL-IW-6) penetrating into a Holocene ice wedge (BEL-IW-4) was sampled together with the Holocene ice wedge in alas deposits near the ice wedge BEL-IW-3 (Figure 5.2.4-6C). The ice of the Holocene ice wedge was clean, milky-white and characterized by large ice crystals (up to 0.5-1.0 cm in diameter). A frost crack and a recent ice wedge were located above the Holocene ice wedge. The thickness of the active layer is about 35 cm. The width of the upper part of recent ice wedge (ice vein) amounts not more than 0.5-0.8 cm (sample BEL-IW-6-1). This Ice was transparent and yellowish. The width of ice vein is increased with the depth up to 4-5 cm (sample BEL-IW-6-2) because of the penetration into older ice veins. The width increased up to 15 cm when the recent ice wedge penetrated into the Holocene ice wedge (sample

BEL-IW-6-3). Transparent and clean ice of the recent ice wedge are visible in the milky-white Holocene ice down to the depth of 30-40 cm (sample BEL-IW-6-4). Four samples of the Holocene ice wedge were also collected.

Ice wedge casts containing lacustrine deposits and allochtonous peat lenses were observed at the sub-profiles Bel-7 and Bel-8 directly above the beach level. The sub-profile Bel-7 is situated 80 m west of Bel-5. A 2 m long and 2.5 m broad ice wedge cast is exposed there (Figure 5.2.4-6D). The layer below the ice wedge cast consists of bluish-grey clay. The cast structure is filled by fine-laminated silt-organic-sand alternations, which are bent parallel to the cast structure. This indicates a post-sedimentary thawing within a thermokarst depression forming ice wedge casts. The cast structure is overlain by greyish-brown silty sand with fine-laminated cryostructure. More disturbed was the ice wedge cast of the sub-profile Bel-8 (Figure 5.2.4-6E), which is situated at about 100 m west Bel-7. Fine-laminated black-white silt-organic alternations occur as well as peaty sands with shrub twigs, allochtonous moss peat with shrub remains, and yellowish fine sand. The ice wedge cast is covered by homogenous grey sediment with mussel-shells.

Finally, large ice wedges of about two meters width were observed in a distance of about 850 m from first sub-profile Bel-3. The ice wedges were overlain by a lacustrine horizon of silt-organic alternation. Further up a smaller milky ice wedge was found, that appeared like a Holocene ice wedge. Numerous sand fans, formed during thawing and flowing out of permafrost deposits, cover the beach there. Various shapes of such sediment fans were measured. A single fan was about 5 m long and 4 m wide. The sand cover was only 3-4 cm thick near the outflow and 40-42 cm thick in front of the sand fan. Numerous fans of various shapes overlay each other. The fan material is eroded periodically by normal wave erosion, hence it is a factor of coastal erosion without strong wind and waves.

Paleontological material from the south coast of Bel'kovsky Island was meagre - only 18 bones were found. The most interesting bones are six bison bones, which were collected on the exposure. According to conservation and position these bones probably belong to one individual.

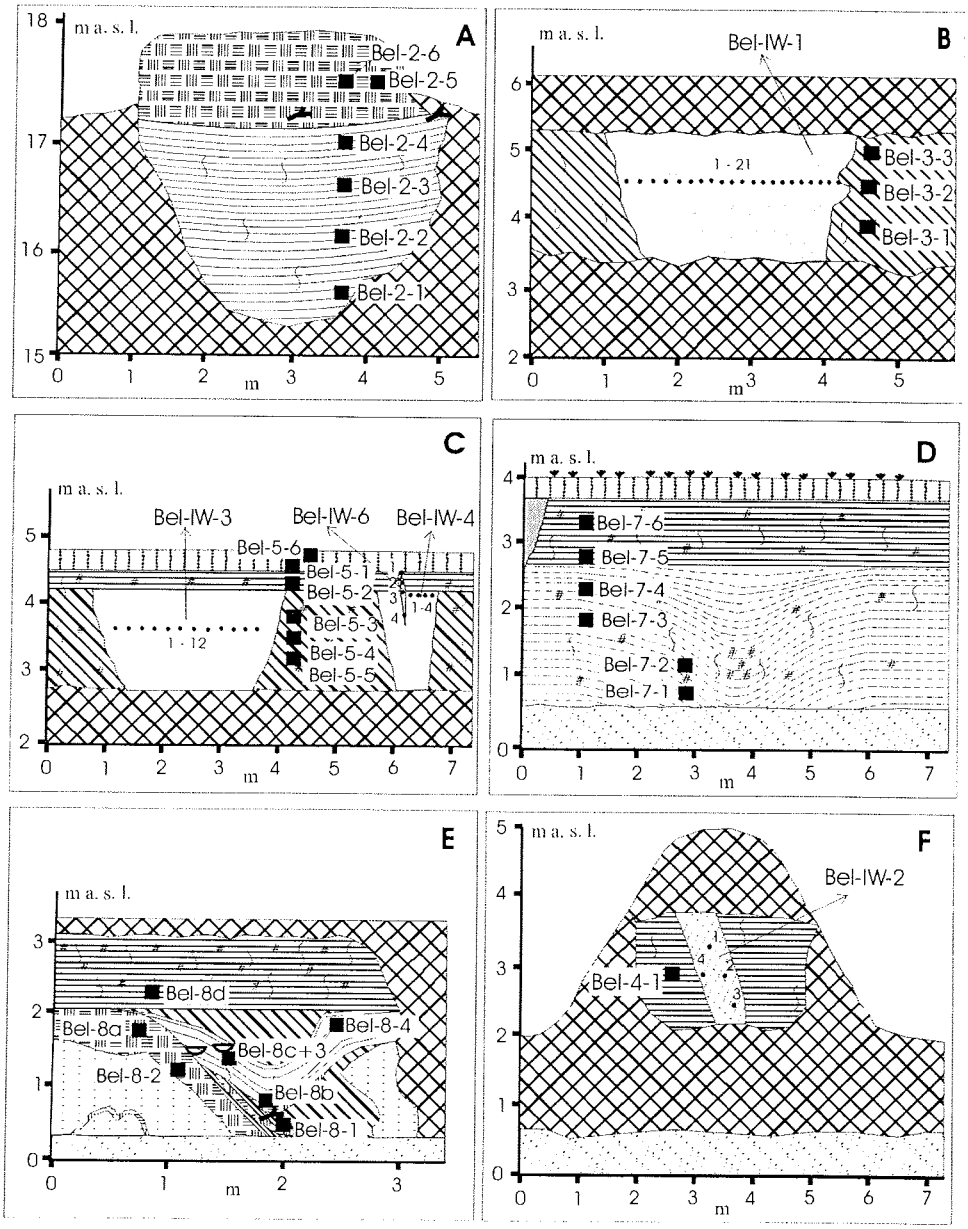
A
m a. s. l.
Bel-2-6
Bel-2-5
Bel-2-4
Bel-2-3
Bel-2-2
Bel-2-1
B
m a. s. l.
Bel-IW-1
1 - 21
Bel-3-3
Bel-3-2
Bel-3-1
C
m a. s. l.
Bel-IW-3
Bel-IW-6
Bel-IW-4
Bel-5-6
Bel-5-1
Bel-5-2
Bel-5-3
Bel-5-4
Bel-5-5
1 - 12
1 - 4
D
m a. s. l.
Bel-7-6
Bel-7-5
Bel-7-4
Bel-7-3
Bel-7-2
Bel-7-1
E
m a. s. l.
Bel-8d
Bel-8a
Bel-8-4
Bel-8c+3
Bel-8-2
Bel-8b
Bel-8-1
F
m a. s. l.
Bel-IW-2
Bel-4-1
m

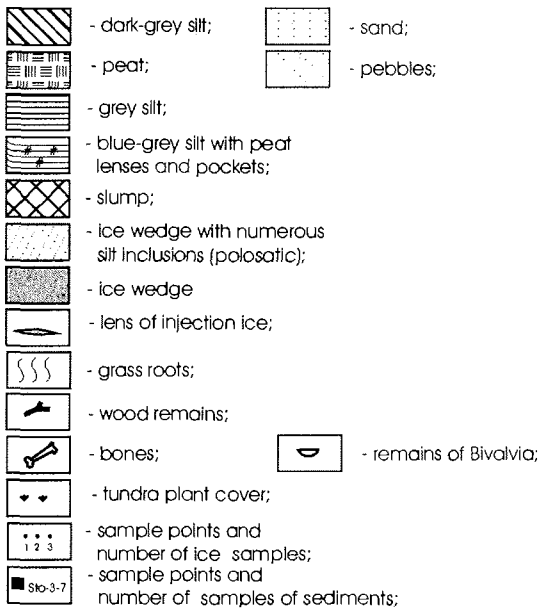

Figure 5.2.4-6: Schematic sketch of the studied sub-profiles of Bel'kovsky Island A – Sub-profile Bel-2, B – Sub-profile Bel 3 with the ice wedge Bel-IW-1, C – Sub-profile Bel 5 with the ice wedges Bel-IW-2, IW-4 and IW-6; D – Sub-profile Bel 7; E Sub-profile Bel 8; F – Sub-profile Bel 4 with the ice wedge Bel-IW-2

5.2.5 Kotel'ny Island, south coast – Khomurgannakh River mouth (18.08)

The general relief at the south coast of Kotel'ny Island again is dominated by cryoplanation terraces reaching from the Sogurum Tas hill (172 m a.s.l.) down to the sea (Figure 5.2.5-1). On the step edges of terraces some snowfields were observed. The lowest terrace at about 20 m a.s.l. is covered by Ice Complex deposits. Thermo-erosional valleys with steep slopes, plain bottoms and shallow brooks, cut the surface there. In these valleys ice wedge polygons of 30 to 40 m diameter were formed. They are 3 to 3.5 times larger than those of the Ice Complex indicated by distances of thermokarst mounds.

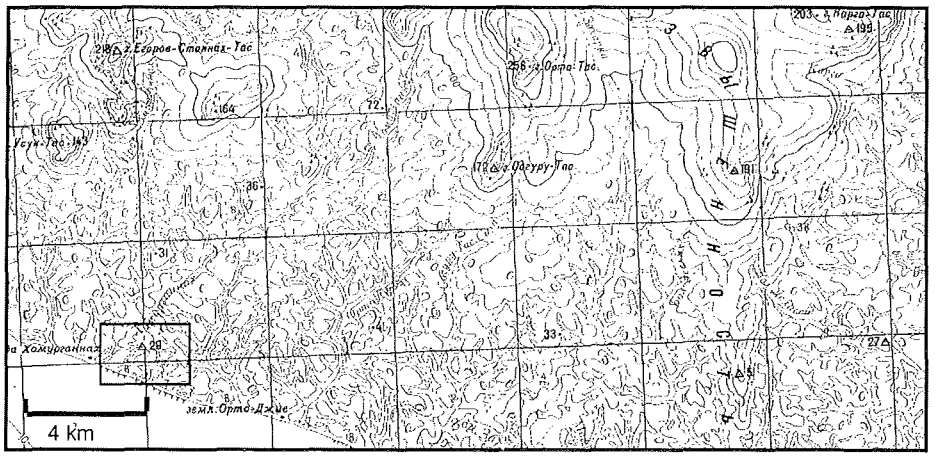

Figure 5.2.5-1: Map of the studied coastal section near the Khomurgannakh River mouth

The TSP was placed on the bottom of a wide and flat depression of the coastal cliff. The surface was covered by scarce vegetation of grass and lichens. Hummocks, frost boils and small polygons formed the patterned ground on the depression floor. Here, the active layer is 45 to 50 cm thick. In addition, several erosion forms were observed during the walk along the coast, e.g. steep ravines with brooks and U-shaped, 25 to 30 m broad thermo-erosional valleys. Brook deposits contain debris and pebbles up to 30 cm in diameter.

At the coast only one section with two sub-profiles in a distance of 1.5 km from the Khomurgannakh River mouth was studied in detail. The general situation is shown in Figure 5.2.5-2. Of the two observed units the lower unit consists of coarse-grained yellowish weathered material (cryogenic eluvium) and contains an about 1.5 m wide ice wedge, which was totally embedded in the coarse-grained deposit.

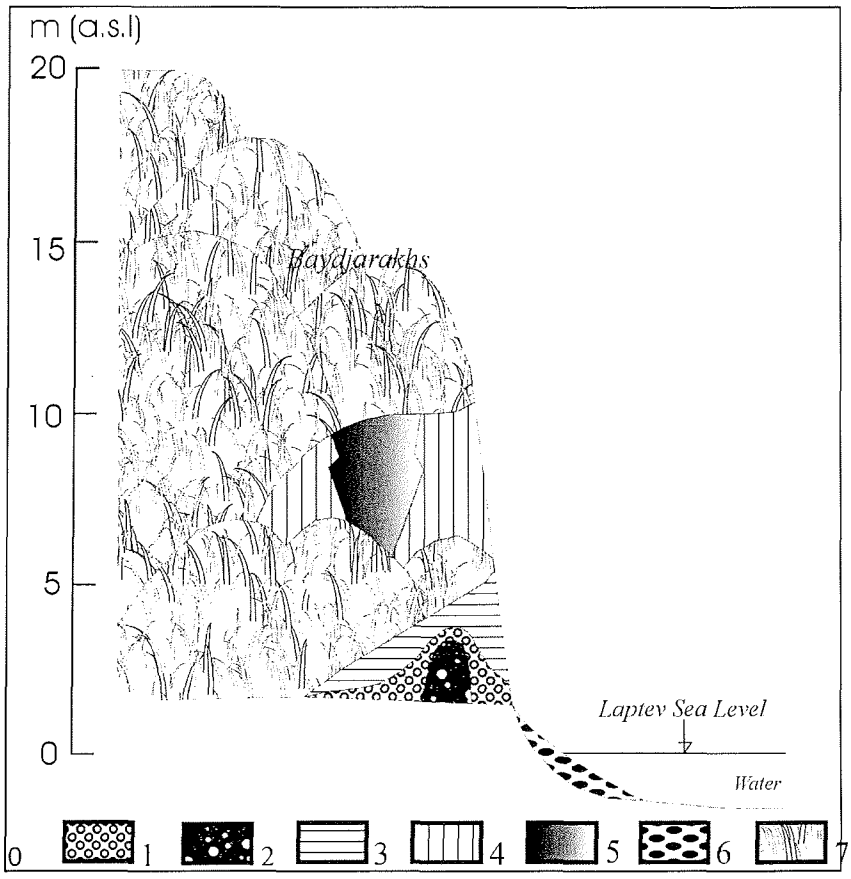

Figure 5.2.5-2: Scheme of the profile Kys 2 of the Ice Complex fragment of the 20 m cryoplanation terrace near the Khomurgannakh River mouth
1 – Gravel layer, yellowish-brown, small, with sandy loamy matrix, crusts and nests of segregation ice, 2 – Ice wedge, yellowish-brown, with a lot of sediment veins and inclusions of gravels, "Polosatic"; 3 – Silty sand, grey-blue to grey, in parts black, small peat nests (5-10 cm Ø), thin ice bands; 4 – Silty sand, dark-grey, with thin grass roots, 3 to 5 cm thick ice belts; 5 – Ice wedge, grey, any grey silt veins, 4 m thick, small rim of brownish silty sand; 6 – Beach pebbles; 7 – Active layer surface with thermokarst mounds

At about 2.5 m a.s.l. an ice wedge (KYS-IW-2), 1.5 m high and 1 m wide, was excavated. It shows a characteristically rounded head with upward bound ice bands above the ice wedge (Figure 5.2.5-3). A similar ice wedge was observed near the beach on Stolbovoy Island (see chap. 5.2.2, Figure 5.2.2-4A). The ice wedge is enclosed in sediment containing at lot of sub-rounded yellowish gravel, and also the ice itself contains some pebbles. A similar feature is found on Bol'shoy Lyakhovsky Island near Zimov'e River (Rachold et al. 2000). Additionally, large gas bubbles (1-2 mm in diameter) were observed in the ice. The ice wedge ice is of white colour interrupted by dark grey to black parts, probably because of a varying content of organic matter in the ice. The vertical structures, such as elementary ice veins, are evident especially in the upper

part of the ice wedge. Six samples were taken in 15 cm intervals in a height of about 3 m a.s.l., additionally one sample of organic matter for radiocarbon dating at about 2.7 m.

The ice wedge was surrounded by yellowish ice-rich sandy gravels and debris (gravimetric ice content about 40-wt %), consisting of sub-rounded pebbles. This material was pressed up by the ice wedge. The deposits were undisturbed and layered horizontally only at a distance of 1 m besides the ice wedge. Ice-rich grayish silty sand (aleurite) with single non-rounded stones, a coarse lens-like cryostructure and ice bands occur. The next layer consists of ice-poor silty sand followed by an alternation of sandy gravels and ice bands. An about 0.5 m thick ice-rich gravel layer was bent by the head of the ice wedge. The next layer was an alternation of peat laminas and ice-rich gray silty sand with lens-like reticulated cryostructure. In general, the coarse-grained layers seem to be of fluvial origin. This unit is covered by a cryoturbated paleosol consisting of sandy and organic-rich layers and have a lens-like reticulated and ice-bent cryostructure. Above the paleosol, a 2 m thick horizon follows, which consists of ice-rich silty sand and contains numerous peat nests (Ø 10 cm) and single stones and ice bands.

The middle part of the section was covered by thermokarst mounds and debris and was not studied therefore. However, below the top of the cliff Ice Complex deposits of about 1.2 m were exposed. Two broad ice wedges framing a sequence of greyish to brownish ice-rich silty sand with small ice bands, broken lens-like cryostructure and small grass roots (gravimetric ice content 52 to 82 wt-%) was found there. A small ice wedge penetrated into the sediment beside the large ice wedge (Figure 5.2.5-3B). A small zone was coloured by brownish iron oxide at the contact between the ice wedges and the sediment packet. In this section at about 8 m a.s.l., two ice wedges were examined. A broad ice wedge at the left side (KYS-IW-1) was sampled in 20 cm intervals from right to left. In total, 18 samples were taken from this 3.5 m wide ice wedge. This ice wedge contained a lot of organic matter, especially lemming coprolithes as well as plant remains. Two of these coprolithes could be sampled in frozen state for radiocarbon analyses. According to former datings, lemming coprolithes have been proven to give highly reliable ^{14}C ages. The ice wedge is characterised by greyish milky ice, which is not typical for the Ice Complex because of its turbidity. This is due to the large quantity of gas bubbles, which mostly are smaller than 0.5 mm. Single ice veins are moderately to recognise and in general between 1.5 and 3 mm thick. From a smaller ice wedge of a younger generation (KYS-IW-3), 2 samples were retrieved. This ice wedge is 8-10 cm wide, and penetrates KYS-IW-1, and crosses the ice belts besides the other sampled ice wedge. The ice veins are easily to recognise and between 2 and 5 mm thick.

30 bones and their fragments were found at the south coast of Kotel'niy Island near the Khomurgannakh River mouth. It is unusual, that there is no one bone from the shore. This can only be explained little coastal erosion. The same processes are on the Belkovsky Island. All bones were collected on the

exposure, on thermokarst mounds in coastal outcrops as well as in the tundra. For parts of them the initial stratigraphical position could be reconstructed (Appendix 5.2-3).

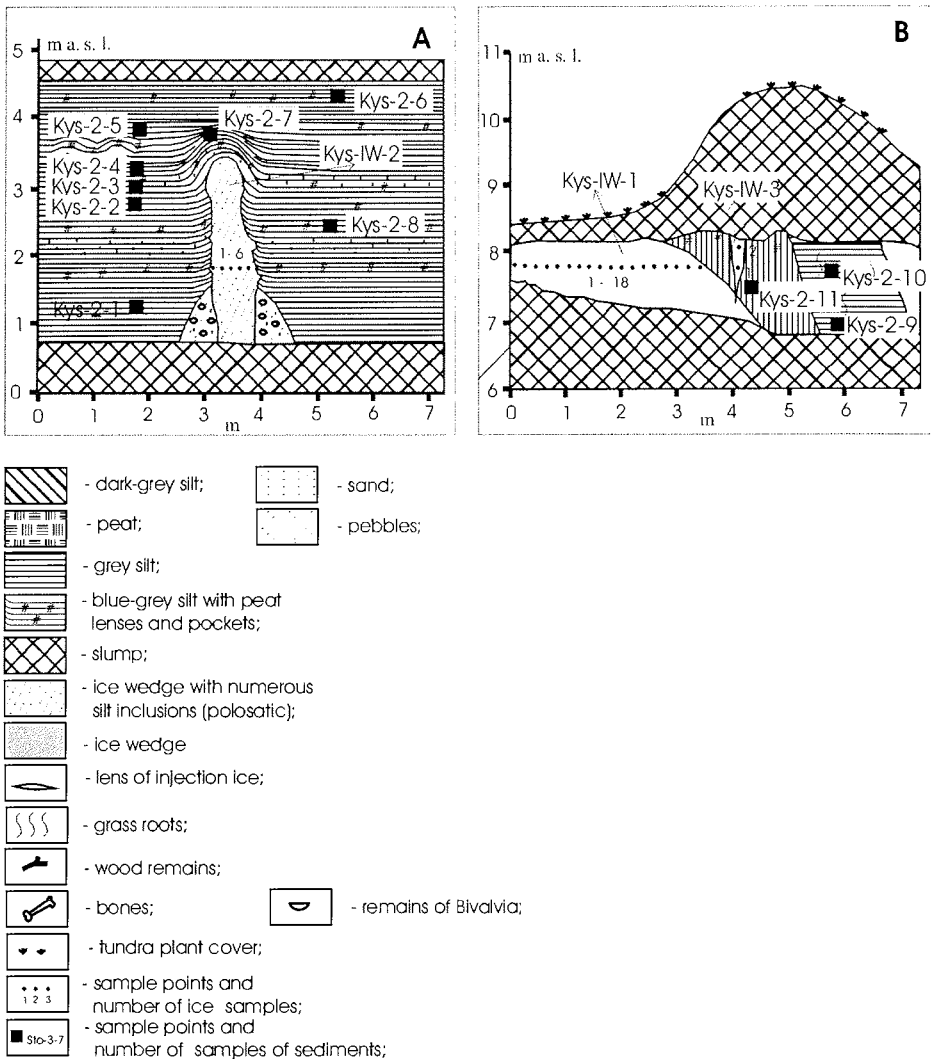

Figure 5.2.5-3: Schematic sketch of the studied sub-profiles of Kotel'ny Island south coast, site Khomurgannakh;
A – Lower part with an old buried ice wedge;
B – Upper part with Ice Complex deposits.

5.2.6 Bunge-Land (19./25.08)

Bunge-Land is one of the least studied regions of the New Siberian Archipelago. The largest part of Bunge-Land is a flat, sandy plain with heights between 2-12 m (low terrace) and a very gentle inclination towards the sea. Only in the southeast a small area of about 25 x 15 km extension has a higher surface (11 to 21 m a.s.l.) with a stronger relief (high terrace). According to the modern map of Quaternary deposits (Ivanenko 1998), the low terrace is a Holocene marine terrace and the higher level a Pleistocene marine terrace.

Large areas of the low terrace are episodically flooded during storm surges mainly up to the level of about 2 m a.s.l. (Figure 5.2.6-1). The surface is not covered by vegetation and can be classified as Arctic desert. Driftwood is found in some kilometres distance from the coast. The surface of this area is covered by water saturated thixotropic sand and the active layer is maximum 0.6 m thick.

The TSP was placed within the wet, homogenous sand surface about 100 m from the shoreline.

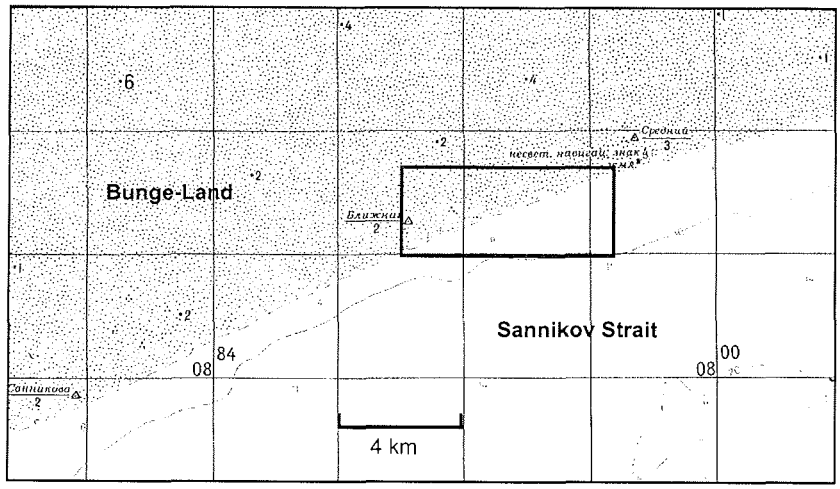

Figure 5.2.6-1: Study area on the low terrace of Bunge Land

A small, elevated (3 m a.s.l.) area close to the coast was scarcely covered by grass tussocks. The size of this area was about 400 x 600 m. Separate grass hummocks occurred in a distance of 1.5-2 m. The active layer there was about 95 cm below grass hummocks and 20-40 cm in the inter-spaces. The small depressions between grass hummocks are comparable with small deflation hollows.

A pit down to the permafrost table was dug on this elevated area (Figure 5.2.6-2). The small profile consisted of frozen silty fine-grained sand (gravimetric ice content 34 wt %), followed by unfrozen dark gray fine sand with clay inclusions or nests. The upper horizon of about 50 cm thickness was formed by a wet, brownish-grey fine to medium sand with grass roots. Three samples were taken there for sedimentological analysis (Bun-7-1 to 7-3) and two samples for OSL-dating (Bunge 4 & 5). Unfortunately, recent ice wedges were not found in this place.

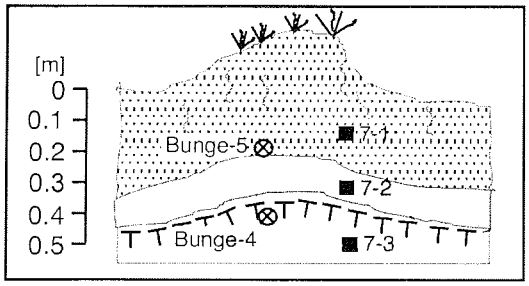

Figure 5.2.6-2:
Sub-profile Bun-7 on the low terrace of Bunge-Land

The relief character of the high terrace of Bunge-Land is totally different. The study area was located southeast of the polar station "Zemlya Bunge". The TSP was placed near the polar station for about 8 hours. The scarce vegetation consists of dry grass tussocks and moss and is covered by yellowish fine sand with pebbles. The surface (20-10 m a.s.l.) is a landscape, weakly inclined towards the sea and crossed by wide valleys with flat bottom and periodical streams. The vegetation of this area is more dense than on the low terrace of Bunge-Land, but also scarce. Only on the valley bottom more grass is growing. Several initial thermokarst lakes occur in the areas between the valleys. The diameter of one small lake amounts to 60 x 80 m. Its water-depth was 0.4 m and the active layer thickness about 0.6 m. Lake deposits (Bun-1) and lake water were sampled there. A depth profile was measured from the shore of a large lake (800 x 600 m) near the polar station. This lake is very shallow – 0.5 m deep at a distance of 100 m from the shore. The active layer thickness is almost constant at about 0.1 m. Lake sediment (Bun-2) and lake water were sampled at a distance of 7 m from the lake shore.

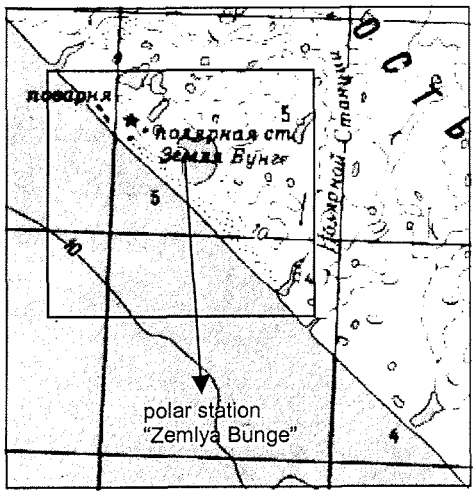

Figure 5.2.6-3:
Study area of Bunge-Land high terrace near the polar station „ Zemlya Bunge".

The detailed studied sections were located about 2 km Southeast of the polar station (Figure 5.2.6-3). Thermokarst mounds were visible at the terrace slopes as well as on valley margins, indicating the existence of ice wedge polygonal nets. Although frost cracks were visible there, we were unable to find recent ice wedges on the beach. The schematic profile of the Bunge-Land high terrace is presented in Figure 5.2.6-4. Ice wedge polygons were found especially in higher areas between the valleys. They have diameters of 18-20 m. Small, 0.3 m deep trenches often outline the polygons. One small frost crack was dug during our studies (Figure 5.2.6-5). A thin ice vein shades away into a composite ice-sand wedge or so-called "Polosatic" – a vertically striped alternation of ice and sediment veins. The ice veins as well as the "Polosatic" structure were sampled for stable isotope and tritium analyses.

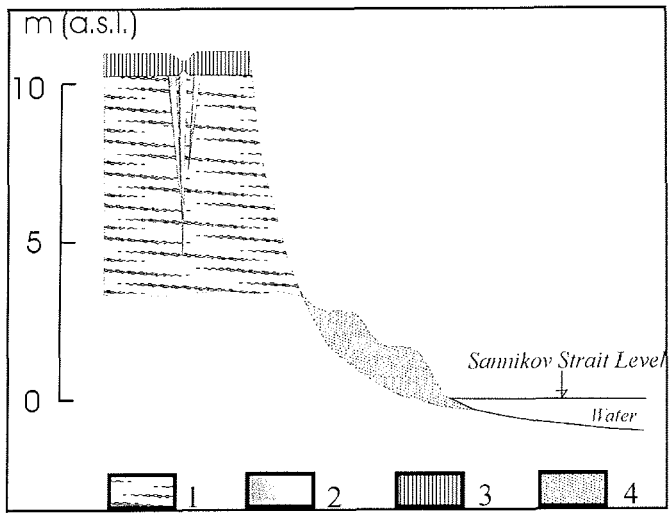

Figure 5.2.6-4:
Schematic profile of Bunge-Land high terrace.
1 – Greyish-blue sand, horizontal and cross-bedded, deformed by ground wedges and microfaulting, frozen;
2 – Ice wedge, white, „Polosatic", ice-sediment stripes; 3 – Active layer;
4 – Beach sand, yellowish-grey, cross-bedded, with gravels and pebbles, permanently frozen.

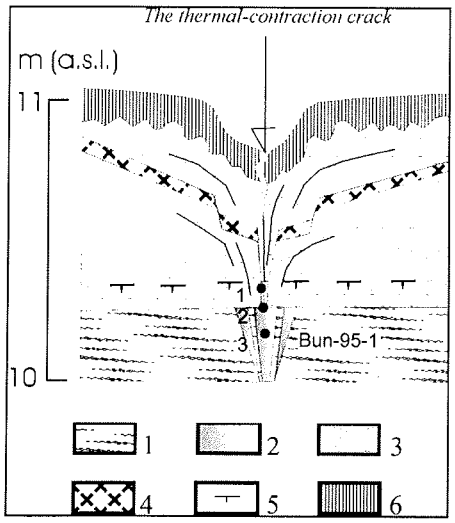

Figure 5.2.6-5: Schematic Profile of the active layer with the upper part of a so-called „Polosatic" on Bunge-Land, high terrace.

1 – Fine and greyish-blue;
2 – Ice wedge, „Polosatic";
3 – Fine sand, lightgrey with humic laminaes;
4 – Fine sand reddish-brown, riddled with iron and manganese;
5 – Permafrost table
6 – Fine sand, dark grey, with roots.

In addition, a 4 m thick section with two sub-profiles was studied in more detail at the steep slope of an erosional valley 2 km southeast of the polar station (Fig. 5.2.6-6). The lower part (1 m) of the sub-profile (Bun-4) consisted of grey frozen, fine sand layers alternating with black organic-rich layers. This interbedding was disturbed syn-sedimentary by small faults. The next part contains thicker sand and organic-rich layers. In general, these two horizons look like lacustrine or stillwater deposits of an old river channel. Their gravimetric ice content was between 18-22 wt-%. The horizon below the permafrost table was brownish coloured spotty, non-bedded, fine sand that was influenced by soil formation. Some 0.4-0.6 m long and about 1 cm wide ground wedges were observed. The gravimetric ice content amounts to about 18 wt-%. The upper horizon of this subprofile consisted of unfrozen, interbedded fine sand, whereas its lower part is strongly cryoturbated.

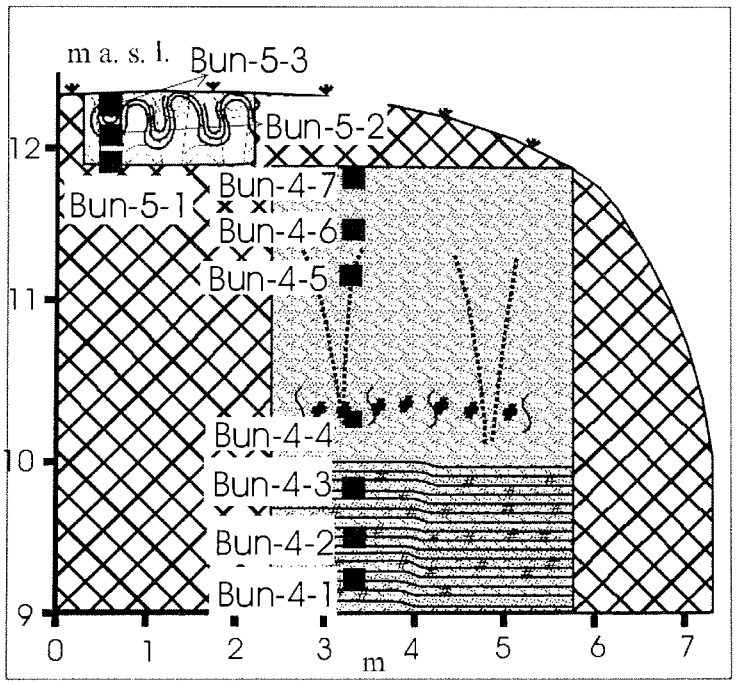

Figure 5.2.6-6: Sub-profiles Bun-4 and Bun-5; Laminated organic-rich sand, cryoturbated soils, ground wedges

The second sub-profile Bun-5 represents the uppermost part of the whole section up to the surface at about 12 m a.s.l.. It is a strongly cryoturbated unfrozen soil, containing dark brown and light brown fine sand layers (Figure 5.2.6-6). In addition to the regular sampled profile 3 samples were taken for IRSL dating there.

Age determination, analysis of grain size, grain shape and heavy minerals as well as pollen analysis could help to understand the genesis of the large desert-like sand plain of Bunge-Land.

5.2.7 Novaya Sibir Island (20./21. 08.)

The southwest coast of the Island Novaya Sibir was the easternmost study region. On August 20th, the very impressive coast section of Derevyannye Gory (Wood hills) and parts of a coastal region named "Urochishche Gedenshtroma" (Location Hedenstrom) were studied (Figure 5.2.7-1).

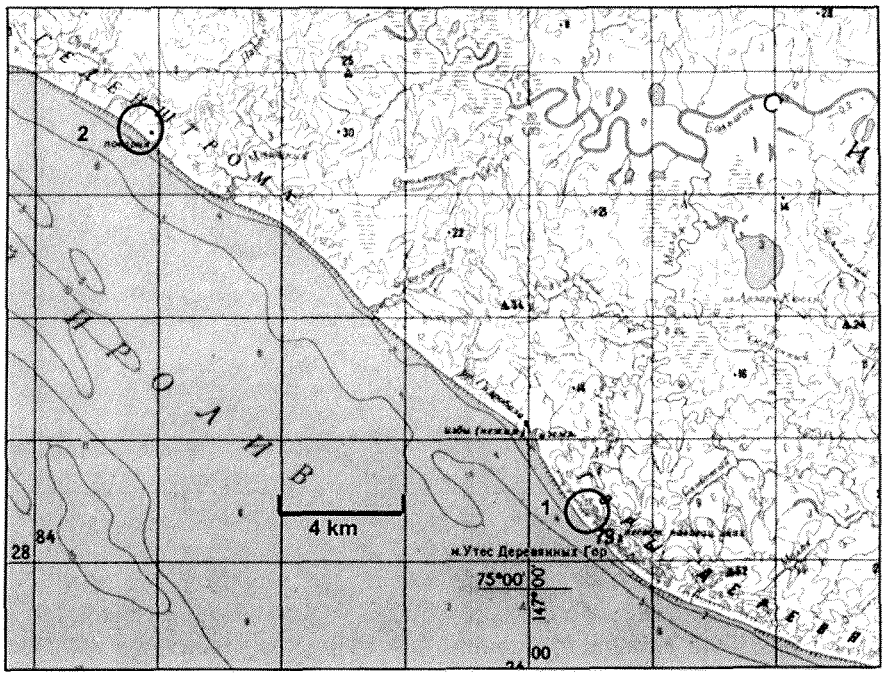

Figure 5.2.7-1: Study areas at the southwest coast of the Novaya Sibir Island
1 – Derevyannye Gory; 2 – Location Hedenstrom

5.2.7.1 Derevyannye Gory

The coast of Derevyannye Gory exposes Upper Cretaceous and Cenozoic loose rocks. By approaching the coast the markant light-dark alternation of sand and coal layers below lighthouse catches the eyes (Figure 5.2.7-3A). This unit is overlain by Paleogene to Neogene silty sands (aleurite) and gravels. The Tertiary deposits were mostly covered by clays, silty sands and sands of the early Quaternary Kanarchasky Suite. According to Parfenov et al. (2001), Jurassic, Upper Cretaceous and Upper Miocene deposits were upfaulted during Late Miocene and early Pliocene (Figure 5.2.7-2).

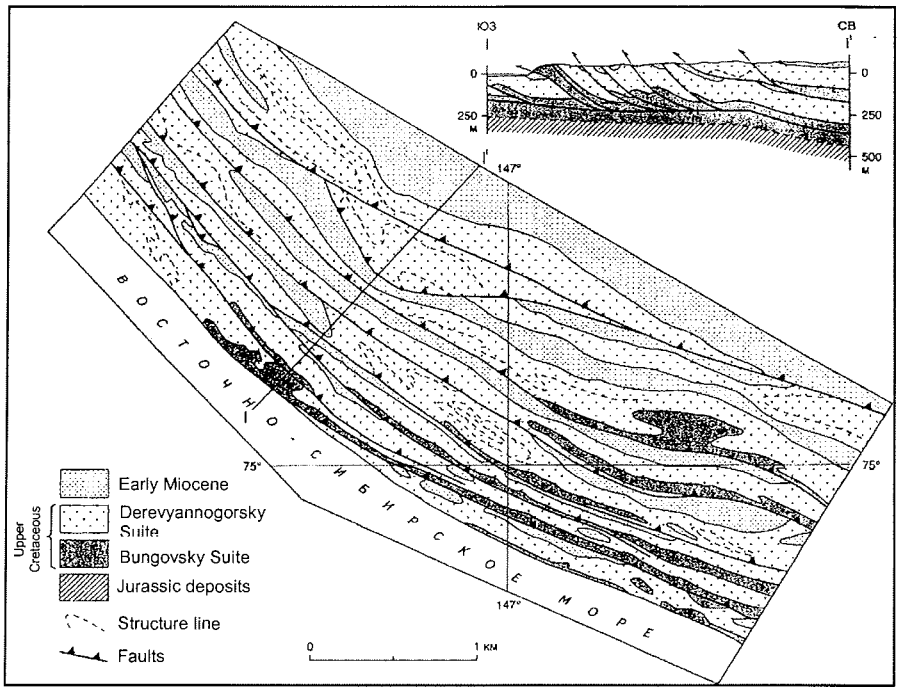

Figure 5.2.7-2: Geological situation of the study site Derevyannye Gory; late Miocene to early Pliocene faults (according to Parfenov et al. 2001)

The upper Cretaceous frozen sand-coal interbedding contained numerous thin coal layers and trunk remains of *Sequoia.* Different types of ice were sampled on Novaya Sibir Island. First, 20 cm long and 5-8 cm wide lenses of injection ice were observed at the contact of old coal deposits with silty gray sediments. Voids in these highly tectonised deposits seem to be filled with very clear and transparent injection ice with a lot of gas bubbles especially in the central part. In addition, remains of snow patches as well as sea ice were observed and sampled near the coast. In a cavity formed by wave erosion, a snow patch was sampled in direct contact with an overlying coal layer. This snow patch consisted of white and brown ice pointing to the percolation of water from above (Figure 5.2.7-3C). A second, 1.5 m thick snow patch was sampled 5 m a.s.l., consisting of clear ice almost without any gas bubbles. These two snow patches are surely influenced by seawater (e. g. by spray), whereas a third one of 1 m (sub)-recent snow was sampled further landwards (without marine influence).

Intensive erosion cuts the island's surface near the coast and the zebra-like stripes of the upper Cretaceous deposits were visible all over (Figure 5.2.7-3B). The erosion seems to be dominated by periodical meltwater runoff from the hills. No vegetation is covering the surfaces, hence the soil is easily transported downhill by running water. These slopes are covered by rock debris with different degrees of rounding. The slopes of Derevyannye Gory hill are also shaped by nivation niches in form of wide kars. The kar bottoms are about 20-

30 m a.s.l.. Single snow fields were observed at the steep walls of such kars. One of these snow patches was about 2 m thick and the thawing-remains, so-called "Chionochonite", did not contain larger amount of plant remains because of the polar desert conditions in the surroundings. Two terraces are formed in about 50 m and 80 m height, respectively. Valley bottoms as well as the terrace surfaces are covered by large pebbles (10-20 cm Ø) and boulders up to 1 m in diameter (Figure 5.2.7-3D). Many of them show traces of striation. They contain a wide spectrum of rocks, like porphyry vulcanite's, gabbroids, granate gneisses, quartzitic sandstones, slates, limestones and others. All these rocks do not occur on Novaya Sibir Island. The origin of this material and the formation of these terraces are still under discussion. The most realistic hypothesis will be the glacio-marine transport of this coarse grained material, perhaps during Early Quaternary periods. Patterned ground with circles, stripes and frost boils were observed in places (Figure 5.2.7-3E).

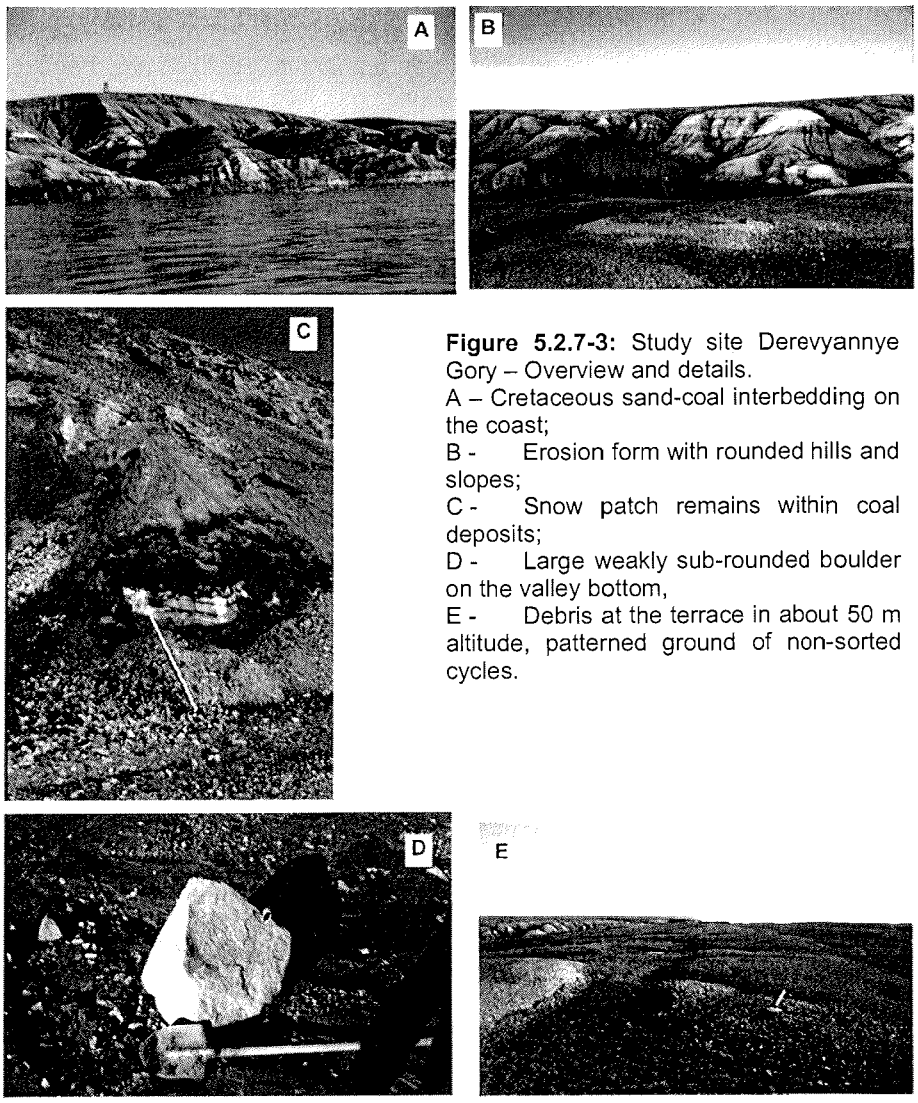

Figure 5.2.7-3: Study site Derevyannye Gory – Overview and details.
A – Cretaceous sand-coal interbedding on the coast;
B - Erosion form with rounded hills and slopes;
C - Snow patch remains within coal deposits;
D - Large weakly sub-rounded boulder on the valley bottom,
E - Debris at the terrace in about 50 m altitude, patterned ground of non-sorted cycles.

5.2.7.2 Island Novaya Sibir - Location Hedenstrom

Frozen marine deposits with terrestrial permafrost deposits were studied for the first time during our expedition at about 40 km NW of Derevyannye Gora along a 2 km long coastal section. The general profile is presented in Figure 5.2.7-4 and shows marine deposits containing ice bodies of unknown origin, Ice Complex deposits as well as alas deposits.

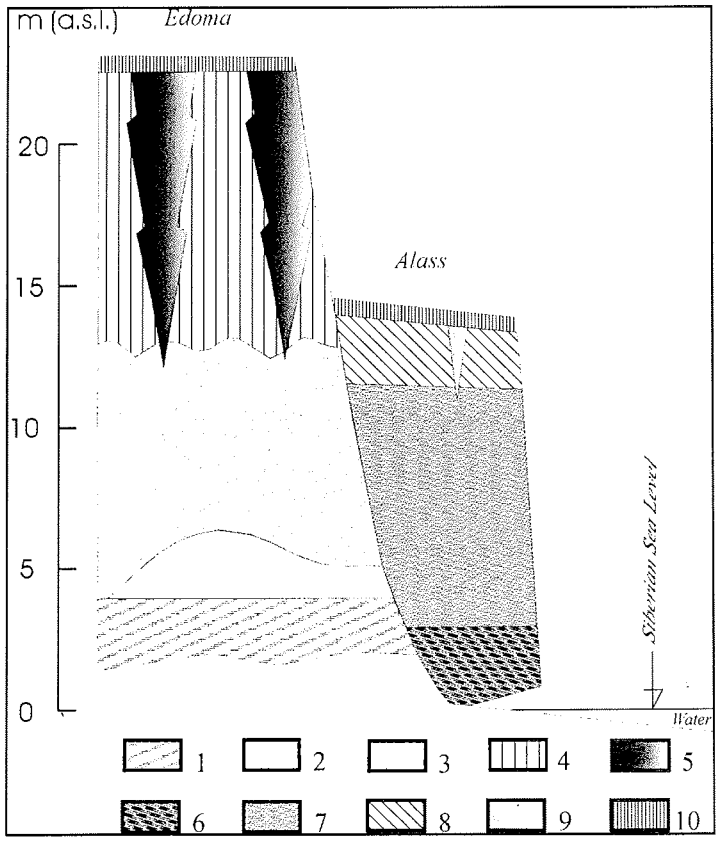

Figure 5.2.7-4: Schematic profile of clayish marine or lacustrine deposits with an ice body framed by alas deposits and covered by Ice complex deposits
1 – Dark-grey, dense silty fine sand (aleurite), bedded, with inclusions of debris, gravels and single pebbles, frozen, blocky cryostructure; 2 – Blue-grey clay, unclearly bedded, with shells of marine molluscs, frozen, blocky or lattice cryostructure; 3 – Transparent ice of unknown origin, dense; 4 – Brownish-grey silty to clayish fine sand (aleurite) with sand lenses with thin grass roots, frozen, ice bands; 5 – Ice wedge, grey, dense, 3 m wide; 6 - Yellow-brown sand of various grain size, with inclusions of gravels, debris and fine sand interlayers, massive cryostructure; 7 – Grey-blue loam, diagonal lattice cryostructure in the lower part, brownish patches and diagonal lens-like cryostructure in the upper part; 8 – Grey loam with thin grass roots, lens-like reticulate or bedded cryostructure, 9 – Small, white ice wedge, 1m wide, 10 – Active layer.

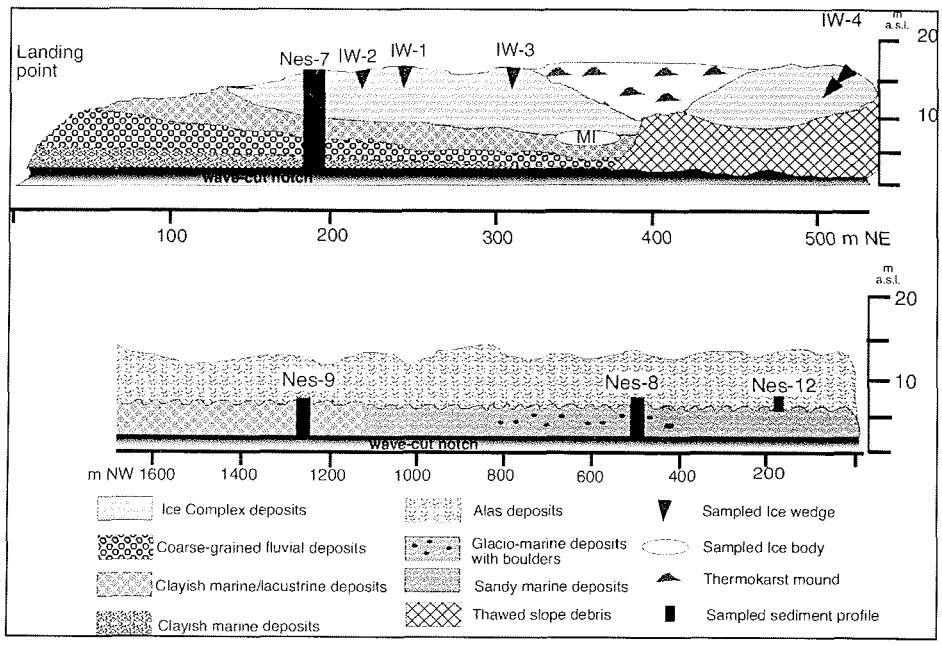

Figure 5.2.7-5: Scheme of sampling positions and general stratification of the study area location Hedenstrom

Several sub-profiles were studied during a stay of 8 hours there (Figure 5.2.7-5). The TSP was placed in a distance of 80 m from the coast line at about 16 m a.s.l.. The surface of this place was characterized by scarce, dry tundra (grass and moss) and frost boils.

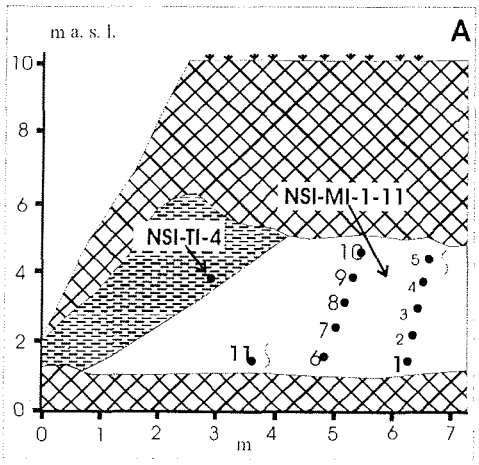

Figure 5.2.7-6: Buried massive ice body NSI-MI with sample positions

In the southern part of the coast section a massive ice body of more than 6 m width and 3 m height was exposed between 3 m and 6 m a.s.l. (Fig.5.2.7-6). Ice-rich deposits overlie the seaward part of the ice body with reticulated cryostructure dipping about 20-30° towards the sea. The inclination of the ice body is similar below the segregated ice. The landward part of the ice body is covered by about 4-5 m of Ice Complex baydzerakhs. This part of the ice body does not show the same inclination, since the structures are rather vertically oriented. This impression is supported by the alternation of different types of ice in this section. A 1.2 m wide zone of milky, white ice with a high amount of very small gas bubbles occurs between two zones of clear transparent ice with some bigger sized gas bubbles (> 1 mm). From this ice body, 11 samples were taken by means of an axe. Five samples were retrieved in different heights from the white and milky ice, six from the clear and transparent ice. Some of these samples contain organic material such as black coal particles (presumably derived from the Dereviannye Gora section) as well as small red organic particles, possibly moss fragments. The genesis of this massive ice body is still unknown yet and its age can be assumed to be older than the Ice Complex. Stable isotope and hydrochemical analyses will help to clarify these questions.

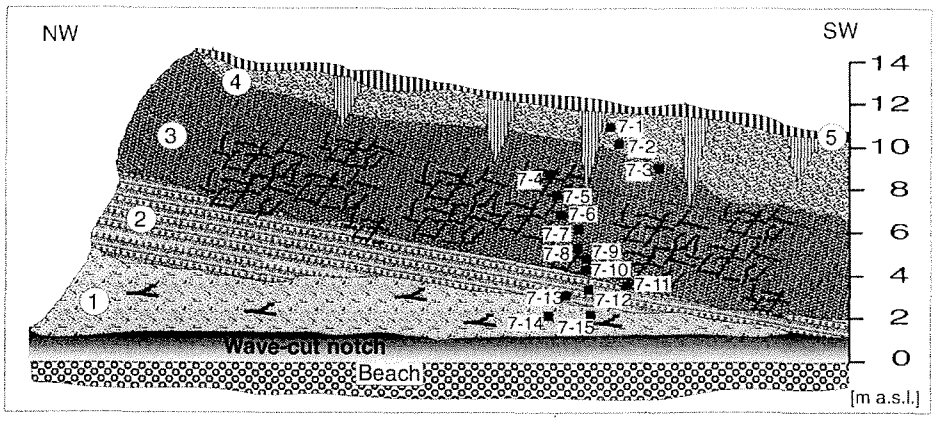

Figure 5.2.7-7: Sub-profile Nes-7, a sequence terrestrial and aquatic deposits at the SW-coast of Novaya Sibir Island; 1 – Silty sand (aleurite), ice banded, shrub fragments; 2 – Interbedding of silty fine sand, coarse-grained sand and gravel; 3 – Bluish-grey clay. diagonal lattice ice veins; 4 – Ice Complex deposits; 5 – Active layer

About 300 m to the north the 10 m thick sub-profile Nes 7 was studied and sampled in detail (Figure 5.2.7-7). Above the wave-cut notch a 0.5-0.8 m thick frozen horizon (gravimetric ice content 47 wt-%) of ice-banded silty fine sand with shrub fragments occurs, which is overlain by 1m thick interbedding of silty fine sand layers and coarse-grained sand with gravels (gravimetric ice content 21-38 wt-%) and thick ice schlieren. Both horizons represent terrestrial deposits and the coarse-grained part was probably of fluvial origin. The following horizon consisted of frozen bluish-grey clayish silt (gravimetric ice content 40-73 wt-%) with a net of diagonal lattice ice veins. Such ice veins are 1-2 cm thick and 10-20 cm long. Ice Complex deposits overlie these aquatic perhaps marine or

lacustrine deposits and show the typical lens-like reticulated cryostructure. The gravimetric ice content amounts to 132 wt-%. Ice wedges at this place penetrated 1 m into the horizon situated below. The transition zone between both horizons is of brown colour because of iron oxide patches. A 0.3-0.4 m thick active layer borders the described profile.

Ice wedges of different generations were studied near this location. In a height of 7 m a.s.l., a 2.2 m wide ice wedge was sampled (Figure 5.2.7-8A). This ice wedge (NSI-IW-1) is of milky, white colour with a lot of very small (0.1-1 mm), slightly elongated gas bubbles. The ice wedge contains a very small amount of sediment and organic particles and vertical structures are poorly recognisable. It is embedded in very ice-rich sediment (Ice Complex ?) with ice belts bound upward near the ice wedge. These features as well as some ice shoulders in the ice wedge point to the synsedimentary growth of this ice wedge. Nevertheless, the appearance of the ice wedge is not typical for Ice Complex but rather for Holocene ice wedges. From this ice wedge, 16 samples were taken (in 15 cm intervals from the left to the right) by means of an ice screw to answer the question, whether this ice wedge is of Holocene age or older, and to understand if these ice wedges are formed without simultaneous sedimentation. Secondly, four samples of ice wedge and four samples of texture ice (ice belts in the contact of the ice wedge) were gained from a narrow ice wedge (NSI-IW-2) approximately in the same level of the (Ice Complex ?) deposits as NSI-IW-1. It shows nice ice belts in the sediment and ice wedge shoulders, the contact of which was sampled in detail (Figure 5.2.7-8B).

80 m further to the SE, a third ice wedge was studied (NSI-IW-3). This 0.4 m wide and 2.2 m high ice wedge is surrounded by ice-rich Ice Complex deposits (Figure 5.2.7-8C), but in contrast to NSI-IW-1, the ice belts are not bound upward near this ice wedge. Therefore, this classical epigenetic ice wedge is assumed to be younger than the Ice Complex, possibly of Holocene age, which is sustained by its white, milky colour. The milky appearance is, again, caused by a lot of small gas bubbles (< 1mm) and some bigger ones, which are slightly elongated. Elementary ice veins are smaller than 3 mm but they are not so easy to differentiate.

The Ice Complex thermokarst mounds on top of the outcrop near the massive ice body have small diameters between 8 and 10 m and contain a lot of debris from different rock types (e.g. quartzite, basalt, sandstone, granite, metamorphic rocks). About 100 m further to the SE, a 20 m high outcrop was studied, the upper 12 m of which consist of Ice Complex deposits. Two generations of Ice Complex ice wedges are observed in this section. Smaller 1.5 m wide and 4-5 m high ice wedges penetrate into an older generation of 3 m wide ice wedges. An ice wedge of 1.2 m in horizontal extension (NSI-IW-4) of the younger generation of Ice Complex ice wedges was sampled (Figure 5.2.8-8C). Because of lack in time, a more detailed study and description of this section was unfortunately not possible.

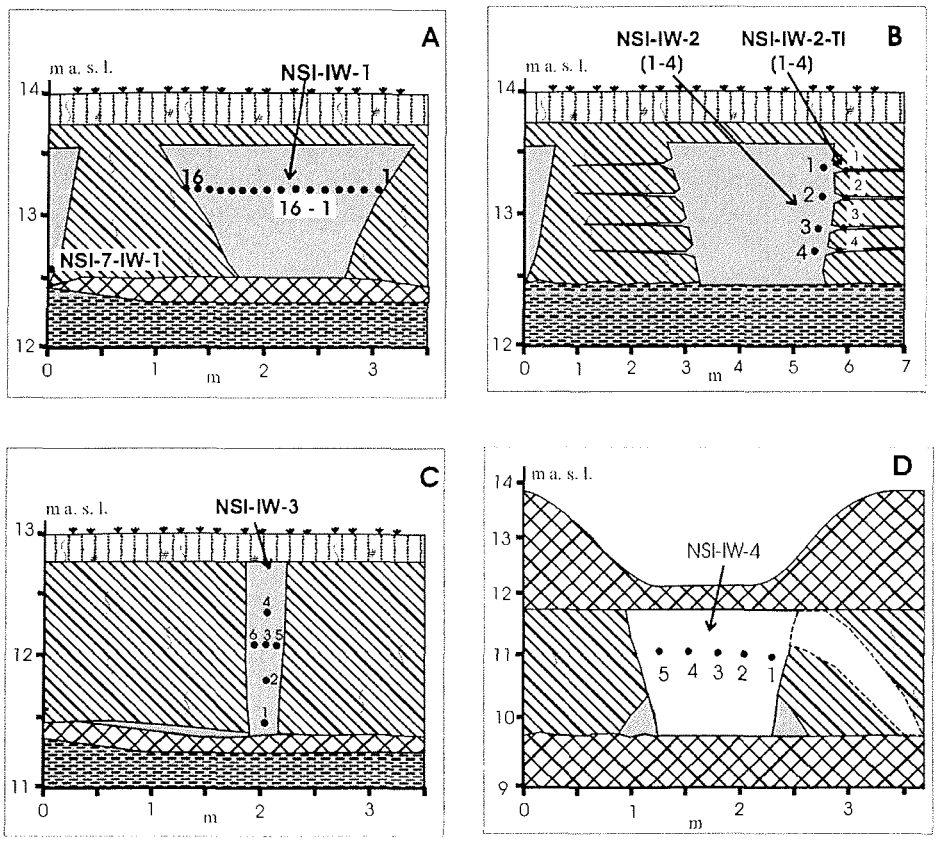

Figure 5.2.7-8: Various studied ice wedges of SW-coast of Novaya Sibir Island

A lateral succession of various marine deposits overlain by thermokarst (alas) deposits was exposed at the coast some 1.4 km further northwest. In the lowermost part, frozen bluish-grey, compact and bedded clay with shells occurs (sub-profile Nes 9, Figure 5.2.7-9A).

This clay contains horizontal 1 cm thick ice bands in a distance of 20 cm. They are 1 cm thick, vertical ice veins forming lattice-like cryostructure (gravimetric ice content 36-40 wt-%). The horizon was regularly wave-like deformed with amplitude of 10 m width (Figure 5.2.7-11A). The marine deposits are covered by 3-4 m thick yellowish-brown alas deposits in a height of 8-9 m a.s.l., which were deformed accordingly. They consist of bedded silty sands and contain layers of plant remains or thin peat layers. After some hundred meters to the SE the lower marine horizon changes to coarse-grained, well-bedded deposits. Cross-bedded, wave-like deformed sands occur, (Figure 5.2.7-11D) overlain by similar alas deposits as described before. Next to the SE (sub-profile Nes 8, Figure 5.2.7-8B) the bedded and also wave-like deformed marine horizon looks like a till because of numerous rounded pebbles (Figure 5.2.7-11E) within a grey-blue fine-grained matrix. In addition, dropstones up to 0.5 m in diameter are embedded within this matrix (Figure 5.2.7-11C). Therefore, a glacio-marine

formation is assumed. The cryostructure is also lattice like with diagonal ice veins. Brownish, bedded and wave-like deformed alas deposits with organic rich interlayers overlay this material in about 3.5 m a.s.l.. In general, a lateral transition from marine clayish deposits to marine sandy deposits and glacio-marine deposits was studied. This marine sequence was totally covered by deposits of thermokarst depression.

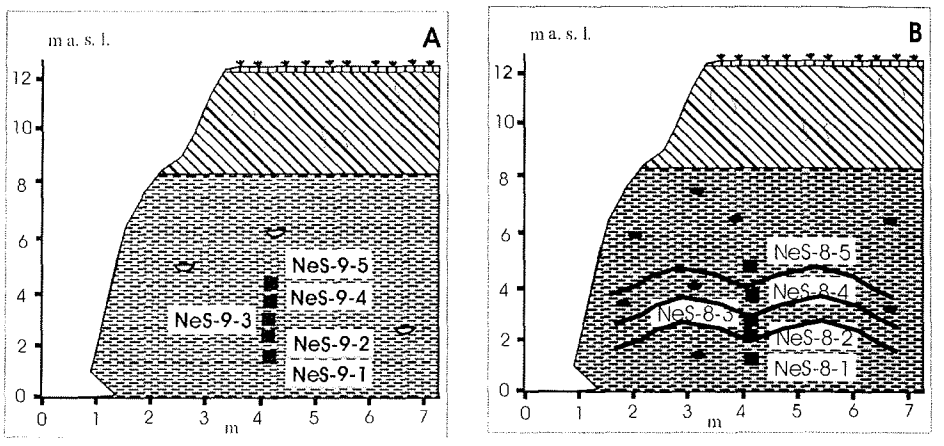

Figure 5.2.7-9: Studied sub-profiles Nes-9 and Nes-8 with marine deposits and thermokarst deposits

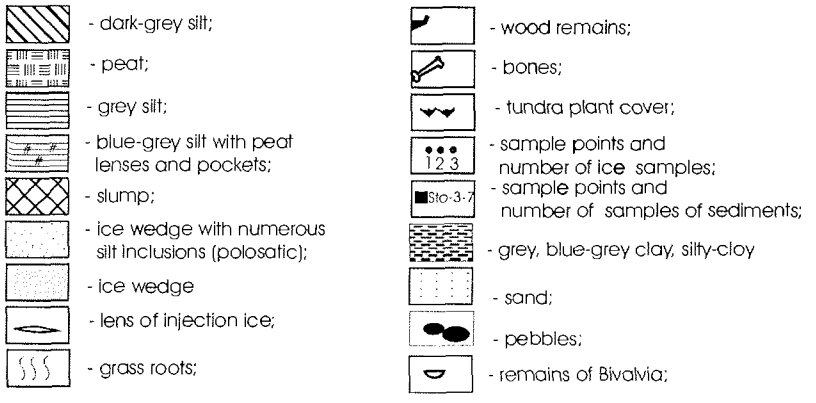

Figure 5.2.8-10: Legend to figures 5.2.7-6, -8, -9

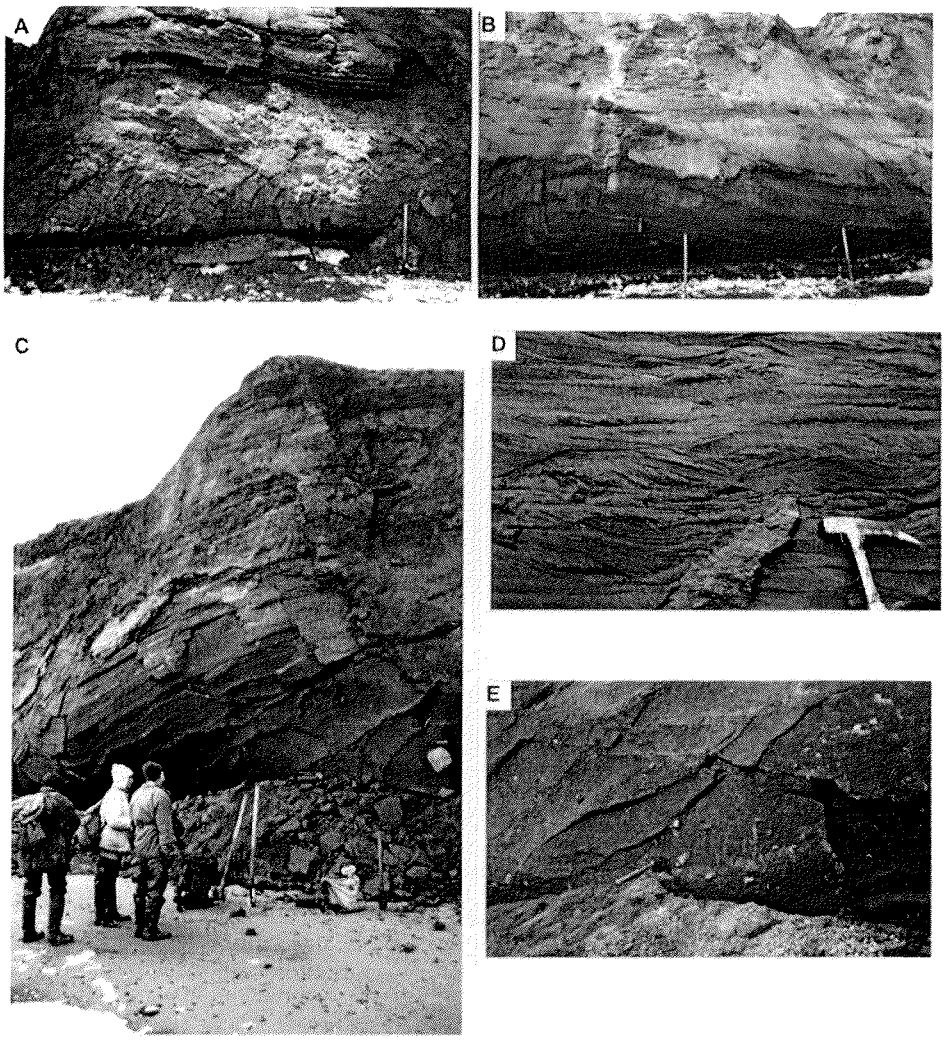

Figure 5.2.7-11: Deposits of a marine to glacio-marine succession on the southeast coast of Novaya Sibir island, location Gedenstrom.
A – Bluish-grey marine clay with shells and lattice-like cryostructure (sub-profile Nes 9) covered by sandy alas deposits with organic-rich interlayers;
B – Bedded marine sands overlain by yellowish-brown alas deposits;
C – Cross-bedded marine sand horizon;
D – Glacio-marine deposits with a large boulder of dropstones, overlain by alas deposits;
E – Detailed section of glacio-marine deposits with numerous well-rounded pebbles.

5.2.8 Maly Lyakhovsky Island (27.08.)

The basement of Maly Lyakhovsky Island consists of upper Jurassic and lower Cretaceous sediments (Lopatin 1998). The highest elevation of the island is about 32 m a.s.l and the islands surface has step-like character with some terraces. Thermokarst lakes occur in the centre of the island at the highest terrace of 30-32 m a.s.l.. The second terrace at about 25 m a.s.l. is characterized by thermokarst valleys with flat bottoms. The third terrace at about 20 m a.s.l. is cut by a net of deeper thermokarst valleys. At the lowest level on the beach numerous pebbles and boulders up to 1-1.5 m occur. The study area was located southeast of Cape Vaygach (Figure 5.2.8-1). The frequent distribution of thermokarst mounds and thermokarst valleys indicate the existence of an Ice Complex cover on these terraces (Figure 5.2.8-2).

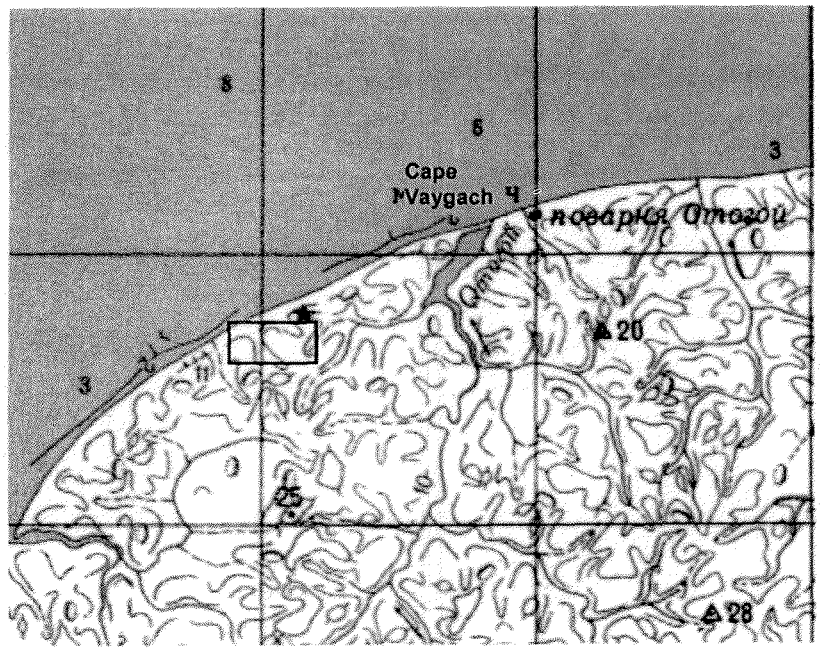

Figure 5.2.8-1: North coast of Maly Lyakhovsky Island with the study area west of Cape Vaygach

The TSP was placed on top of the coastal cliff near a thermokarst valley about 7 m a.s.l.. Dry cryoturbated soil, dried grass, and lichens covered the surface. The vegetation was generally denser than the Arctic tundra and than Arctic desert of Kotel'ny Island and Novaya Sibir Island. The valley bottom was wet and a dense grass cover was growing, whereas the higher located surface between the valleys was quite dry.

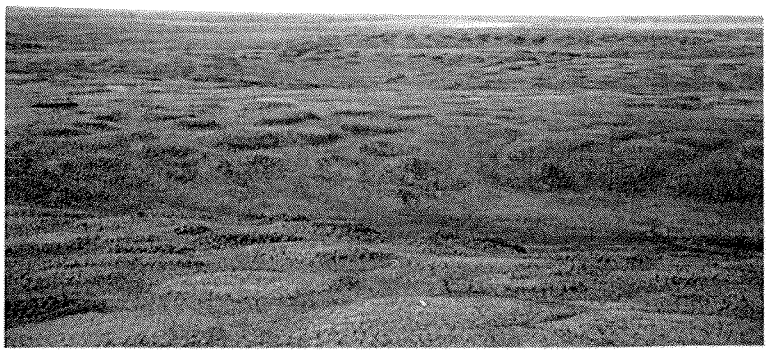

Figure 5.2.8-2: The step-like surface of Maly Lyakhovsky Island; terraces with thermokarst mounds and thermokarst valleys.

Thermokarst mounds were measured at a valley slope. They are between 1-2.5 m high and have mostly a flat top. The distance of thermokarst mounds reflecting the size of a former ice wedge polygon net is between 8-18.5 m (in average 12 m). The surface of the mounds is also covered by cryoturbated ground and dry grass.

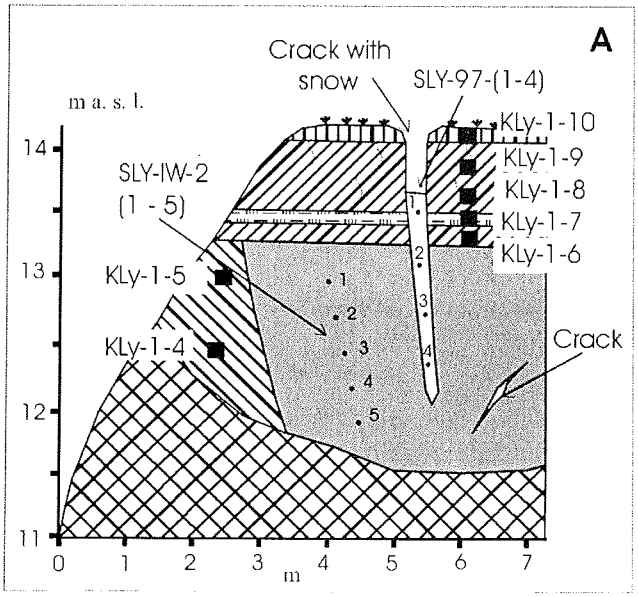

Figure 5.2.8-3: Ice Complex deposits covered by laminated deposits of a thermokarst valley (profile Kly 1)

Only one permafrost sequence of about 8 m in length could be dug on two sub-profiles at a thermokarst mound situated at the steep slope of a deep thermokarst valley near the sea (Figure 5.2.8-3). The first sub-profile on the foot of the mound consists of grey ice-rich silty fine sand (aleurite) with broken reticulated cryostructure and 2 cm thick ice belts (samples Kly 1-1 to 1-3, gravimetric ice content 74-132 wt-%). The second sub-profile in a higher position continued these Ice Complex deposits (samples Kly 1-4, 1-5). In addition, the contact of an ice wedge was exposed there. Both, ice wedge and Ice Complex deposits were firstly covered by a horizon of buried cryosol containing small peat nests followed by fine-laminated light-brown and dark-brown interbedding of silty fine sand and organic-rich layers (samples Kly 1-6 to 1-10). A frost crack penetrating from the surface 3 m down into the ice wedge was filled by snow of the preceding year, which also was sampled. In general, the described profile presents presumably a late Pleistocene Ice Complex sequence, covered by Holocene deposits of a thermokarst valley.

The largest paleontological collection of New Siberian Islands is from the north coast of Maly Lyakhovsky Island (59 samples). In comparison with other islands we found there a lot of bones at the shore and at the slopes of small brooks in tundra. That indicates an active erosion of Pleistocene deposits in this part of Maly Lyakhovsky Island. The taxonomic composition is typical for the "Mammoth" fauna. All finds were separately found. Only four bones of rein deer were found together and they probably belong to one individual (Appendix 5.2-3).

5.2.9 Cape Svyatoy Nos (22.08.)

A chain of Cretaceous granite domes up to 433 m a.s.l. dominates the landscape of Cape Svyatoy Nos (Lopatin 1998) (Figure 5.2.9-1). Cryoplanation terraces are formed around these elevations at various levels. The lowest terrace was studied about 8 km south of this cape near the former polar station "Mys Svyatoy Nos". Former studies by Russian colleagues point to the occurrence of early Pleistocene deposits there (Figure 5.2.9-2). According to them, the upper part of the basement of the 30 m terrace consists of greenish-grey sands of various grain sizes below a peat horizon with up to 15 cm thick wood remains. This wood was radiocarbon dated of > 30 ka BP (PI-2014). The described sand horizon is comparable with similar deposits west of Cape Svyatoy Nos, which were assigned to the Ebelyakhsky Suite (Nikolsky et al. 1999). The Ebelyakhsky Suite was dated paleomagnetically with more than 700 ka (Nikolaev et al. 2000). The main part of the early Pleistocene sands was probably eroded during cryoplanation processes.

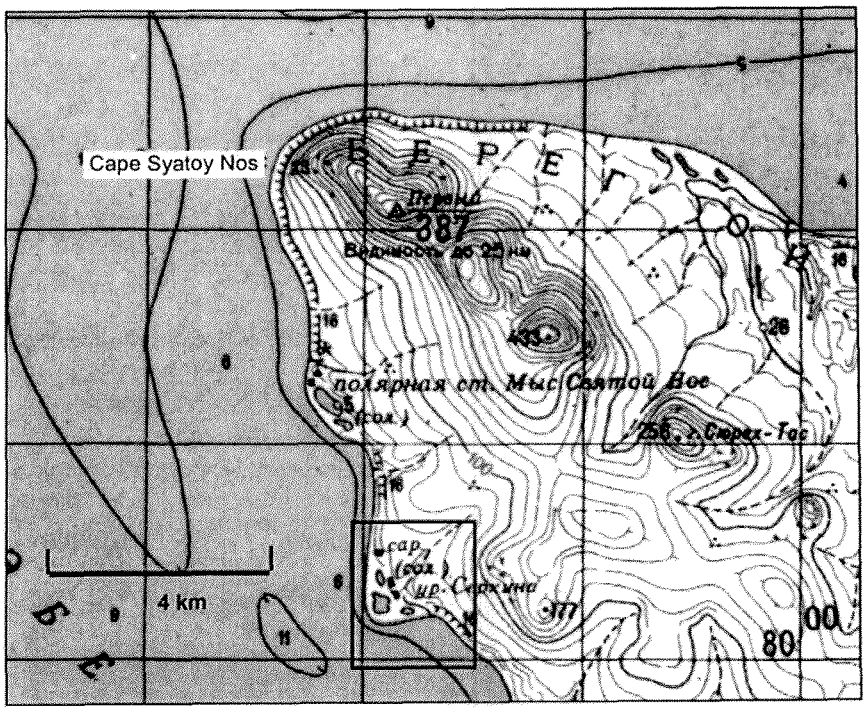

Figure 5.2.9-1: Study area south of Cape Svyatoy Nos

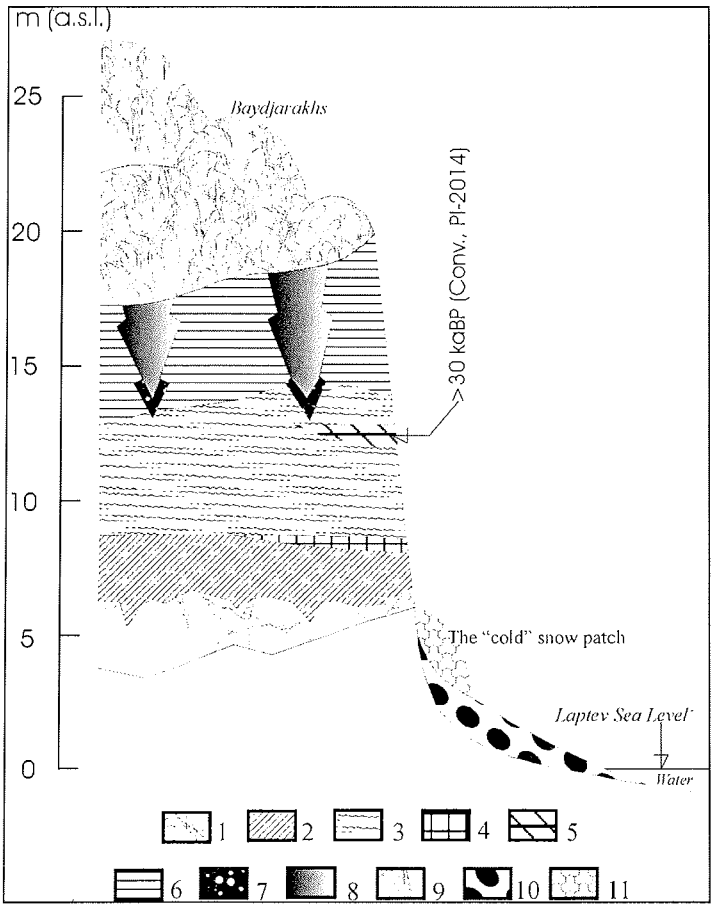

Figure 5.2.9-2: Schematic profile of the Ice Complex fragment as part of the 30 m cryoplanation terrace near Cape Svyatoy Nos, Compilation of former Russian expeditions by V.V. Kunitsky.

1- Strongly weathered light grey granite, frozen, with ice filled cracks;
2 – Dark-grey loam;
3 – Dark-brown peat, grass, moss shrub remains (up to 15 cm Ø);
4 – Greenish-grey sand, cross-bedded, with gravel interlayers;
5 – Brown alluvial peat, small plant detritus with shrub fragments;
6 – Ice Complex deposits, brown silty sand with gravel inclusions and ice belts;
7 – Ice wedge with sediment veins ("Polosatic")
8 – Ice wedge, grey
9 – Surface with thermokarst mounds;
10 - Large pebbles on the beach (up to 3 m Ø)
11 - Snow patch

Table 5.2.9-1: Radiocarbon age determination of *Mammuthus primigenius* found east of the Svyatoy Nos Cape

Lab.No.	Age (a BP)	Bone	Reference
GIN-9555	>16000	bone	Nikolaev et al., 2000
GIN-9556	17100±300	bone	Nikolaev et al., 2000
GIN-9045	25200±300	bone,	Nikolsky et al., 1999
GIN-9563	26100±600	bone	Nikolaev et al., 2000
GIN-9559	>36900	bone	Nikolaev et al., 2000
GIN-9566	40900±1200	bone	Nikolaev et al., 2000
GIN-9552	42900±900	bone	Nikolaev et al., 2000
GIN-9568	43100±1000	bone	Nikolaev et al., 2000
GIN-9557	47400±1200	tusk ?	Nikolaev et al., 2000
GIN-9044	48800±1400	tooth?	Nikolsky et al., 1999

Unfortunately, only a stop of two hours was possible in the evening of August, 22 because of bad weather conditions. Therefore, no detailed coastal section but only some landscape observations and sampling of small reconnaissance profiles were made.

The TSP was placed at the stony slope of the coastal cliff 8 m a.s.l.. The cliff was about 10 m high, and cut by V-shaped thermo-erosional valleys. A snow patch was preserved at the bottom of the southern slope of one of the valleys. Three samples were taken from this snow patch for stable isotope analyses. The surface on top of the cliff was covered by cryoturbated soil with frost boils containing a lot of rock debris. Boulders of sub-rounded weathered granite and dolerite (up to 1 m in diameter) occur at this surface as well as in the valley bottom and on the beach (samples Svy 4-1 to 4-4). Similar boulders also occur further north near the abandoned polar station. They were shaped by sea ice and seawater but not by glacial processes (Kunitsky & Grigoriev 2000). The visible material of the coastal cliff mostly consists of reworked material from higher levels. About 350 m south of the landing point bedded sediments were found containing large remains of shrubs. They were interpreted as stillwater deposits. The lowest horizon of the studied profile was a 5 m thick laminated silty fine-sand (aleurite) at 2.5 m a.s.l.. Laminas were 0.1-4 cm thick and consisted of light-grey silty sand with orange coloured clay lenses alternating with plant detritus (sample Svy 1-1). This horizon was spotted with iron oxide. The next horizon was a 5 m thick, bedded alluvial peat (sample Svy 1-2), containing a shrub root horizon in the lower part (sample Svy 1-3) covered by a 0.5 m thick layer of grey silty fine sand. An additional wood horizon with shrub remains was found 200 m to the north in 15 m a.s.l. (sample Svy 1-4). The wood remains of both horizons showed bluish-grey thin Vivianite crusts on the surface. We collected only tree bones on the shore during the two hours stop.

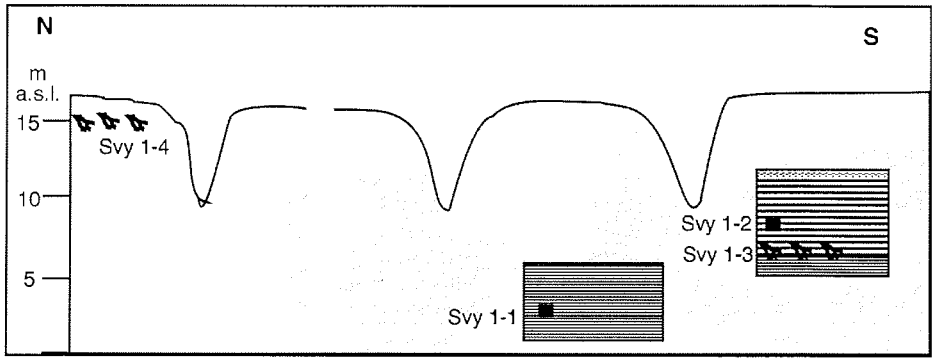

Figure 5.2.9-3: Scheme of the only studied profile at the coastal section 5 km south of Svyatoy Nos polar station; laminated deposits with shrub remains.

5.2.10 Oyogos Yar coast (30.08.)

The coast of Oyogos Yar was already the study object of some Russian scientist during the last decades. Two main units characterize the coastal section. They are separated by a thermo-terrace (Figures 5.2.10-1 and 10-3). The stratigraphical classification of the lower unit is still under discussion. Opinions vary between middle to upper Pleistocene (Kayalaynen & Kulakov 1966, Ivanov 1972, Vereshagin 1982). This dark bluish-grey, bedded deposit with shells is clearly a subaquatic formation and was named Khomsky-Suite (Vereshagin1982). The Khomsky-Suite is exposed in the Yana-Indigirka Lowland up to 100 m a.s.l. and above (Kayalaynen & Kulakov 1966) and contains freshwater diatoms as well as saline forms.

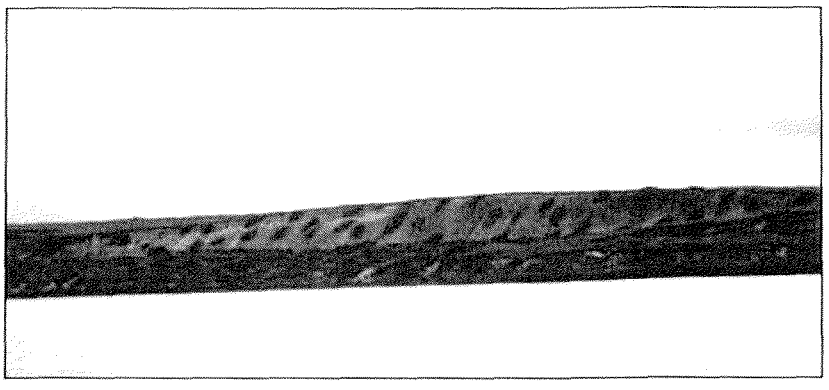

Figure 5.2.10-1: The studied coastal cliff of Oyogos Yar; a thermo-terrace devides the Ice Complex horizon from the underlaying subaquatic deposits

The upper unit with large ice wedges is named Oyogossky-Suite and presents the Ice Complex in this region. Ice Complex deposits cover the less inclined step-like surface of the Yana-Indigirka Lowland and were formerly interpreted as sequences of interlocked lake terraces (Kayalaynen & Kulakov 1966). The step-like distribution of this horizon is supposed to be connected with steps of cryoplanation terraces (Kunitsky 1996). The outcrops of Oyogos Yar were also studied by Gravis (1978). He found shrub remains below the Ice Complex, which were dated > 42 ka BP, as well as shrub remains and peat of Holocene age (about 3-8 ka BP) at the top of the Ice Complex. Gravis (1978) and also Konishev and Kolesnikov (1981) supposed that the Oyogossky-Suite was formed within a thermokarst depression (alas). But Tomirdiaro (1970, 1980) assumed an eolian origin of these deposits. Some age determinations from Oyogos Yar sections dated by other authors are summarized in table 5.2.10-1. In general, the situation is comparable with that of the Laptev Strait coast on Bol'shoy Lyakhovsky Island.

Table 5.2.10-1: Radiocarbon age determinations of the Oyogos Yar Section

sample Index	Location	Depth [m]	Material	Radiocarbon age [y BP]	Reference
IM-235				> 42 000	Gravis 1978
IM-233	Cliff	6	Peat	33720±1500	Gravis, 1978
IM 230			Peat	5750±230	Gravis 1978
IM 229			Peat	3890±250	Gravis 1978
NUTA3521	Cliff	5		22 940±390	Nagaoka et al 1995
OG 34	Ice Complex top	1	Methane	3539±87	Moriizumi et al 1995
MAG-544	Mouth of Rebrov River	5	Peat	34200±2300	Kaplina & Lozhkin, 1985
MAG-543	- " -	8.5	Peat	37700±2200	Kaplina & Lozhkin, 1985
MAG-545	- " -	17	Peat	> 41 000	Kaplina & Lozhkin, 1985

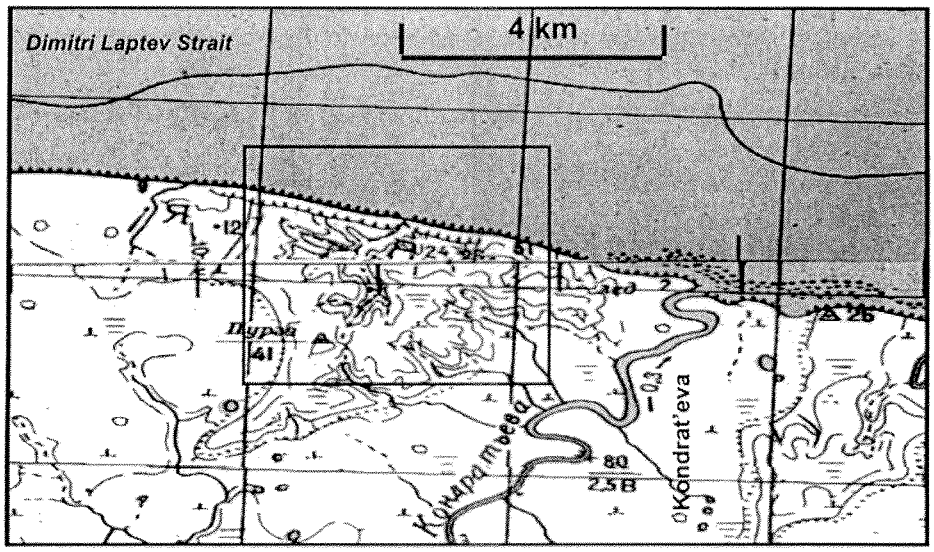

Figure 5.2.10-2: Study area of Oyogos Yar coast west of the Kondrate'eva River mouth

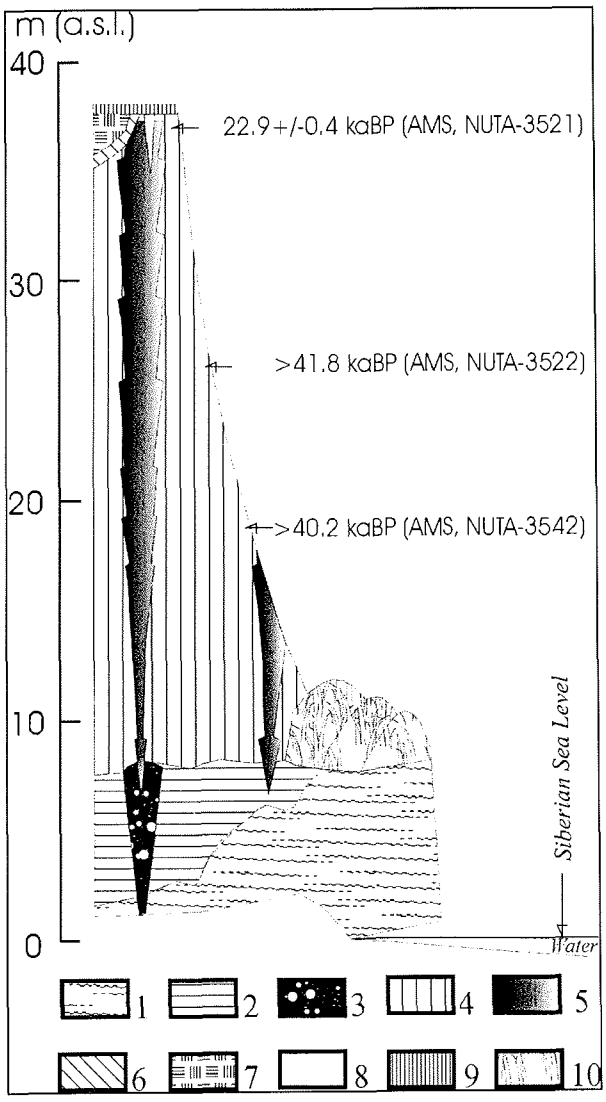

Figure 5.2.10-3:
Schematic profile of the Oyogos Yar coast west of the Kondrateva River:

1 – Dark-blue silt, bedded with shells, slanting ice lenses;

2 – Brownish-grey silty fine sand, bedded, dense, with shrub fragments and grass roots, diagonal cryostructures;

3 – Ice wedge with sediment veins

4 – Dark-grey loess-like silty fine sand (aleurite) with peat nests and ice belts, Ice Complex deposit;

5 – Ice wedge of the Ice Complex horizon;

6 - Dark-grey aleurite, involution layer, with peat, shrub remains, bedded and reticulated cryostructure;

7 – Brown moss peat;

8 – Ice wedge, white, less

In order to get an overview of the stratigraphical, cryolithological and geomorphological situation, profiles were studied 2 km along the cliff of Oyogos Yar (Figure 5.2.10-4) as well as some outcrops in the hinterland. The coast is dominated by Ice Complex elevations (20-30 m a.s.l.) interrupted by thermokarst valleys and thermokarst depressions.

The TSP station was placed at the slope of the Ice Complex elevation (Yedoma) in 8 to 9 m a.s.l.. The surface was completely covered by alternating dry and wet grass vegetation. In addition, a lot of *Salix* and mosses occurred there.

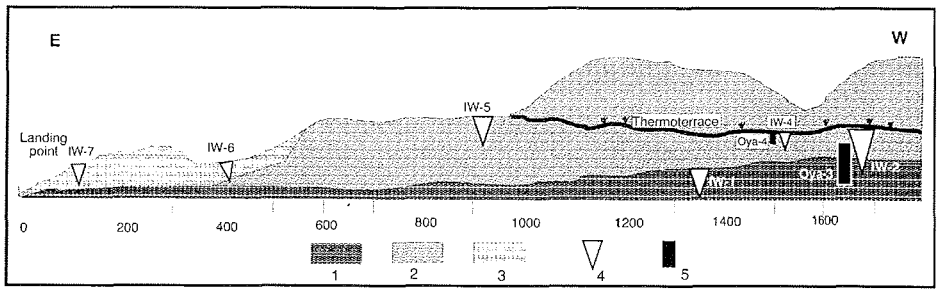

Figure 5.2.10-4: Schematic overview and study locations at the coast of Oyogos Yar; 1 – Subaquatic deposits, 2 – Ice Complex deposits; 3 – Alas deposits; **4** – Studied ice wedges; 5 – Studied sediment profiles.

In the lower part of the section near the beach, three profiles were studied. They involved possible lacustrine deposits, a buried sediment-rich ice wedge ("Polosatic) with rounded head, horizons with large ice wedge casts and shrub remains and the lower part of the Ice Complex with roots of large ice wedges. Such special buried ice wedges were also found in the lower level of the coastal section on Stolbovoy Island (chapter 5.2.2) and on Kotel'ny Island, south coast (chapter 5.2.5). The ice wedge (0.75 m wide) is incorporated in a well-bedded silty fine-sand (aleurite) with banded cryostructure (Figure 5.2.10-5).

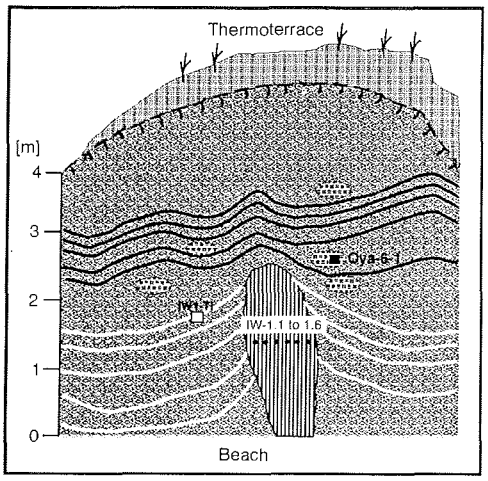

Figure 5.2.10-5: Buried ice wedge in the lowest horizon of Oyogos Yar covered by laminated peaty sand.

Six samples were taken from this ice wedge (OYA-IW-1) and one from the ice belt near the ice wedge in a height of about 1.5 m a.s.l. The width of the ice wedge is about 0,7-0,8 m. The visible height is about 2,5-3 m. The head of this ice wedge was thawed and buried under the yellow-grey aleurite with numerous peat nests and lenses. The ice wedge showed belts, shoulders and tracks of up-ward-squeeze of ice wedge, which are typically for syngenetic formation. The Ice is dirty, turbid with vertical oriented striation. The ice crystals are very big and reach about 0.5-0.7 cm in diameter.

A second study site of the lower level was located some hundred metres further to the north (Figure 5.2.10-3) exposing deposits and ice wedges below the

thermo-terrace (Figure 5.2.10-6). Bluish-grey, clayish laminated lacustrine deposits with a net-like, broken cryostructure (gravimetric ice content 38-99 wt-%) contained a horizon of ice wedge casts. These ice wedge pseudomorphs are 1-2 m long and consist of grey, laminated clayish sand with peat nests and wood remains. They occur in distances of 10-20 m to each other. These probably lacustrine deposits are covered by a greyish-brown transition horizon of iron oxide colour (gravimetric ice content 48-57 wt-%). The overlying grey silty fine sand (aleurite) of the Ice Complex had a lens-like cryostructure (gravimetric ice content 37-50 wt-%) with ice bands. The lower part of an ice wedge of the Ice Complex penetrated downward into the lacustrine deposits. The ice wedge was about 1.2 m wide and consisted of yellowish ice, possibly due to a high amount of organic matter in the ice.

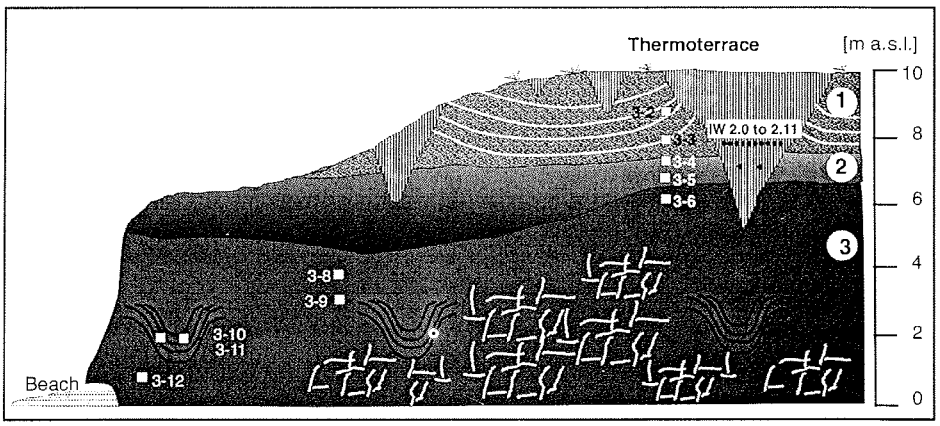

Figure 5.2.10-6: Studied profile Oya-3 and ice wedge OYA-IW-2 below the thermo terrace; 3 – Lacustrine deposits with ice wedge casts, 2 – Oxidic transition zone, Ice wedge of the Ice Complex penetrating lacustrine sediments.

The sampling for OYA-IW-2 was carried out in a height of about 7 m a.s.l. and in total, 12 samples were taken. The ice wedge is characterised by narrow ice veins of 0.5-2.5 mm, which may penetrate into each other, and also by low sediment content and very small gas bubbles < 1 mm leading to a milky appearance of this ice wedge. Small vertical ice veins, up to 4 cm wide and 0.8 m long occur on the left side of the ice wedge.

A high amount of shrub fragments was found in the upper part of the lacustrine horizon (sample Oya 3-13). Two additional samples were taken from the lower unit further to the west – at first from subaquatic deposits with shells (sample Oya-5-1) and secondly from alder shrub fragments (sample Oya-5-2).

Further ice wedges, belonging to the Ice Complex horizon were studied at the level below the edge of the thermoterrace (IW-4, IW-5). Ice wedge OYA-IW-4 was sampled (6 samples, in a distance of about 30 cm) in a height of about 35 m a.s.l. and a depth of 4 m below the cliff top edge. Ice wedge ice was dirty, turbid, and contained numerous air bubbles. Elementary ice veins were not

observed. The ice wedge OYA-IW-5 was about 5 m high and 3 m wide and was surrounded by very ice-rich brownish-grey silty sand with ice belts bound upward (in an angle of up to 80°) and peat inclusions. 15 samples were taken in a horizontal sampling transect (20 cm intervals) in a height of about 16 m a.s.l. (Figure 5.2.10-7A). This typical Ice Complex ice wedge is composed of yellowish slightly milky ice. Elementary ice veins are between 1-3 mm thick.

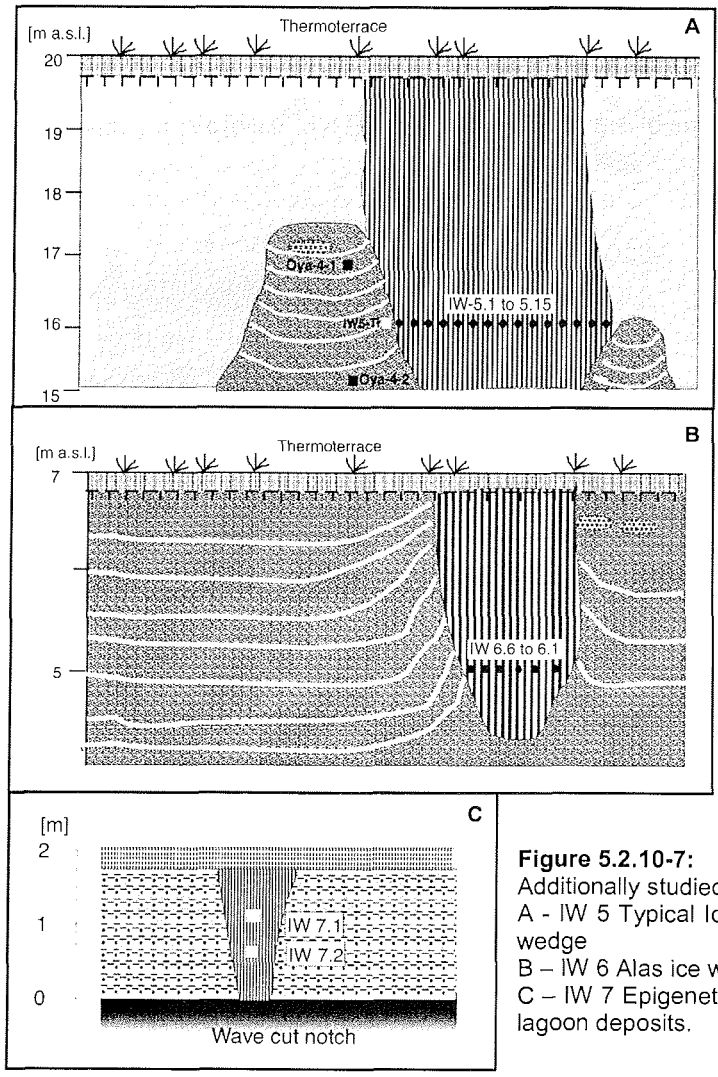

Figure 5.2.10-7:
Additionally studied Ice wedges
A - IW 5 Typical Ice Complex ice wedge
B – IW 6 Alas ice wedge
C – IW 7 Epigenetic ice wedge in lagoon deposits.

Two generations of ice wedges younger than the Ice Complex were observed at the Oyogos Yar coast. Six samples were taken in a height of 5 m a.s.l. of an ice wedge which was about 1.5 m wide, probably belonging to alas deposits (OYA-IW-6) (Figure 5.2.10-7B). These deposits consist of ice-rich brownish silty sand with peat inclusions and ice belts bound upward. The ice wedge consists of

yellowish to white, milky ice. A second ice wedge was sampled just above the wave-cut notch near the landing point in grey sediments (oxygen reducing conditions) with oxidised fissures of yellowish-brown colour and lens-like reticulate to laminated cryostructure. These sediments were possibly associated with lagoon deposits. The ice wedge OYA-IW-7 is 0.3 m wide and 1.2 m high and it is composed of grey to white milky ice. It is assumed to be epigenetic and of Holocene age (Figure 5.2.10-7C).

The landscape was studied about 1.5 km to the south as supplement to the general investigations on coastal sections. The surface rises up to 40-50 m a.s.l.. Larger and smaller thermokarst depressions occur in various levels. The various bottom levels of these depressions might reflect the altitude of former cryoplanation terraces. Additionally, U-shaped thermokarst valleys with flat, wet, and grass-covered bottom characterised the coastal hinterland. Such valleys are 50-60 m wide on the top and 10 m at the bottom. Brooks flowing at the valley bottom formed small cascades of about 2-3 m height in distances of 400 to 500 m. These cascades were possibly formed at the edges of a step-like bottom surface. Such barriers may also reflect the relief of former cryoplanation terraces, which is now covered by Ice Complex deposits.

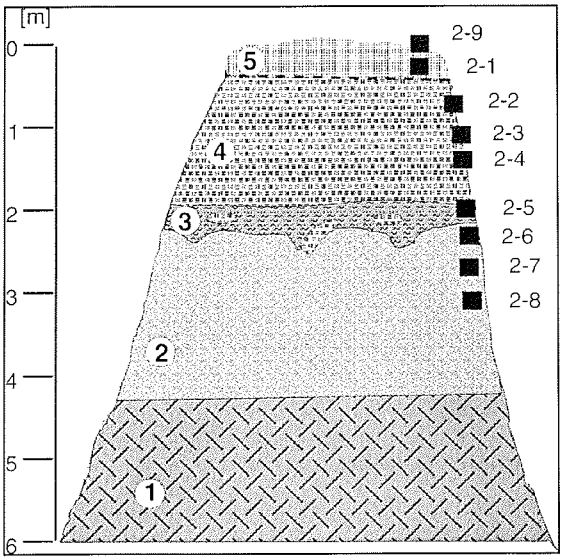

Figure 5.2.10-8:
Profile Oya-2; Thermokarst mound at the slope of a thermokarst valley about 1.5 km south of the coastal section;
1 – Talus
2 – Ice complex deposit, ice-rich silty fine sand (aleurite);
3 – Cryoturbated peaty paleosol;
4 – Moss peat, fresh, with twigs;
5 – Active layer:

A thermokarst mound at the steep slope of a thermokarst valley was exemplarily studied, as it was thought to be the highest Ice Complex level (Figure 5.2.10-8). This profile consists of frozen silty fine sand with twig fragments and coarse lens-like reticulated cryostructure (gravimetric ice content 54-118 wt-%). The Ice Complex horizon is covered by a cryoturbated peaty paleosol and an about 2 m thick, non-decomposed peat horizon with a lot of twigs. All thermokarst mounds at the valley slopes also had a peat cover.

An ice wedge of the highest Ice Complex level was studied 200 m to the north at the top of a small thermo-cirque (Figure 5.2.10-9). This ice wedge was

vertically striped, dense and contains small gas bubbles and only a few clastic inclusions. The wall of the thermo-cirque cuts the ice wedge at an angle of 10-20 ° and, therefore the ice wedge looks very broad. The ice wedge was covered by frozen slope material with banded and reticulated cryostructure. This horizon

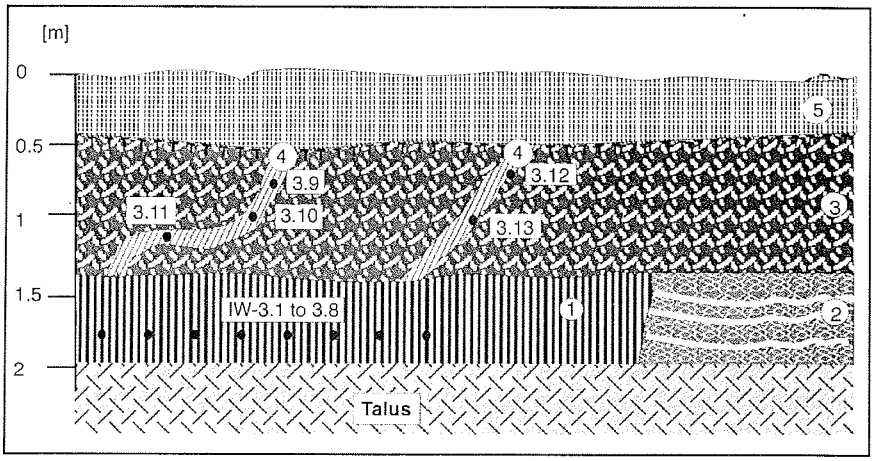

Figure 5.2.10-9: Ice wedge of the upper Ice Complex level exposed at a small thermo-erosional cirque about 1.3 km south of the coastal section;
1 – Old Ice wedge; 2 – Ice Complex deposits, buried by talus, 3 – Frozen slope deposits; 4 – Young disturbed ice wedges, 5 – Active layer.

contains additional small ice wedges, which were disturbed during solifluction processes. Both types of ice wedges were sampled but unfortunately the Ice Complex deposits were buried by talus material and sampling therefore was impossible.

Figure 5.2.10-10:
Small part of the collection of woolly mammoth found at the Oyogos Yar section

Apart from geomorphological, geocryological and sedimentological studies, which had been carried out the stop at Oyogos Yar was very useful for paleontological studies (Figure 5.2.10-10, Table 5.2.10-1). The paleontological collection from Oyogos Yar site is the most comprehensive. We collected 369 bones and their fragments. Unfortunately we worked on this outcrop one day only. Bones were collected from the 5 different types of location groups. 48 bones were found at the exposure itself. Among them one bone (group "a") – rib of woolly mammoth - was collected strictly *in situ*, from the coastal outcrop on

the altitude 1m from the water level. Nearby we also saw small pieces of several limb bones, which stuck still within frozen sediments. Probably they are part of one skeleton of *Mammuthus primigenius*. Two half of pelvis, left femur and left humerus already fell out from the cliff sediments and we had found they nearby. Concerning preservation and position of these bones, they probably belong to an individual. Large amount of bones (47) was found on the termoterrace of the exposure (location group "c"). The possible altitude range of their initial stratigraphical position could be estimated between the height of their occurrence (height of termoterrace) and the height of the upper cliff. On tundra surface were found 4 bones only (group "d" and "f"). One of them (NS-OgK-O430 - mammoth ulnare) is submitted to determination of radiocarbon age.

The largest group of bones – 317 samples was collected from the shore (group "e"), which is typical for permafrost regions in Arctic Siberia. All these bones divided into three subgroups. Two subgroups contain bones from the open shore (west and east part). The third subgroup (68 bones) was collected on the small part of shore near the small stream mouth. All large limb bones of *Mammuthus primigenius* were usually measured, photographed and finally cut off in pieces of 2 – 3 kg. These are samples of mammoth for the radiocarbon dating. We are planning to determine the radiocarbon age near 20 bones of different species on mammals from the Oyogos Yar at the Radiocarbon Laboratory of the Geological Institute, Russian Academy of Sciences. Taxonomic composition of the Oyogos Yar collection is the same to our collection from the New Siberian Islands and differs in the found of *Panthera spelaea* bone only (Tab. 5.2.10-2). The main dominants of both collections are woolly mammoth, horse, bison and reindeer. It is typical for all known Late Quaternary collections from the Arctic Siberia. But the percentage correlation is different for our two collections. In collection from the Oyogos Yar bones of *Mammuthus primigenius* dominate (39,8%), than *Bison priscus* (22,0%), *Equus caballus* (15,7%) *and Rangifer tarandus* (11,7%) follow (Figure 5.2.10-11).

Table 5.2.10-2: Preliminary list of mammal taxa of the Oyogos Yar collection.

Class MAMMALIA – mammals
- Order Proboscidea
  - *Mammuthus primigenius (Blum).* (woolly mammoth)
- Order Artiodactyla
  - Family Cervidae
    - *Rangifer tarandus (L.)* (reindeer)
  - Family Bovidae
    - *Ovibos moschatus Zimm.* (muskox)
    - *Bison priscus (Boj.)* (Pleistocene bison)
- Order Perissodactyla
  - Family Equidae
    - *Equus caballus L.* (horse)
- Order Carnivora
  - Family Felidae
    - *Panthera spelaea (Gold.)* (Pleistocene "lion")
- Order Lagomorpha
  - *Lepus sp.* (hare)

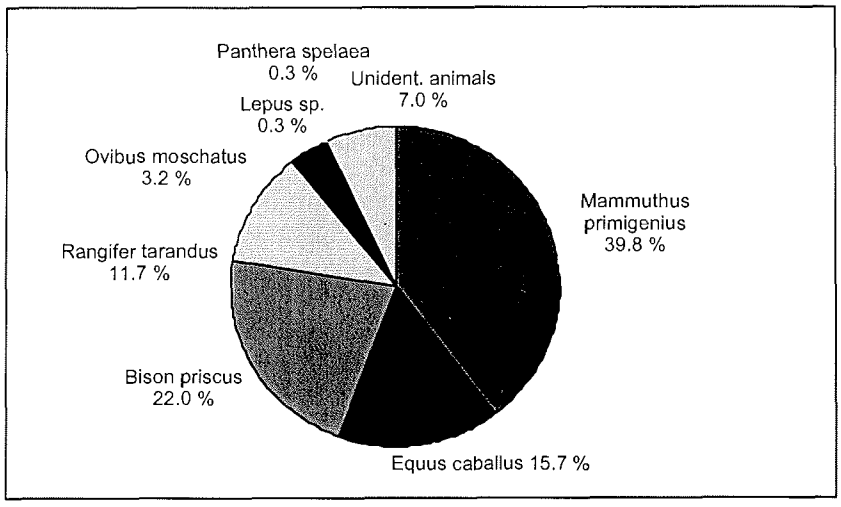

Figure 5.2.10-11: Composition of mammal bones collection from Oyogos Yar, 369 specimens.

5.2.11 Muostakh Island (02.09.)

The last stop was made on Muostakh Island during the return to Tiksi. This slender island of about 10 km length and less than 750 m width, is located 25 km north-east of the mainland and 15 km south-east of Bykovsky Peninsula. It presents the southeastern continuation of the Bykovsky Peninsula coast (Figure 5.2.11-1, 11-2). The island mainly consists of Ice Complex deposits, which are exposed at the east coast from sea level up to the island's surface at about 23 m a.s.l.

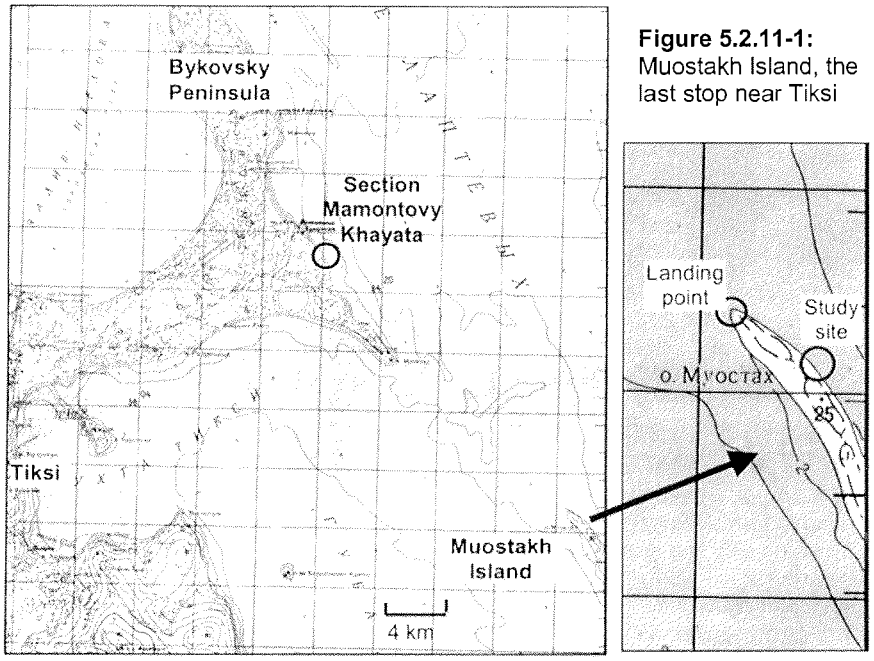

Figure 5.2.11-1: Muostakh Island, the last stop near Tiksi

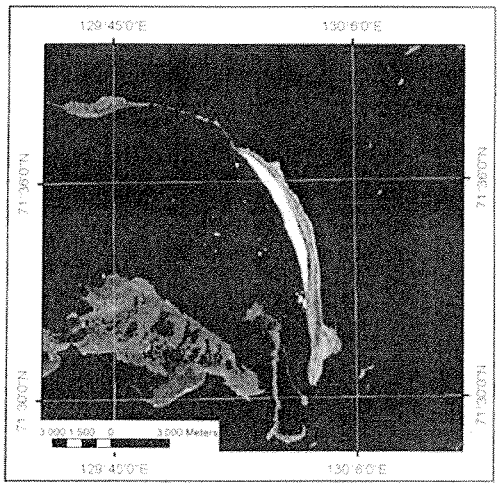

Figure 5.2.11-2: Cloudy Landsat-7 picture of Muostakh Island (August 1999)

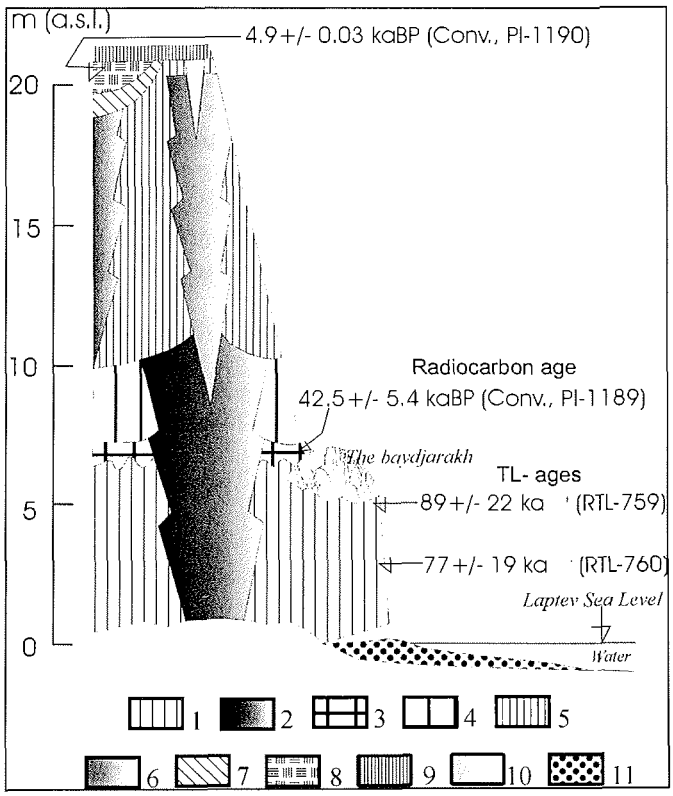

Figure 5.2.11-3: Columnar section of Muostakh Island, compiled by V.V. Kunitsky according to former Russian studies;
1 – Grey-blue silty fine sand laminated, ice banded;
2 – Grey dense ice wedge, single sediment veins, 3-4 m wide;
3 – Black peat, autochtonous
4 – Dark-grey, bedded silty fine sand with sandy interlayers and lenses,
5 – Black sand, gravels and debris, bedded cryostructure;
6 – Small (1-2 m), grey ice wedge;
7 – Dark-grey sandy loam, with sand lenses and shrub remains;
8 – Dark-brown, frozen moss peat;
9 - Dark-brown, thawed moss peat;
10 - White, small (0.5 m wide) ice wedge,
11 - Grey beach sand.

The columnar section of Muostakh Island is shown in Figure 5.2.11-3, as compilation of former Russian studies and datings. The aim of the study was to obtain samples of a large ice wedge sequence and permafrost sediment for comparison with the section Mamontovy Khayata at the Bykovsky Peninsula studied in detail before (Meyer et al. 2002, Schirrmeister et al. 2002, Siegert et al. 2002).

The TSP was placed at the black sandy beach near the landing point about 1 m a.s.l.. The active layer there was 1 m thick. There did not occur any vegetation at the beach. However the plain surface of the island (20-25 m a.s.l.) was dense

covered by moss, grass, lichen and single small shrubs. Ice wedge polygons were observed, indicating recent ice wedge formation. A study site was chosen on the east coast 160 m southeast of the landing point (Figure 5.2.11-1).

A large ice wedge was sampled by chain saw in order to gather ice samples, which were transported to Germany in the frozen state. Consequently, the ice crystallography, all gaseous, liquid and solid inclusions and their distribution in the ice as well as internal structures can be studied in detail in the ice laboratory at AWI Bremerhaven. Additionally, samples can be taken in very high resolution for all kinds of analyses, such as for stable isotopes, hydrochemistry, gas content etc.

The 4.5 m wide ice wedge was sampled in a height of 1 m a.s.l. above the wave-cut notch (Figure 5.2.11-4). 18 blocks of ice (up to 30 cm long and between 10 and 15 cm high) were cut. Altogether only 3 m (out of 4.5 m) were retrieved in a horizontal transect starting from the right side. Because of lack in time and due to technical problems with the chain saw 1.8 m from the left side could not be sampled.

The left side (samples Muo-01 to -04) was characterised by relatively white ice without clear internal structures, except a few vertical sediment stripes. The right side (samples Muo-05 to -11) was composed of rather typical Ice Complex ice with yellowish-grey tiger-striped ice with clear, transparent ice veins, which were relatively easy to recognise. Muo-12 and -13 were taken from the grey ice-rich silty sand in the left continuation of the sampling transect. These samples were taken for a detailed study on exchange processes (hydrochemical and stable isotopes) between the ice wedge and adjacent segregated ice, which were identified for ice wedges on the Bykovsky Peninsula (Meyer et al. 2002).

The Ice Complex deposits next to the studied ice wedge consist of ice-rich grey silty fine sand (gravimetric ice content 97-136 wt%) with small peat nests and thin grass roots. The lens-like reticulated cryostructure and ice belts are typical for most of the studied Ice Complex deposits. In addition, Ice Complex deposits were sampled in higher levels about 100 m to the south. Here above a thermoterrace peat horizons and sand-silty interbeddings occurred (Figure 5.2.11-3 and 11-4).

We collected only six bones from the shore of Muostakh Island (Appendix 5.2-3) and one bone (NS-Mst-O535) from the exposure about 3 - 6 m a.s.l..

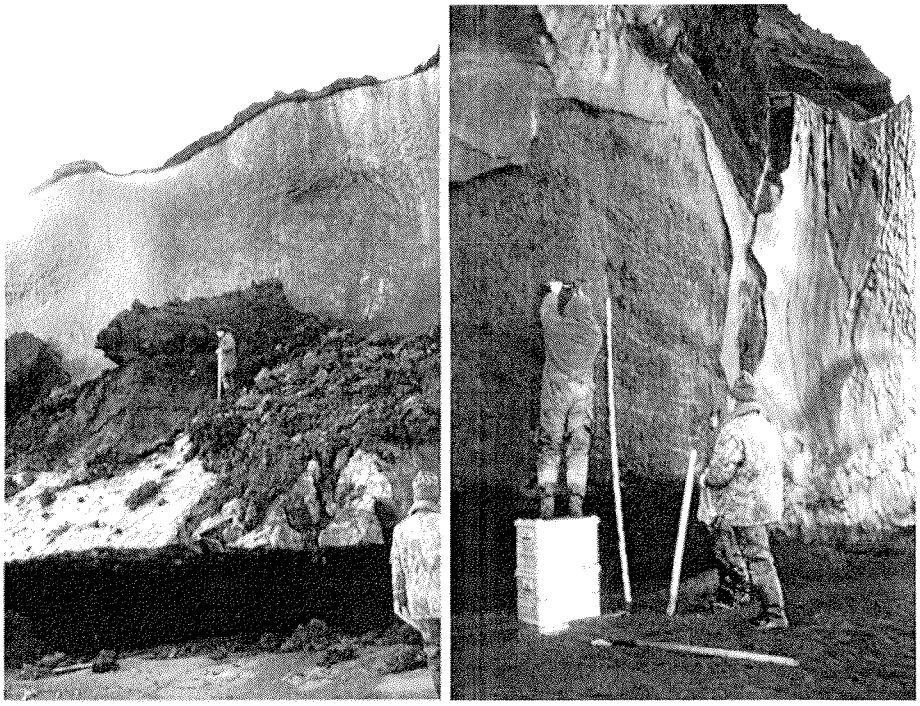

Figure 5.2.11-4: Sampling of Ice Complex profiles on Muostakh Island

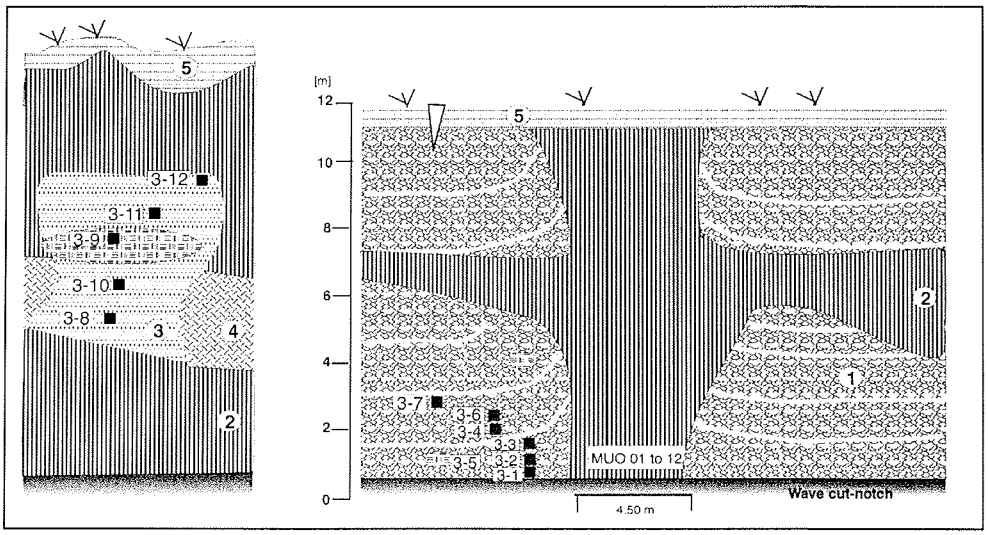

Figure 5.2.11-5: Schemes of sampled permafrost profiles on Muostakh Island
1 – Ice Complex deposits; 2 – Large Ice wedges; 3 – Sandy bedded horizon; 4 – Debris; 5 – Active layer; 6 – Peat lens

5.2.12 Paleontological study on New Siberian Islands

Paleontological studies of Pleistocene and Holocene deposits on the New Siberian Islands included the collection and research of large fossil mammal bones. All participants of the expedition helped to collect and work on bone material. During our stay on the New Siberian Islands we collected 176 bones. As in previous expeditions (1998, 1999, 2000) all of the bones and fragments found were registered in order to obtain fairy most complete statistics of the species composition.

The bones were collected from 7 different places and 5 islands (Stolbovoy, Kotel'ny, Bel'kovsky, New Siberia, Maly Lyakhovsky). Unfortunately, we had only a very short time, not more than one day for each locality. The largest collection on New Siberian Islands is from Maly Lyakhovsky Island (near Cape Vaygach) – 54 samples, and followed by that Kotel'ny Island (Cape Anisy and Khomurgunakh River mouth).

Bones were collected from 6 different types of localities. An unexpected amount of material - 31 bones and fragments - were found *in situ* (group "a"). All these bones are from Kotel'ny Island (Cape Anisy). They belong to mammoth's and horse's skeletons. On Cape Anisy 6 bones from one single mammoth skeleton (bones from forelegs and hind legs) were found *in situ* (samples from NS-Kan-O13-a to O13-f). At the same place several vertebrae and some bones from legs were also found *in situ*.

The second group "b" includes only 5 bones found within the exposures and the altitude of their occurrence was instrumentally determined as well as the level of minimum height of the original position of these bones. Group "c" – 15 samples – includes also bones found at the exposure, but in talus debris. For these bones it is not possible to reconstruct their original position in the exposure.

The most comprehensive material was collected within thawed sediments in different outcrops and valleys. It is group "d" which contains 86 bones. 26 bones (group "e") were collected on the shore and 13 bones were collected in various areas of islands, mainly in tundra.

Table 5.2.12-1: Preliminary list of mammal taxa identified in the New Siberians collection.

Class MAMMALIA – mammals
- Order Perissodactyla
  - Family Equidae
    - *Equus caballus L.* (horse)
- Order Proboscidea
  - *Mammuthus primigenius (Blum).* (woolly mammoth)
- Order Artiodactyla
  - Family Cervidae
    - *Rangifer tarandus (L.)* (reindeer)
  - Family Bovidae
    - *Ovibos moschatus Zimm.* (muskox)
    - *Bison priscus (Boj.)* (Pleistocene bison)
- Order Lagomorpha
  - *Lepus sp.* (hare)

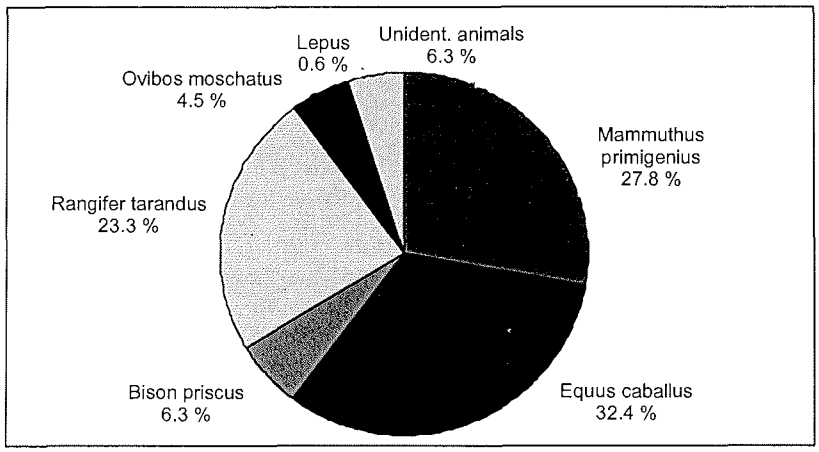

Figure 5.2.12-1: Composition of mammal bones collection from New Siberian Islands, 176 specimens.

Figure 5.2.12-2: Mammoth humerus *(in situ)* in the high Arctic tundra near Cape Anisy (Kotel'ny Island)

5.2.13 Results and Conclusions

The studies made during our three week's expedition have shown the large potential for further geocryological, paleo-ecological and geomorphological research on the New Siberian Islands and the neighbouring coasts of the mainland. Some general remarks and results of our fieldwork should be concluded in short:

Landscapes concerning to three different vegetation zones were observed: Subarctic tundra (Muostakh Island, Stolbovoy Island, Oyogos Yar coast), Arctic tundra (Bel'kovsky Island, Kotel'ny Island, Maly Lyakhovsky Island), Arctic desert (Bunge-Land, Novaya Sibir Island).

Repeatedly step-like cryoplanation terraces were observed, especially close to basement elevations. Snow patches were often situated at the terrace edges. Their occurrence supports the important role may play nival processes during relief formation, already discussed by Kunitzky et al. (2002). The lowest terraces in general consist of Ice Complex deposits. This ice-rich permafrost formation is widely distributed in the coastal regions of the New Siberian Islands and the neighbouring coasts. U-shaped thermo-erosional valleys with flat, grass-covered bottoms always cut the terrace surface. In addition, thermokarst depressions occur if the surface inclination is very low.

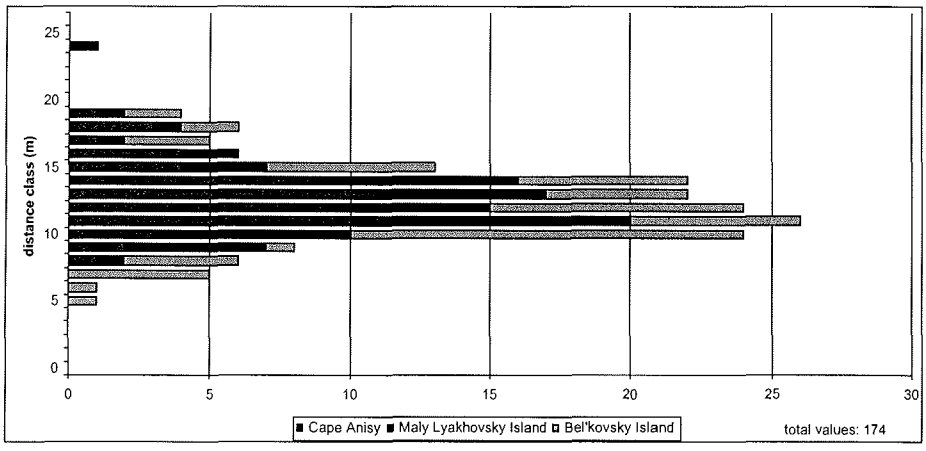

Figure 5.2.13-1: Frequency of distance classes (classes = 1, 2, 3, 4 ... 24, 25 m) for central tops of thermokarst mounds: the values originate from three denudated Ice Complex localities on New Siberian Islands; Most distances from top to top are between 10-15 m, the mean is situated at 12.2 m

Thermokarst mounds at the slopes of thermokarst depressions and valleys reflect the former ice wedge polygon systems. They had various shapes (flat, broad, peaky). Distances of the thermokarst mounds, representing the distances of former polygonal centres, were measured from their centre top to the neighbouring mounds. They mostly vary in a narrow range of 10-15 m, which seems to be typical for former ice-rich, silty to sandy deposits like the Ice Complex in NE Siberia (Figure 5.2.13-1).

Ground-truth activities are an integral part of the analysis of remote sensing data. Until now we collected ground data for calibration from geomorphological, geological, sedimentological and cryological fieldwork. Further, vegetation investigations were done and soil moisture as well soil temperature data were collected for this purpose. For future remote sensing studies it would be most desirable, to employ a field spectrometer. Such a field spectrometer should have a spectral range from 300-2500 nm wavelength, comparable to the Landsat-7 spectral range. This will help to characterise individual surface covers. Such spectra can be compared directly with multi-spectral satellite data in a much more accurate way. Especially for the classification of Landsat-7 multi-spectral images it is favourable to collect on-site reflectance spectra for individual vegetation components, bare surfaces or periglacial structures, hence such data for typical periglacial landscapes are very rare in spectral libraries. A field spectrometer is not equally replaceable with a laboratory spectrometer for serious reasons:

- In-situ atmospheric conditions and natural illumination are different from lab conditions
- A lot of material changes from being sampled until reaching the lab (e.g. thawing of ground ice, drying out of soils, wilting of vegetation, etc.).

Besides late Pleistocene Ice Complex deposits and Holocene thermokarst formation, subaquatic (marine and/or lacustrine) and glacio-marine deposits were found at the coast of Novaya Sibir Island and Oyogos Yar. These horizons perhaps point to the early and middle Pleistocene history of this region. Old buried ice wedges of a special conus-like shape with rounded heads were studied in three different sites. They are traces of an older stage of permafrost formation and are possibly linked with melting processes after ice wedge growth. Together with such ice wedges, a so-called cryogenic eluvium occurs. It consists of coarse-grained debris and yellowish loam and seems to be material of a reworked weathering crust.

Bunge-Land is a completely different formed landscape. Its origin is not associated with periglacial permafrost conditions. The area of the high terrace of Bunge-Land does in fact seem to be of terrigeneous and not of marine origin. Thermokarst phenomena indicate the existence of ice-rich permafrost in this location. For future studies on Bunge-Land, tracked vehicles and / or helicopters and drilling equipment are necessary because of the broad flat shore, the remoteness of interesting investigation sites from the coast and the absence of relief exposures.

The best study conditions were found at the coasts of Stolbovoy Island, Bel'kovsky Island, at the south coast of Kotel'ny Island (Khomurgannakh River mouth), at the southwest coast of Novaya Sibir Island (location Hedenshtrom) and at the Oyogos Yar coast. This concerns the excellent outcrop conditions as well as the occurrence of driftwood (heating material), freshwater and protected places for field camps. For future expeditions at least 2-3 weeks are necessary for detailed stratigraphical studies.

In total, 395 samples of ice, surface water and precipitation were taken during the expedition to the New Siberian Islands (Appendix 5.2-2), among them 30 ice wedges of different generations were sampled (see Table 5.2.13-1).

Table 5.2.13-1: Total number of samples and ice wedges of every location visited during the expedition as well as the occurrence of snow patches and recent ice wedges. A rough estimate of the ice wedge stratigraphy is given in the right column of the table (R= recent ice wedges, H= Holocene ice wedges, I= Ice Complex ice wedges, O= ice wedges older than the Ice Complex).

Location	No. (ice wedges)	No. (samples)	Recent ice wedges	Snow	Ice wedge stratigraphy
Stolbovoy Island	5	48	X	X	O, I, H, R
Bel'kovsky Island	6	63	X	-	O, I, H, R
Kotel'ny Island - Cape Anisy	1	10	-	X	?
Kotelny Island - Khomurgannakh R.	3	36	-	-	O, I
Bunge-Land. Low terrace	-	3	-	-	?
Bunge-Land, High terrace	-	12	X	-	?, R
Novaya Sibir Island - Derevyannye Gory	-	14	-	X	?
Novaya Sibir Island Location Hedenstrom	4	52	-	-	I, H
Maly Lyakhovsky Island	2	18	-	X	I?
Oyogos Yar coast	7	72	X?	-	O, I, H, R?
Cape Svyatoy Nos	-	14	-	X	?
Muostakh Island	1	11	-	-	I, H
Bykovsky Peninsula	1	42	-	-	I
Total	30	395			

Additionally, 210 sediment samples (Appendix 5.2-1) and 556 mammal fossil remains were collected (Appendix 5.2-3).

New study ideas are:

- Obtaining regional climate information by studying ice wedges in a great number of places as well as in extended areas,

- Study of connections the between geological basement construction, surface relief and the distribution of Ice Complex deposit and thermokarst formation;

- Comparison of coastal profiles along the Dimitri Laptev Strait (Bol'shoy Lyakhovsky Island, Oyogossky Yar, Svyatoy Nos area) in order to reconstruct Eemian and Pre-Eemian conditions,

- Study of marine deposits on Novaya Sibir Island and Faddeyevsky Island to estimate Quaternary sea level variations in the region;

- Facies analysis of Bunge-Land area (marine, glacigene, periglacial ?).

5.2.14 Appendices

Appendix 5.2-1. List of sediment samples collected on the New Siberian Islands.

No.	Sample	Sample description		Position			Depth below surface [m]	Ice content, abs./grav. [wt %]	Remarks	Date	Ice/water samples
		Sedimentology	Cryolithology	N	E	Height. a.s.l. [m]					
	East coast of Stolbovoy Island			**74°**	**136°**						
1	Sto-0-1	Silty fine sand	Ice rich, broken cryotexture				0.3	37.4/59.6	Below an Holocene ice wedge	15.08.	STO-IW-4 STO-95/01
2	Sto-1-1	Silty fine sand, small roots	Active layer, unfrozen	03.598	04.798	27	0.25		Recent cryosoil	15.08.	Sto-IW-1
3	Sto-1-2	Silty fine sand	Active layer trasition zone			27	0.5		Reducing horizon		
4	Sto-1-3	Silty fine sand	Few ice, massive texture			27	0.8	38.0/61.4	With small grass roots		
5	Sto-1-4	Silty fine sand	Few ice, massive texture			27	1.3	28.8/38.6	With small grass roots		
6	Sto-1-5	Silty fine sand	Few ice, massive texture			27	1.8	34.0/51.6	With small grass roots		
7	Sto-1-6	Grass roots				27	1	-	AMS-dating		
8	Sto-2-1	Silty fine sand	Few ice, massive texture	03.598	04.798	10		34.3/52.2		15.08.	STO-IW-5
9	Sto-2-2	Silty fine sand	Few ice, massive texture	03.598	04.798	1		33.3/50.0		15.08.	STO-IW-3
10	Sto-2-3	Silty fine sand	Few ice, massive texture	03.598	04.798	3		37.4/59.7		15.08.	STO-IW-2
11	Sto-3-1	Silty fine sand, gray, with small peat inclusions	Small ice lenses	03.598	04.798	5		36.1/56.4	Thermokarst mound with large peat lense (145 m long, 1.5-2 m thick)	15.08.	
12	Sto-3-2	Silty peat				5.25		38.8/63,4			

Appendix 5.2-1. continuation.

No.	Sample	Sample description: Sedimentology	Sample description: Cryolithology	Position: N	Position: E	Position: Height. a.s.l. [m]	Depth below surface [m]	Ice content, abs/grav. [wt %]	Remarks	Date	Ice/water samples
13	Sto-3-3	Peat, brown, fresh				5.5		50.1/100.4			
14	Sto-3-4	Peat, brown, fresh	Transparent injection ice			5.75		49.6/98.3			
15	Sto-3-5	Peat, brown, fresh				6		63.0/170.1			
16	Sto-3-6	Peat, brown, fresh	Transparent injection ice			6.25		72.7/266,2			STO-3-6
17	Sto-3-7	Peat, brown, fresh				6.5		49.6/ 98,4			
18	Sto-3-8	Silty fine sand, grayish-brown, grass roots				6.75		36.1/56.5			
19	Sto-4-0	Peat		03.915	04.544	ca. 10	0.9		Top of a thermokarst mound	15.08.	
20	Sto-4-1	Peat		03.915	04.544	ca. 10	0.7				
21	Sto-4-2	Peat		03.915	04.544	ca. 10	0.5				
22	Sto-4-3	Peat		03.915	04.544	ca. 10	0.3				
23	Sto-5	Beach pebbles		03.915	04.544	0				15.08.	
	Kotel'nylsland, Kap Anisii			**76°**	**139°**						
24	Mya-1-1	Silty fine sand, cryoturbated soil, twigs	Fine lense like cryotextur	10.220	00.816		1.5	--	Thermokarst mound	16.08.	MYA-IW-1.1 to 1.3
25	Mya-1-2	Silty fine sand, twigs					1	--	With many bones		
26	Mya-1-3	Silty fine sand					0.5				
27	Mya-peat-1	Peat		Ca. 1km to North			0.2				ANS-96-1 to 2
28	Mya-peat-2	Peat					0.6				

Appendix 5.2-1. continuation.

No.	Sample	Sample description		Position			Depth below surface [m]	Ice content, abs/grav. [wt %]	Remarks	Date	Ice/water samples
		Sedimentology	Cryolithology	N	E	Height. a.s.l. [m]					
	South cape of Bel'kovsky Island			**75°**	**135°**						
29	Bel-1	Beach pebbles		21.949	35.337		0		Up to 0.2 cm in diameter	17.08.	
30	Bel-2-1	Silty fine sand, cryoturbated	Lens like, vertical streaks (1-3 cm)	21.961	35.247	12.3	2.7	40.6/68.4	Thermokarst mound	17.08.	
31	Bel-2-2	Silty fine sand	Fine lens like cryostructure			12.8	2.2	46.2/86.5			
32	Bel-2-3	Silty fine sand	Fine lens like reticulated, ice bands			13.2	1.8	46.7/87.6			
33	Bel-2-4	Silty fine sand, single grass roots	Lens like reticulated, ice bands			13.4	1.6	45.2/82.4			
34	Bel-2-5	Peat inclusion				13.7	1.3				
35	Bel-2-6	Silty fine sand, with peat inclusions				13.75	1.25				
36	Bel-2-7	Twigs inthe peat horizon				14.6	0.6		AMS-dating, peat horizon of the next thermokarst mound		
37	Bel-3-1	Silty fine sand, plant roots	Fine lenslike reticulated	21.953	35.620	3.7		29.3/41.4		17.08.	BEL-IW-
38	Bel-3-2	Silty fine sand, plant roots				4.2				17.08.	1.1 to
39	Bel-3-3	Silty fine sand, plant roots				4.6				17.08.	1.21

Appendix 5.2-1. continuation.

No.	Sample	Sample description		Position			Depth below surface [m]	Ice content, abs/grav. [wt %]	Remarks	Date	Ice/water samples
		Sedimentology	Cryolithology	N	E	Height. a.s.l. [m]					
40	Bel-4-1	Silty fine sand, small grass roots	Fine lenslike reticulated	21.950	35.391	2.5				17.08.	BEL-W-2.1 to 2.4
41	Bel-AA-1	Recent surface		22.012	35.275		0-0.10		Thermokarst mound, pollen analyses	17.08.	
42	Bel-AA-2	Recent surface					0-0.10		Thermo-erosional valley		
43	Bel-5-1	Silty fine sand	Active layer, unfrozen	21.985	34.432		0.2			17.08.	BEL-IW-3.1 to 3.12
44	Bel-5-2	Silty fine sand	Transition zone frozen				0.6				
45	Bel-5-3	Silty fine sand					0.9				
46	Bel-5-4	Silty fine sand					1.3				
47	Bel-5-5	Silty fine sand					1.6				
48	Bel-5-6	Recent surface					0-0.05				
49	Bel-6	Gravels		22.005	34.160		0		Brock bed of a thermo-erosional valley	17.08.	
50	Bel-7-1	Silty clay, gray-blue	Fine laminated cryostructure	21.995	34.275	1			Lake deposit, ice wedge cast	17.08.	
51	Bel-7-2	Interbedding				1.8					
52	Bel-7-3	Of silt, sand				2.5					
53	Bel-7-4	And organic				3					
54	Bel-7-5	Detritus lamines				3.5					
55	Bel-7-6					3.8					

Appendix 5.2-1. continuation.

No.	Sample	Sample description: Sedimentology	Sample description: Cryolithology	Position: N	Position: E	Position: Height. a.s.l. [m]	Depth below surface [m]	Ice content, abs/grav. [wt %]	Remarks	Date	Ice/water samples
56	Bel-8-1	Shrub fragments, peat, sand		50 m		1.2			Ice wedge cast	17.08.	
57	Bel-8-2 Bel-8a	Allochton moss peat with twigs, weakly decomposed		West of		2			Ice wedge cast		
58	Bel-8b	Interbedding of organic and fine sand lamines		Bel-6		2.1					
59	Bel-8-3 Bel-8c	Silty fine sand with shells				2.2-2.3			Lake deposits		
60	Bel-8-4	Silty fine sand with shells				2.7-2.8			Lake deposits		
61	Bel-8d	Fine laminated fine sand				3			Lake deposits		
		Kotel'ny Island Southwest coast		**74°**	**138°**						
62	Kys-1	Beach boulder		43.991	27.229	1	0			18.08.	
63	Kys-2-1	Sandy silt, gray, single non subrounded gravels	Ice band, coarse lens like reticulated cryostructure	44.003	27.071	1.6		48.4/93.8	Thermokarst mound at the beach	18.08.	KYS-IW-2.1 to 2.6
64	Kys-2-2	Coarse-grained sandy gravels	Ice bands			2.1		33.7/50.8			
65	Kys-2-3	Coarse-grained sandy gravels	Ice bands, fine lens-like cryostructure			2.35		39.2/64.6			
66	Kys-2-4	Silty sand, small roots	Fine lenslike cryostructure			2.7		46.5/87.0			

Appendix 5.2-1. continuation.

No.	Sample	Sample description		Position			Depth below surface [m]	Ice content, abs/grav. [wt %]	Remarks	Date	Ice/water samples
		Sedimentology	Cryolithology	N	E	Height. a.s.l. [m]					
67	Kys-2-5	Silty fine sand, cryoturebated paleosol	Few ice			3		49.5/97.8			
68	Kys-2-6	Silty fine sandwith peat inclusions (3-7 cm)	Coarse lenslike reticulated			4		60.8/155			
69	Kys-2-7	Selcted gravels				1.75-2.4					
70	Kys-2-8	Yelloish sandy gravel, subrounded	Ice lenses			1.5		28.4/39.7	"cryogenic alluvium", weathered material		
71	Kys-2-9	Silty fine sand	Ice bands (0.5 mm), broken lenslike cryostructure	44.003	27.071	ca. 7.3		33.6/50.5	Themokarst mound about 8 m above the beach	18.08.	KYS-IW-1.1 to 1.18
72	Kys-2-10	Silty fine sand, small grass roots	Ice bands, broken lenslike cryostructure			ca. 8.4		45.0/81.8			
73	Kys-2-11	Silty fine sand, brownish	Near the ice wedge			ca. 8.1		38.0/61.2			
74	Kys-3	Beach material				ca. 1	0		Shells, sponges	18.08.	
75	Kys-AA	Surface material		44.321	24.200	ca. 3.5	0-0.05		Thermokarst depression, pollen analyses	18.08.	

Appendix 5.2-1. continuation.

No.	Sample	Sample description		Position			Depth below surface [m]	Ice content, abs/grav. [wt %]	Remarks	Date	Ice/water samples
		Sedimentology	Cryolithology	N	E	Height. a.s.l. [m]					
	Bunge Land upper terrace			74°	142°						
76	Bun-1	Recent lake deposit		52.050	09.703		0-0.05		Small thermokarst lake, 10 m from the bank, 0.4 m water depth	19.08.	Surface water ?
77	Bun-2	Recent lake deposit		52.357	09.470		0-0.05		Large thermokarst lake, 7m from the bank, 0.2 m water depth	19.08.	
78	Bun-3-1 AA	Fine sand		52.163	09.651		0		Surface of the valley bottom, pollen analyses	19.08.	
79	Bun-3-2 AA	Fine sand					0		Surface of the valley rim, pollen analyses		
80	Bun-4-1	Interbedding of fine sand and black organic-rich laminae		52.163	09.651		3	18.3/22.3	Section in the step valley rim	19.08.	
81	Bun-4-2	See above					2.70-2.80	-	Sand layers 2-30 mm thick		
82	Bun-4-3	See above					2.40-2.30	25.3/33.9	Organic-rich layers 2-6 mm thick		
83	Bun-4-4	Sand, organic rich					1.80-1.90	15.9/18.9			
84	Bun-4-5	Fine sand, oxiding, cryoturbated					1.50-1.60	15.1/17.8	Paleosol		
85	Bun-4-6	Fine sand					0.80-0.90				
86	Bun-4-7	Fine sand					0.30-0.40				

Appendix 5.2-1. continuation.

No.	Sample	Sample description		Position			Depth below surface [m]	Ice content, abs/grav. [wt %]	Remarks	Date	Ice/water samples
		Sedimentology	Cryolithology	N	E	Height. a..s.l. [m]					
87	Bun-5-1	Fine sand		52.163	09.651		0.50-0.60		Valley rim	19.08.	
88	Bun-5-2	Cryoturbated soil		52.163	09.651		0.20-0.30				
89	Bun-5-3	Fine sand		52.163	09.651		0.10-0.20				
90	Bun-5-AA	Surface sample		52.163	09.651		0-0.05		Pollen analyses		
91	Bun-6	Fine sand, middle sand, gravels		52.458	07.920		0		Collected from the surface		
92	Bunge-1	Interbedding of fine sand and black organic-rich laminae	Frozen	52.163	09.651		3		Drilled, like Bun-4-1	19.08.	
93	Bunge-1-y						3		γ-spectrometry		
94	Bunge-2	Fine sand	Unfrozen				0.7	0	Hammered, like Bun-4-7		
95	Bunge-2-y						0.7	0	γ-spectrometry		
96	Bunge-3	Fine sand	Unfrozen				0.7	0	Hammered, like Bun-5-1		
97	Bunge-3-y						0.7	0	γ-spectrometry		
98	Bun-95-I	Fine sand		50m E of Bun-4				--	Near of a recent ice wedge		BUN-95

Appendix 5.2-1. continuation.

No.	Sample	Sample description		Position			Depth below surface [m]	Ice content, abs/grav. [wt %]	Remarks	Date	Ice/water samples
		Sedimentology	Cryolithology	N	E	Height. a.s.l. [m]					
	Bunge Land lower terrace			**74°**	**140°**						
99	Bun-7-1	Silty fine sand	Frozen	50.352	23.206	ca.1-1.5	0.6	25.7/34.5	Small pit	25.08.	
100	Bun-7-3-Eis		Texture ice				0.6				
101	Bun-7-2	Clayish fine sand	Unfrozen				0.5				
102	Bun-7-3	Fine sand, recent roots	Unfrozen, dry				0.25				
103	Bun-7-4	Carex-species					0		Vegetation, pollen analyses		
104	Bun-7-5	Fine sand					0.3		Pit		
105	Bun-8	Fine sand				ca. 0.3	0		Beach sand		
106	Bun-9	Beach material							Shells, sponges	19./25, 08.	
107	Bunge-4	Silty fine sand	Frozen				0.6		Drilled like Bun-7-1	25.08.	
108	Bunge-4-y	Silty fine sand					0.6		γ-spectrometry		
109	Bunge-5	Sand	Unfrozen				0.4		Hammered		
110	Bunge-5-y	Sand					0.4		γ-spectrometry		
	New Siberian Island, Derevyaniy Gora			**75°**	**147°**						
111	Nes-AA-1	Surface material					0-0.05		Pollen analyses	20.08.	
112	Nes-4	Boulders		01.096	05.136	ca. 50	0				
113	Nes-5	Boulders					0				
114	Nes-6	Boulders		01.096	05.136	ca. 50	0				
115	Nes-1-1	Coal							Cretaceous wood coal stems		
116	Nes-1-2	Coal									
117	Nes-2	Coal									

Appendix 5.2-1. continuation.

No.	Sample	Sample description		Position			Depth below surface [m]	Ice content, abs/grav. [wt %]	Remarks	Date	Ice/water samples
		Sedimentology	Cryolithology	N	E	Height. a.s.l. [m]					
	New Siberian Island, Urositse Hedenstrom			**75°**	**146°**						
118	Nes-7-1	Clayish silt	Horizontal to subhorizontal ice lenses, reticulated	07.156	38.857	ca. 12.3	1.2	56.9/ 132.3	Coastal outcrop	21.08.	
119	Nes-7-2	Clayish silt	Thin ice streaks			ca. 11.7	1.8	42.1/72.6	Marine or alas deposit		
120	Nes-7-3	Bluish-gray fine sandy silt	Diagonal ice streaks			ca. 11.4	2.1	30.8/44.6	With brownish oxydations patches		
121	Nes-7-4	Bluish-gray fine sandy silt	Diagonal ice streaks			ca. 11	2.5	29.6/42.0	Marine or alas deposit		NSI-IW-
122	Nes-7-5	Bluish-gray fine sandy silt	Diagonal ice streaks			ca. 10.5	3	34.5/52.6			1.1 to 1.16
123	Nes-7-6	Bluish-gray fine sandy silt	Diagonal ice streaks			ca 10.1	3.4	39.5/65.2			
124	Nes-7-7	Bluish-gray fine sandy silt	Thick ice streaks			ca 9	4.5	32.8/48.7			NSI-TI-1
125	Nes-7-8	Bluish-gray fine sandy silt	Diagonal ice streaks			ca. 7.7	5.8	42.4/75.5			
126	Nes-7-9	Bluish-gray fine sandy silt	Diagonal ice streaks			ca. 6.5	7	36.7/58.0			
127	Nes-7-10	Bluish-gray fine sandy silt	Diagonal ice streaks			caa. 5	8.5	27.6/38.1			
128	Nes-7-11	Bluish-gray fine sandy silt, small subrounded gravels	Diagonal ice streaks			ca. 4	9.5	27.7/38.4			
129	Nes-7-12	Sand-silt-interbedding, ripple marks				ca. 3.8	9.7	17.1/20.7			
130	Nes-7-13	Gravels, subrounded,1cm				ca. 3.7	9.8	19.7/24.6			
131	Nes-7-14	Silty fine sand, twig fragments	Ice bands			ca. 2.7	10.8	31.8/46.7			NSI-TI-3
132	Nes-7-15	Twig fragments				ca. 2.7	10.8		AMS-dating		

Appendix 5.2-1. continuation.

No.	Sample	Sample description		Position			Depth below surface [m]	Ice content, abs/grav. [wt %]	Remarks	Date	Ice/water samples
		Sedimentology	Cryolithology	N	E	Height. a.s.l. [m]					
133	Nes-8-1	Clayish silt to silty clay, bluish-gray, with dropstones	Diagonal ice streaks	07.331	37.559	1.3			Marine deposit	21.08.	
134	Nes-8-2	Clayish silt to silty clay, bluish-gray, with dropstones	Diagonal ice streaks			2.2			Marine deposit		
135	Nes-8-3	Clayish silt to silty clay, bluish-gray, with dropstones	Diagonal ice streaks			3			Marine deposit		
136	Nes-8-4	Clayish silt to silty clay, bluish-gray, with dropstones	Diagonal ice streaks			4			Marine deposit		
137	Nes-8-5	Silty fine sand				5			Alas deposit (?)		
138	Nes-8-6	Pebbles							Dropstones (IRD), selected		
139	Nes-9-1	Silty clay		07.594	36.340	1.4		26.7/39.6	Marine deposit	21.08.	
140	Nes-9-2	Silty clay		07.594	36.340	2		28.4734.5	Marine deposit		
141	Nes-9-3	Silty clay		07.594	36.340	2.6		25.6/36.3	Marine deposit		
142	Nes-9-4	Silty clay		07.594	36.340	3.5		--	Marine deposit		
143	Nes-9-5	Clayish silt, laminated with organic layers		07.594	36.340	4		--	Lacustrine deposits		
144	Nes-AA-3	Surface material		07.196	38.535	ca. 3	0-0.05		Pollen analyses		
145	Nes-10	Pebbles				2-3.5			Dropstones (IRD), selected		
146	Nes-11	Pebbles					0		Pebbles from various *thermokarst* mounds		

Appendix 5.2-1. continuation.

No.	Sample	Sample description		Position			Depth below surface [m]	Ice content, abs/grav. [wt %]	Remarks	Date	Ice/water samples
		Sedimentology	Cryolithology	N	E	Height. a.s.l. [m]					
	Maly Lyakhov Island			**74°**	**140°**						
147	Kly-1-1	Fine sandy silt	Ice banded	14.763	21.052		5	42.4/73.5	Thermokarst mound	27.08.	
148	Kly-1-2	Fine sandy silt	Ice banded				4.5	37.4/59.6			
149	Kly-1-3	Fine sandy silt	Ice banded				4	57/132.5			
150	Kly-1-4	Fine sandy silt	Ice banded				3.3	48.1/92.8			
151	Kly-1-5	Fine sandy silt	Ice banded				2.8	45/81.8			
152	Kly-1-6	Fine sandy silt, soil horizon with peat inclusions	Transition zone of the active layer				2.1	43.7/77.6			
153	Kly-1-7	Allochtonous peat layer					2				
154	Kly-1-8	Silty fine sand, laminated					1.8				
155	Kly-1-9	Silty fine sand, laminated					1.5				
156	Kly-1-10	Recent soil, rooted					0-0.05		Pollen analyses		
157	Kly-AA-1	Surface material				25-28	0-0.05		Pollen analyses		
158	Kly-2	Beach material		14.591	19.181				Sponges		

Appendix 5.2-1. continuation.

No.	Sample	Sample description		Position			Depth below surface [m]	Ice content, abs/grav. [wt %]	Remarks	Date	Ice/water samples
		Sedimentology	Cryolithology	N	E	Height. a.s.l. [m]					
S of Cape Svyatoy Nos				72°	140°						
159	Svn-1-1	Silty fine sand light gray, laminated		47.095	50.542	2.5			Cliff	28.08.	
160	Svn-1-2	Allochtonous peat		47.095	50.542	6				28.08.	
161	Svn-1-3	Shrub fragments		47.095	50.542	3				28.08.	
162	Svn-1-4	Shrub fragments		47.095	50.542	ca. 15			Thermokarst mound	28.08.	
163	Svn-1-5	Shrub fragments				ca. 15			Thermokarst mound	28.08.	
164	Svn-2	Twigs, vivianite				3			Cliff, 350 m SE of the landing point	28.08.	
165	Svn-3	Beach sand							Beach, 300 m NW of the landing point	28.08.	
166	Svn-4-1	Pebble.surface lineation		47.415	49.186				Valley with snow patch	28.08.	
167	Svn-4-2	Beach pebbles									
168	Svn-4-3	Beach pebbles									
169	Svn-4-4	Stones							Valley with snow patch, comparison granite dolerit	28.08.	

Appendix 5.2-1. continuation.

No.	Sample	Sample description		Position			Depth below surface [m]	Ice content, abs/grav. [wt %]	Remarks	Date	Ice/water samples
		Sedimentology	Cryolithology	N	E	Height. a.s.l. [m]					
	Oyogosky Ya			**72°**	**143°**						
170	Oya-1	Surface material		40.519	35.922	ca. 8-9	0-0.05		Pollenanalyses	30.08.	
171	Oya-2-1	Peat, non-decomposed with wood fragments	Ice rich	39.166	33.500	40	0.4-0.5		Co-ordinates according to the map	30.08.	
172	Oya-2-2	Peat, non-decomposed with wood fragments					0.7-0.8				
173	Oya-2-3	Peat, non-decomposed with wood fragments					1.2-1.3		Thermokarst mound,		
174	Oya-2-4	Peat, non-decomposed with wood fragments					1.6-1.7				
175	Oya-2-5	Peat with vertically twigs, cryoturbated soil					1.9-2.0				
176	Oya-2-6	Silty fine sand, cryoturbated paleosol					2.2-2.3	35.3/54.4	Ice Complex deposit		
177	Oya-2-7	Silty fine sand, twigs	Coarse lens like reticulated				2.3-2.4	54.1/118			
178	Oya-2-8	Silty fine sand, twigs	Coarse lens like reticulated				3.0-31.0	51/ 104.1			
179	Oya-2-9	Surface material					0-0.05		Pollen analyses		

Appendix 5.2-1. continuation.

No.	Sample	Sample description		Position			Depth below surface [m]	Ice content, abs/grav. [wt %]	Remarks	Date	Ice/water samples
		Sedimentology	Cryolithology	N	E	Height. a.s.l. [m]					
180	Oya-3-2	Silty fine sand	Lens like reticulated	40.759	33.085		1.4		Coastal cliff, lowest part, Ice Complex	30.08.	
181	Oya-3-3	Silty fine sand, fine-laminated, with thin organic layers	Injection ice				2.4	49.7/99.0	Ice Complex deposit		OYA-IW-2.0 to 2.11
182	Oya-3-4	Silty fine sand	Few ice				3	36.7/58.0	Oxidic transition zone		
183	Oya-3-5	Silty fine sand	Few ice				3.6	35.9/55.9	Oxidic transition zone		
184	Oya-3-6	Grayish-blue silt	Few ice				4.1	32.2/47.6	Reductic part, lacustrine deposit		
185	Oya-3-8	Dark-gray clayish silt	Few ice				5.8	27.6/38.0	Lacustrine deposit		
186	Oya-3-9	Dark-gray clayish silt	Ice rich				6.4	49.1/96.6	Lacustrine deposit		
187	Oya-3-10	Gray, clayish silt, laminated	Few ice				7.4		Ice wedge cast with lacustrine deposit		
188	Oya-3-11	Peat, wood	Frozen				7.4		Pseudomorphose, like Oya-3-10		
189	Oya-3-12	Gray, clayish silt, laminated	Frozen				8.2		Lacustrine deposit		
190	Oya-3-13	Shrub wood							Selected, near ice wedge casts		
191	Oya-4-1	Silty fine sand		40.669	33.857			60.5/ 153.2	Ice Complex, middle part	30.08.	Oya- iW-5.1
192	Oya-4-2	Silty fine sand		40.669	33.857					30.08.	to 5.15
193	Oya-5-1	Silt, gray				3.5			With shells	30.08.	
194	Oya-5-2	Wood				13			Alass at the end of the thermocirque	30.08.	
195	Oya-6-1	Peat inclusion		40.524	36.024	3.25			Near of an old ice wedge	30.08.	OYA-IW-1.1 to 1.6

Appendix 5.2-1. continuation.

No.	Sample	Sample description: Sedimentology	Sample description: Cryolithology	Position: N	Position: E	Position: Height. a.s.l. [m]	Depth below surface [m]	Ice content, abs/grav. [wt %]	Remarks	Date	Ice/water samples
Muostakh Island					**71 129**						
196	Muo-1	Surface material		36.820	56.179	ca. 23			Vegetation cover, pollen analyses Frost boil, pollen analyses	02.09.	
197	Muo-2	Surface material		36.623	56.179	23					
198	Muo-3-1	Silty fine sand	Fine lenslike	36.804	56.446	0.5		49.3/97.4	Section 1	02.09.	
199	Muo-3-2	Silty fine sand	Rediculated			1		53.4/ 114.5			MUO-IW
200	Muo-3-3	Silty fine sand	Cryostructure,			1.5		57.6/ 135.8			01 to 12
201	Muo-3-4	Silty fine sand	Ice bands			2		54.5/ 119.6			
202	Muo-3-5	Peat inclusion				1					
203	Muo-3-6	Silty fine sand				2.5		55/122.2			
204	Muo-3-7	Silty fine sand				3					
205	Muo-3-8	Fine sand	Massive cryostructure	36.773	56.615	5		37/ 58.7	Section 2	02.09.	
206	Muo-3-9	Peat, roots				7.5					
207	Muo-3-10	Middle sand				6.5		52.5/ 110.5			
208	Muo-3-11	Sand-silt-interbedding	Unfrozen			9.7					
209	Muo-3-12	Sand	Frozen			8.5					
210	Muo-4	Beach sand		36.820	56.179	1				02.09.	

Ice content, abs./grav. [wt %]
abs. = absolut; ratio of ice mass to wet sample mass
grav. = gravimetric; ratio of ice mass to dry sample mass (> 100 % indicates an ice oversaturation)

Appendix 5.2-2. List of ice and water samples collected on the New Siberian Islands.

				Isotopes			Chemistry				
Nr.	date	sample	type	^{18}O	^{2}H	^{3}H	anion/ cation	LF [µS/cm]	pH	filter	Remarks
1	15.08.	STO-97/01	SP	x	x	x	x	30.5	6.89	-	
2	15.08.	STO-IW-1.1	IW	x	x	-	x	131.6	8.15	-	
3	15.08.	STO-IW-1.2	IW	x	x	-	-	-	-	CAF	
4	15.08.	STO-IW-1.3	IW	x	x	-	x	161.0	8.03	-	
3	15.08.	STO-IW-1.4	IW	x	x	-	-	-	-	CAF	
6	15.08.	STO-IW-1.5	IW	x	x	-	x	180.8	7.91	-	
7	15.08.	STO-IW-1.6	IW	x	x	-	-	-	-	-	
8	15.08.	STO-IW-1.7	IW	x	x	-	x	145.5	7.87	-	
9	15.08.	STO-IW-1.8	IW	x	x	-	-	-	-	CAF	
10	15.08.	STO-IW-1.9	IW	x	x	-	x	159.2	7.82	-	
11	15.08.	STO-IW-1.10	IW	x	x	-	-	-	-	-	
12	15.08.	STO-IW-1.11	IW	x	x	-	x	177.6	7.89	-	
13	15.08.	STO-IW-1.12	IW	x	x	-	-	-	-	-	
14	15.08.	STO-IW-1.13	IW	x	x	-	x	204	7.96	-	
15	15.08.	STO-IW-1.14	IW	x	x	-	-	-	-	-	
16	15.08.	STO-IW-1.15	IW	x	x	-	x	104.2	8.34	-	
17	15.08.	STO-IW-1.16	IW	x	x	x	x	157.9	7.91	-	
18	15.08.	STO-IW-4.1	IW	x	x	-	x	97.7	7.67	-	
19	15.08.	STO-IW-4.2	IW	x	x	-	-	-	-	CAF	
20	15.08.	STO-IW-4.3	IW	x	x	x	x	83.5	7.73	-	
21	15.08.	STO-IW-4.4	IW	x	x	-	-	-	-	CAF	
22	15.08.	STO-IW-4.5	IW	x	x	-	x	82.9	7.67	-	
23	15.08.	STO-94/01	RIW	x	x	x	x	273	7.56	-	
24	15.08.	STO-3-6	II	x	x	x	-	-	-	-	
25	15.08.	STO-IW-3.1	IW	x	x	-	x	158	7.92	-	
26	15.08.	STO-IW-3.2	IW	x	x	x	-	-	-	-	
27	15.08.	STO-IW-3.3	IW	x	x	x	-	-	-	-	
28	15.08.	STO-IW-3.4	IW	x	x	-	x	122	7.83	-	
29	15.08.	STO-IW-3.5	IW	x	x	-	-	-	-	-	
30	15.08.	STO-IW-3.6	IW	x	x	-	-	-	-	CAF	
31	15.08.	STO-TI-1	IW	x	x	-	-	550	7.76	-	
32	15.08.	STO-IW-2.1	IW	x	x	-	x	120	7.94	-	
33	15.08.	STO-IW-2.2	IW	x	x	x	-	-	-	CAF	
34	15.08.	STO-IW-2.3	IW	x	x	-	x	95.1	8.04	-	
35	15.08.	STO-IW-2.4	IW	x	x	x	-	-	-	CAF	
36	15.08.	STO-IW-2.5	IW	x	x	-	x	-	-	-	
37	15.08.	STO-IW-5.1	IW	x	x	-	-	136	7.75	CAF	
38	15.08.	STO-IW-5.2	IW	x	x	-	x	129	7.98	-	
39	15.08.	STO-IW-5.3	IW	x	x	-	-	116	7.82	CAF	
40	15.08.	STO-IW-5.4	IW	x	x	-	x	117.2	8.00	-	
41	15.08.	STO-IW-5.5	IW	x	x	-	-	-	-	-	
42	15.08.	STO-IW-5.6	IW	x	x	x	x	104.1	7.73	-	
43	15.08.	STO-IW-5.7	IW	x	x	-	-	407	8.01	CAF	
44	15.08.	STO-IW-5.8	IW	x	x	-	x	395	7.88	-	
45	15.08.	STO-IW-5.9	IW	x	x	-	-	200	8.02	-	
46	16.08.	ANS-96-1	SW	x	x	x	-	-	-	-	
47	16.08.	ANS-96-2	SW	x	x	x	-	-	-	-	
48	16.08.	MYA-96/01	SW	x	x	x	-	284	7.96	-	
49	16.08.	ANS-97-1	SP	x	x	x	-	-	-	CAF	
50	16.08.	ANS-97-2	SP	x	x	x	-	-	-	CAF	
51	16.08.	MYA-IW-1.1	IW	x	x	x	-	-	-	-	
52	16.08.	MYA-IW-1.2	IW	x	x	-	x	111.1	8.37	CAF	
53	16.08.	MYA-IW-1.3	IW	x	x	-	x	114.2	7.94	-	
54	16.08.	MYA-TI-1	TI	x	x	-	-	-	-	-	
55	17.08.	BEL-IW-1.1	IW	x	x	-	x	265	7.57	-	

				Isotopes				Chemistry				
Nr.	date	sample	type	^{18}O	^{2}H	^{3}H	anion/ cation	LF [µS/cm]	pH	filter	Remarks
56	17.08.	BEL-IW-1.2	IW	x	x	-	x	128	7.76	-	
57	17.08.	BEL-IW-1.3	IW	x	x	-	x	114	7.8	-	
58	17.08.	BEL-IW-1.4	IW	x	x	x	-	-	-	-	
59	17.08.	BEL-IW-1.5	IW	x	x	-	x	213	7.85	-	
60	17.08.	BEL-IW-1.6	IW	x	x	-	-	-	-	CAF	
61	17.08.	BEL-IW-1.7	IW	x	x	-	x	170	7.81	-	
62	17.08.	BEL-IW-1.8	IW	x	x	-	-	-	-	-	
63	17.08.	BEL-IW-1.9	IW	x	x	-	x	152	7.75	-	
64	17.08.	BEL-IW-1.10	IW	x	x	-	-	-	-	CAF	
65	17.08.	BEL-IW-1.11	IW	x	x	-	x	163	7.71	-	
66	17.08.	BEL-IW-1.12	IW	x	x	-	-	-	-	-	
67	17.08.	BEL-IW-1.13	IW	x	x	-	x	152	7.63	-	
68	17.08.	BEL-IW-1.14	IW	x	x	-	-		-	CAF	
69	17.08.	BEL-IW-1.15	IW	x	x	-	x	147	7.69	-	
70	17.08.	BEL-IW-1.16	IW	x	x	x	-	-	-	-	
71	17.08.	BEL-IW-1.17	IW	x	x	-	x	125	7.75	-	
72	17.08.	BEL-IW-1.18	IW	x	x	-	-	-	-	CAF	
73	17.08.	BEL-IW-1.19	IW	x	x	-	x	117	7.75	-	
74	17.08.	BEL-IW-1.20	IW	x	x	-	-	-	-	CAF	
75	17.08.	BEL-IW-1.21	IW	x	x	-	x	160	7.88	-	
76	17.08.	BEL-IW-2.1	IW	x	x	-	-	-	-	CAF	
77	17.08.	BEL-IW-2.2	IW	x	x	-	x	284	7.79	-	
78	17.08.	BEL-IW-2.3	IW	x	x	-	-	-	-	CAF	
79	17.08.	BEL-IW-2.4	IW	x	x	x	x	180	7.56	-	
80	17.08.	BEL-IW-3.1	IW	x	x	-	x	97.4	6.64	GFF	
81	17.08.	BEL-IW-3.2	IW	x	x	x	-	-	-	-	
82	17.08.	BEL-IW-3.3	IW	x	x	-	x	65.4	6.37	GFF	
83	17.08.	BEL-IW-3.4	IW	x	x	-	-	-	-	-	
84	17.08.	BEL-IW-3.5	IW	x	x	-	x	73.3	6.48	-	
85	17.08.	BEL-IW-3.6	IW	x	x	-	-	-	-	CAF	
86	17.08.	BEL-IW-3.7	IW	x	x	-	x	50.5	6.24	-	
87	17.08.	BEL-IW-3.8	IW	x	x	-	x	75.4	6.12	-	
88	17.08.	BEL-IW-3.9	IW	x	x	-	-	-	-	CAF	
89	17.08.	BEL-IW-3.10	IW	x	x	-	x	68.7	6.51	-	
90	17.08.	BEL-IW-3.11	IW	x	x	-	x	38.3	6.38	-	
91	17.08.	BEL-IW-3.12	TI	x	x	-	-	-	-	-	
92	17.08.	BEL-IW-4.1	IW	x	x	x	-	-	-	CAF	
93	17.08.	BEL-IW-4.2	IW	x	x	-	x	166	6.23	-	
94	17.08.	BEL-IW-4.3	IW	x	x	x	-	-	-	CAF	
95	17.08.	BEL-IW-4.4	IW	x	x	-	x	68.5	6.08	-	
96	17.08.	BEL-IW-5.1	IW	x	x	x	-	-	-	CAF	
97	17.08.	BEL-IW-5.2	IW	x	x	-	x	155	6.77	-	
98	17.08.	BEL-IW-5.3	TI	x	x	-	x	370	5.53	-	
99	17.08.	BEL-IW-6.1	IW	x	x	x	-	-	-	-	
100	17.08.	BEL-IW-6.2	IW	x	x	x	x	79.3	5.84	CAF	
101	17.08.	BEL-IW-6.3	IW	x	x	x	-	-	-	CAF	
102	17.08.	BEL-IW-6.4	IW	x	x	x	x	131	5.86	-	
103	17.08.	BEL-96/01	SW	x	x	-	x	423	7.19	-	
104	17.08.	BEL-96/02	SW	x	x	x	x	27700	7.72	-	SAL=18.9‰
105	17.08.	BEL-95/01	SI	x	x	x	x	287	6.43	-	
106	18.08.	KYS-IW-1.1	IW	x	x	-	x	73.6	-	-	
107	18.08.	KYS-IW-1.2	IW	x	x	-	x	64.5	-	-	
108	18.08.	KYS-IW-1.3	IW	x	x	-	x	63.5	7.3	-	
109	18.08.	KYS-IW-1.4	IW	x	x	x	-	-	-	CAF	
110	18.08.	KYS-IW-1.5	IW	x	x	-	x	71.3	6.99	-	
111	18.08.	KYS-IW-1.6	IW	x	x	-	-	-	-	CAF	
112	18.08.	KYS-IW-1.7	IW	x	x	-	x	120	7.38	-	

				Isotopes			Chemistry				
Nr.	date	sample	type	^{18}O	^{2}H	^{3}H	anion/ cation	LF [µS/cm]	pH	filter	Remarks
113	18.08.	KYS-IW-1.8	IW	x	x	-	-	-	-	CAF	
114	18.08.	KYS-IW-1.9	IW	x	x	-	x	70.8	7.38	-	
115	18.08.	KYS-IW-1.10	IW	x	x	-	-	-	-	-	
116	18.08.	KYS-IW-1.11	IW	x	x	-	x	87.6	7.44	-	
117	18.08.	KYS-IW-1.12	IW	x	x	-	-	-	-	CAF	
118	18.08.	KYS-IW-1.13	IW	x	x	-	x	111	7.67	-	
119	18.08.	KYS-IW-1.14	IW	x	x	-	-	-	-	-	
120	18.08.	KYS-IW-1.15	IW	x	x	-	x	70.5	7.43	-	
121	18.08.	KYS-IW-1.16	IW	x	x	x	-	-	-	CAF	
122	18.08.	KYS-IW-1.17	IW	x	x	-	x	149	7.48	-	
123	18.08.	KYS-IW-1.18	IW	x	x	-	-	-	-	-	
124	18.08.	KYS-IW-2.1	IW	x	x	-	x	125	7.37	-	
125	18.08.	KYS-IW-2.2	IW	x	x	x	-	-	-	CAF	
126	18.08.	KYS-IW-2.3	IW	x	x	-	x	93.5	7.7	-	
127	18.08.	KYS-IW-2.4	IW	x	x	x	-	-	-	CAF	
128	18.08.	KYS-IW-2.5	IW	x	x	-	x	89.3	7.85	-	
129	18.08.	KYS-IW-2.6	IW	x	x	-	-	-	-	CAF	
130	18.08.	KYS-IW-3.1	IW	x	x	x	x	378	6.68	-	
131	18.08.	KYS-IW-3.2	IW	x	x	-	x	149	6.72	-	
132	18.08.	KYS-96-1	SW	x	x	x	-	-	-	-	
133	18.08.	KYS-96/02	SW	x	x	x	x	25300	7.77	-	SAL=17.2‰
134	18.08.	KYS-95/01	SI	x	x	x	x	1352	6.78	-	
135	17.08.	BEL-5-2.TI	TI	x	x	-	x	1263	5.84	-	SAL=0.5‰
136	17.08.	BEL-5-3.TI	TI	x	x	-	x	137	6.74	-	
137	17.08.	BEL-5-4.TI	TI	x	x	-	x	218	6.55	-	
138	17.08.	BEL-5-5.TI	TI	x	x	-	x	211	6.43	-	
139	19.08.	BUN-96/01	SW	x	x	x	x	64.1	6.99	-	
140	19.08.	BUN-96/02	SW	x	x	x	x	37.2	6.56	-	
141	19.08.	BUN-96/03	SW	x	x	x	x	24200	7.58	-	SAL=16.4‰
142	19.08.	BUN-95/01	RIW	x	x	x	x	60.0	6.65	-	
143	19.08.	BUN-95/02	RIW	x	x	x	-	-	-	-	
144	19.08.	BUN-95/03	RIW	x	x	-	-	-	-	-	
145	19.08.	BUN-95/04	SI	x	x	x	x	13.4	6.13	-	
146	19.08.	BUN-96/04	SW	x	x	x	-	-	-	-	
147	17.08.	BEL-2-1.TI	TI	x	x	-	x	546	7.35	-	
148	17.08.	BEL-2-2.TI	TI	x	x	-	x	556	6.57	-	
149	17.08.	BEL-2-4.TI	TI	x	x	-	x	-	-	-	
150	17.08.	BEL-2-6.TI	TI	x	x	-	-	63.2	6.1	-	
151	17.08.	BEL-3-2.TI	TI	x	x	-	x	-	-	-	
152	17.08.	BEL-3-3.TI	TI	x	x	-	x	-	-	-	
153	17.08.	BEL-4-1.TI	TI	x	x	-	-	5320	7.39	-	SAL=3.2‰
154	17.08.	BEL-7-1.TI	TI	x	x	-	x	-	-	-	
155	15.08.	STO-0-1.TI	TI	x	x	-	x	1595	7.19	-	
156	15.08.	STO-1-3.TI	TI	x	x	-	x	-	-	-	
157	15.08.	STO-2-3.TI	TI	x	x	-	x	4160	7.21	-	SAL=2.4‰
158	16.08.	MYA-1-1.TI	TI	x	x	-	-	-	-	-	
159	18.08.	KYS-2-1.TI	TI	x	x	-	x	450	7.55	-	
160	18.08.	KYS-2-2.TI	TI	x	x	-	-	-	-	-	
161	18.08.	KYS-2-3.TI	TI	x	x	-	x	471	6.89	-	
162	18.08.	KYS-2-4.TI	TI	x	x	-	-	376	5.86	-	
163	18.08.	KYS-2-8.TI	TI	x	x	-	x	-	-	-	
164	18.08.	KYS-2-9.TI	TI	x	x	-	x	1219	7.16	-	
165	18.08.	KYS-2-10.TI	TI	x	x	-	-	930	7.3	-	
166	20.08.	NSI-95/01	II	x	x	x	x	903	4.93	-	
167	20.08.	NSI-95/02	II	x	x	x	-	-	-	-	
168	20.08.	NSI-97/01	SP	x	x	x	x	800	5.93	-	
169	20.08.	NSI-97/02	SP	x	x	x	-	-	-	CAF	

			Isotopes			Chemistry				
Nr.	date	sample	type	^{18}O	^{2}H	^{3}H	anion/ cation	LF [μS/cm]	pH	filter	Remarks
170	20.08.	NSI-97/03	SP	x	x	x	x	608	6.15	-	
171	20.08.	NSI-97/04	SP	x	x	x	-	921	6.21	-	
172	20.08.	NSI-97/05	SP	x	x	x	x	392	5.56	CAF	
173	20.08.	NSI-97/06	SP	x	x	x	x	317	6.14	-	
174	20.08.	NSI-97/07	SP	x	x	x	-	-	-	CAF	
175	20.08.	DER-97/01	SP	x	x	x	-	-	-	CAF	
176	20.08.	DER-97/02	SP	x	x	x	x	23.6	6.06	CAF	
177	20.08.	DER-97/03	SP	x	x	x	-	-	-	CAF	
178	20.08.	DER-97/04	SP	x	x	x	x	31.5	6.36	-	
179	20.08.	DER-97/05	SP	x	x	x	-	-	-	-	
180	20.08.	DER-96/01	SW	x	x	x	-	-	-	-	
181	20.08.	DER-96/02	SW	x	x	x	-	-	-	-	
182	21.08.	NSI-IW-1.1	IW	x	x	-	x	496	7.61	-	
183	21.08.	NSI-IW-1.2	IW	x	x	-	x	218	7.91	-	
184	21.08.	NSI-IW-1.3	IW	x	x	-	x	145	7.71	-	
185	21.08.	NSI-IW-1.4	IW	x	x	-	-	-	-	CAF	
186	21.08.	NSI-IW-1.5	IW	x	x	-	x	118	7.62	-	
187	21.08.	NSI-IW-1.6	IW	x	x	-	-	-	-	-	
188	21.08.	NSI-IW-1.7	IW	x	x	-	x	276	7.72	-	
189	21.08.	NSI-IW-1.8	IW	x	x	-	-	-	-	CAF	
190	21.08.	NSI-IW-1.9	IW	x	x	-	x	196	7.7	-	
191	21.08.	NSI-IW-1.10	IW	x	x	-	-	-	-	CAF	
192	21.08.	NSI-IW-1.11	IW	x	x	-	x	231	7.92	-	
193	21.08.	NSI-IW-1.12	IW	x	x	x	-	-	-	CAF	
194	21.08.	NSI-IW-1.13	IW	x	x	-	-	-	-	-	
195	21.08.	NSI-IW-1.14	IW	x	x	-	x	112	7.78	-	
196	21.08.	NSI-IW-1.15	IW	x	x	-	x	246	7.76	-	
197	21.08.	NSI-IW-1.16	IW	x	x	x	x	580	7.86	-	
198	21.08.	NSI-IW-2.1	IW	x	x	-	x	85.3	7.72	-	
199	21.08.	NSI-IW-2.2	IW	x	x	x	-	-	-	CAF	
200	21.08.	NSI-IW-2.3	IW	x	x	-	x	194.8	7.88	-	
201	21.08.	NSI-IW-2.4	IW	x	x	x	-	-	-	CAF	
202	21.08.	NSI-IW-3.1	IW	x	x	-	x	194.5	7.4	-	
203	21.08.	NSI-IW-3.2	IW	x	x	-	-	-	-	CAF	
204	21.08.	NSI-IW-3.3	IW	x	x	-	x	169.5	7.43	-	
205	21.08.	NSI-IW-3.4	IW	x	x	x	-	-	-	-	
206	21.08.	NSI-IW-3.5	IW	x	x	-	x	246	7.53	-	
207	21.08.	NSI-IW-3.6	IW	x	x	-	-	-	-	CAF	
208	21.08.	NSI-IW-4.1	IW	x	x	-	x	169.5	7.91	-	
209	21.08.	NSI-IW-4.2	IW	x	x	x	-	-	-	CAF	
210	21.08.	NSI-IW-4.3	IW	x	x	-	x	192	7.91	-	
211	21.08.	NSI-IW-4.4	IW	x	x	-	-	-	-	CAF	
212	21.08.	NSI-IW-4.5	IW	x	x	-	x	210	7.59	-	
213	21.08.	NSI-MI-1	MI	x	x	x	-	391	7.34	-	
214	21.08.	NSI-MI-2	MI	x	x	x	-	-	-	-	
215	21.08.	NSI-MI-3	MI	x	x	x	x	440	7.37	-	
216	21.08.	NSI-MI-4	MI	x	x	x	-	-	-	GFF	
217	21.08.	NSI-MI-5	MI	x	x	x	x	1441	7.36	GFF	
218	21.08.	NSI-MI-6	MI	x	x	x	-	-	-	-	
219	21.08.	NSI-MI-7	MI	x	x	x	-	-	-	-	
220	21.08.	NSI-MI-8	MI	x	x	x	x	247	7.41	GFF	
221	21.08.	NSI-MI-9	MI	x	x	x	-	-	-	-	
222	21.08.	NSI-MI-10	MI	x	x	x	x	231	7.3	-	
223	21.08.	NSI-MI-11	MI	x	x	x	x	321	6.89	GFF	
224	21.08.	NSI-TI-1	TI	x	x	x	x	1666	7.34	-	
225	21.08.	NSI-TI-4	TI	x	x	x	-	3880	7.36	-	
226	21.08.	NSI-TI-2	TI	x	x	-	x	1876	7.37	-	

Nr.	date	sample	type	Isotopes ^{18}O	^{2}H	^{3}H	Chemistry anion/ cation	LF [µS/cm]	pH	filter	Remarks
227	21.08.	NSI-TI-3	TI	x	x	-	x	224	7.52	-	
228	21.08.	NSI-IW2-TI1	TI	x	x	-	x	515	7.75	-	
229	21.08.	NSI-IW2-TI2	TI	x	x	x	-	-	-	-	
230	21.08.	NSI-IW2-TI3	TI	x	x	-	x	337	7.93	-	
231	21.08.	NSI-IW2-TI4	TI	x	x	x	-	-	-	-	
232	21.08.	NES-7-IW-1	IW	x	x	-	-	-	-	CAF	
233	20.08.	NSI-St.6-6m	SW	x	x	-	-	26600	7.71	-	SAL=18.2‰
234	20.08.	NSI-St.6-6.7m	SW	x	x	-	-	27300	7.73	-	SAL=18.5‰
235	21.08.	NES-7-1.TI	TI	x	x	-	x	-	-	-	
236	21.08.	NES-7-2.TI	TI	x	x	-	-	-	-	-	
237	21.08.	NES-7-10.TI	TI	x	x	-	-	-	-	-	
238	21.08.	NES-7-14.TI	TI	x	x	-	x	-	-	-	
239	23.08.	BUN-99/01	RW	x	x	x	x	29.1	6.63	-	
240	23.08.	BUN-99/02	RW	x	x	x	x	-	-	-	
241	24.08.	BUN-99/03	RW	x	x	-	-	-	-	-	
242	25.08.	BUN2-96/01	SW	x	x	x	-	-	-	-	
243	25.08.	BUN2-96/02	SW	x	x	x	x	-	-	-	
244	25.08.	BUN2-98/01	GW	x	x	x	-	-	-	-	
245	25.08.	BUN-7-1.TI	TI	x	x	-	x	1736	6.23	-	
246	27.08.	SLY-96/01	SW	x	x	x	x	27000	7.72	CAF	SAL=18.0‰
247	27.08.	SLY-IW-1.1	IW	x	x	x	x	117.2	7.09	CAF	
248	27.08.	SLY-IW-2.1	IW	x	x	-	x	116.3	7.74	-	
249	27.08.	SLY-IW-2.2	IW	x	x	x	-	-	-	CAF	
250	27.08.	SLY-IW-2.3	IW	x	x	-	x	100.2	7.47	-	
251	27.08.	SLY-IW-2.4	IW	x	x	x	-	-	-	CAF	
252	27.08.	SLY-IW-2.5	IW	x	x	-	x	101.6	7.49	-	
253	27.08.	SLY-97/01	SP	x	x	x	-	-	-	CAF	
254	27.08.	SLY-97/02	SP	x	x	x	x	50.8	7.7	-	
255	27.08.	SLY-97/03	SP	x	x	x	-	-	-	CAF	
256	27.08.	SLY-97/04	SP	x	x	x	x	70	7.59	-	
257	27.08.	SLY-96/02	SW	x	x	x	x	390	-	-	
258	27.08.	KLY-1-1.TI	TI	x	x	-	x	695	7.17	-	
259	27.08.	KLY-1-2.TI	TI	x	x	-	x	1295	7.05	-	
260	27.08.	KLY-1-3.TI	TI	x	x	x	x	373	7.38	-	
261	27.08.	KLY-1-4.TI	TI	x	x	-	x	655	7.12	-	
262	27.08.	KLY-1-5.TI	TI	x	x	-	x	499	7.13	-	
263	27.08.	KLY-1-6.TI	TI	x	x	-	-	-	-	-	
264	28.08.	SVN-99/01	RW	x	x	-	-	-	-	-	
265	28.08.	SVN-96/01	SW	x	x	x	x	47	7.23	-	
266	28.08.	SVN-96/02	SW	x	x	x	x	23800	7.58	-	SAL=16.4‰
267	28.08.	SVN-96/03	SW	x	x	x	x	23200	7.7	CAF	SAL=15.8‰
268	28.08.	SVN-97/01	SP	x	x	x	-	-	-	CAF	
269	28.08.	SVN-97/02	SP	x	x	x	x	23.4	6.63	-	
270	28.08.	SVN-97/03	SP	x	x	x	-	-	-	CAF	
271	29.08.	SVN-99/02	RW	x	x	-	x	440	6.6	-	
272	30.08.	OYA-96/01	SW	x	x	x	x	23700	7.63	CAF	SAL=15.9‰
273	30.08.	OYA-IW-1.1	IW	x	x	-	x	94	8.05	CAF	
274	30.08.	OYA-IW-1.2	IW	x	x	-	-	-	-	-	
275	30.08.	OYA-IW-1.3	IW	x	x	-	x	97	7.89	-	
276	30.08.	OYA-IW-1.4	IW	x	x	x	-	-	-	CAF	
277	30.08.	OYA-IW-1.5	IW	x	x	-	x	125	7.94	-	
278	30.08.	OYA-IW-1.6	IW	x	x	-	-	-	-	-	
279	30.08.	OYA-IW-2.1	IW	x	x	-	x	200	7.53	-	
280	30.08.	OYA-IW-2.2	IW	x	x	-	-	75.3	6.86	CAF	
281	30.08.	OYA-IW-2.3	IW	x	x	-	-	79.1	6.26	-	
282	30.08.	OYA-IW-2.4	IW	x	x	-	x	58.6	6.28	-	

Nr.	date	sample	type	Isotopes ^{18}O	Isotopes ^{2}H	Isotopes ^{3}H	Chemistry anion/ cation	Chemistry LF [µS/cm]	Chemistry pH	Chemistry filter	Remarks
283	30.08.	OYA-IW-2.5	IW	x	x	-	-	-	-	CAF	
284	30.08.	OYA-IW-2.6	IW	x	x	x	-	-	-	-	
285	30.08.	OYA-IW-2.7	IW	x	x	-	x	57.1	6.23	-	
286	30.08.	OYA-IW-2.8	IW	x	x	-	-	-	-	CAF	
287	30.08.	OYA-IW-2.9	IW	x	x	-	x	135	7.37	-	
288	30.08.	OYA-IW-2.10	IW	x	x	-	-	-	-	-	
289	30.08.	OYA-IW-2.11	IW	x	x	-	x	63.9	6.88	CAF	
290	30.08.	OYA-IW-2.0	IW	x	x	-	-	79.4	7.42	-	
291	30.08.	OYA-IW-4.1	IW	x	x	-	x	90.2	7.51	-	
292	30.08.	OYA-IW-4.2	IW	x	x	-	-	-	-	CAF	
293	30.08.	OYA-IW-4.3	IW	x	x	-	x	81.6	7.31	-	
294	30.08.	OYA-IW-4.4	IW	x	x	x	-	-	-	CAF	
295	30.08.	OYA-IW-4.5	IW	x	x	-	-	-	-	-	
296	30.08.	OYA-IW-4.6	IW	x	x	-	x	62.6	7.25	CAF	
297	30.08.	OYA-IW-5.1	IW	x	x	-	x	54.9	6.99	-	
298	30.08.	OYA-IW-5.2	IW	x	x	-	-	-	-	CAF	
299	30.08.	OYA-IW-5.3	IW	x	x	-	x	102	7.57	-	
300	30.08.	OYA-IW-5.4	IW	x	x	-	-	-	-	-	
301	30.08.	OYA-IW-5.5	IW	x	x	-	x	83.4	7.38	-	
302	30.08.	OYA-IW-5.6	IW	x	x	-	-	-	-	CAF	
303	30.08.	OYA-IW-5.7	IW	x	x	-	-	114	7.47	-	
304	30.08.	OYA-IW-5.8	IW	x	x	x	-	-	-	-	
305	30.08.	OYA-IW-5.9	IW	x	x	-	x	123	7.65	-	
306	30.08.	OYA-IW-5.10	IW	x	x	-	-	-	-	CAF	
307	30.08.	OYA-IW-5.11	IW	x	x	-	-	-	-	-	
308	30.08.	OYA-IW-5.12	IW	x	x	-	x	77.3	7.45	-	
309	30.08.	OYA-IW-5.13	IW	x	x	-	-	-	-	-	
310	30.08.	OYA-IW-5.14	IW	x	x	-	-	-	-	CAF	
311	30.08.	OYA-IW-5.15	IW	x	x	-	x	73.9	7.41	-	
312	30.08.	OYA-IW-6.1	IW	x	x	-	x	56.3	6.56	CAF	
313	30.08.	OYA-IW-6.2	IW	x	x	x	-	-	-	-	
314	30.08.	OYA-IW-6.3	IW	x	x	-	x	51.3	6.09	CAF	
315	30.08.	OYA-IW-6.4	IW	x	x	-	-	-	-	-	
316	30.08.	OYA-IW-6.5	IW	x	x	-	x	60.0	6.07	CAF	
317	30.08.	OYA-IW-6.6	IW	x	x	-	-	-	-	-	
318	30.08.	OYA-IW-7.1	IW	x	x	x	-	-	-	CAF	
319	30.08.	OYA-IW-7.2	IW	x	x	-	x	114	6.52	-	
320	30.08.	OYA-IW-3.1	IW	x	x	-	x	60.3	6.67	CAF	
321	30.08.	OYA-IW-3.2	IW	x	x	-	-	-	-	-	
322	30.08.	OYA-IW-3.3	IW	x	x	-	x	62.0	7.04	-	
323	30.08.	OYA-IW-3.4	IW	x	x	x	-	-	-	CAF	
324	30.08.	OYA-IW-3.5	IW	x	x	-	x	68.9	7.12	-	
325	30.08.	OYA-IW-3.6	IW	x	x	-	-	-	-	CAF	
326	30.08.	OYA-IW-3.7	IW	x	x	-	-	-	-	-	
327	30.08.	OYA-IW-3.8	IW	x	x	-	-	-	-	-	
328	30.08.	OYA-IW-3.9	RIW	x	x	x	x	69.7	6.30	-	
329	30.08.	OYA-IW-3.10	RIW	x	x	x	-	-	-	-	
330	30.08.	OYA-IW-3.11	RIW	x	x	x	x	71.4	6.42	-	
331	30.08.	OYA-IW-3.12	RIW	x	x	x	-	-	-	-	
332	30.08.	OYA-IW-3.13	RIW	x	x	x	x	29.7	6.57	-	
333	30.08.	OYA-3-2.TI	TI	x	x	-	x	2400	7.61	-	SAL=1.3‰
334	30.08.	OYA-3-4.TI	TI	x	x	-	-	-	-	-	
335	30.08.	OYA-3-9.TI	TI	x	x	-	x	747	7.38	-	
336	30.08.	OYA-4-1.TI	TI	x	x	-	x	486	5.66	-	
337	30.08.	OYA-4-2.TI	TI	x	x	x	-	-	-	-	
338	30.08.	OYA-IW1.TI	TI	x	x	-	x	182	7.70	-	
339	30.08.	OYA-IW-5.TI	TI	x	x	-	x	67.8	5.80	-	

			Isotopes			Chemistry				
Nr.	date	sample	type	^{18}O	^{2}H	^{3}H	anion/ cation	LF [µS/cm]	pH	filter	Remarks
340	30.08.	OYA-2-1.TI	TI	x	x	-	-	-	-	-	
341	30.08.	OYA-2-2.TI	TI	x	x	x	-	-	-	-	
342	30.08.	OYA-2-6.TI	TI	x	x	-	x	323	6.24	-	
343	30.08.	OYA-2-8.TI	TI	x	x	-	x	563	5.76	-	
344	30.08.	STAT-11-5 (2 m)	SW	x	x	-	-	-	-	-	
345	30.08.	STAT-11-1 (6 m)	SW	x	x	-	-	-	-	-	
346	27.08.	BW SERGEY	SW	-	-	-	-	26400	6.43	-	SAL=17.9‰
347	01.09.	aqua dest. Blank	-	-	-	-	x	-	-	-	
348	01.09.	tap water ship	-	-	-	-	x	-	-	-	
349	02.09.	MUO-3-1.TI	TI	-	-	-	-	-	-	-	
350	02.09.	MUO-3-2.TI	TI	-	-	-	-	-	-	-	
351	02.09.	MUO-3-3.TI	TI	-	-	-	x	-	-	-	Unfiltered. Frozen
352	02.09.	MUO-3-6.TI	TI	-	-	-	x	-	-	-	Unfiltered. Frozen
353	02.09.	MUO-3-7.TI	TI	-	-	-	x	-	-	-	Unfiltered. Frozen
354	02.09.	MUO-3-8.TI	TI	-	-	-	x	-	-	-	Unfiltered. Frozen
355	02.09.	MUO-3-10.TI	TI	-	-	-	x	-	-	-	Unfiltered. Frozen
356	02.09.	MUO-01	IW	x	x	-	x	-	-	-	Frozen
357	02.09.	MUO-02	IW	x	x	-	x	-	-	-	Frozen
358	02.09.	MUO-03	IW	x	x	-	x	-	-	-	Frozen
359	02.09.	MUO-04	IW	x	x	-	x	-	-	-	Frozen
360	02.09.	MUO-05	IW	x	x	-	x	-	-	-	Frozen
361	02.09.	MUO-06	IW	x	x	-	x	-	-	-	Frozen
362	02.09.	MUO-07	IW	x	x	-	x	-	-	-	Frozen
363	02.09.	MUO-08	IW	x	x	-	x	-	-	-	Frozen
364	02.09.	MUO-09	IW	x	x	-	x	-	-	-	Frozen
365	02.09.	MUO-10	IW	x	x	-	x	-	-	-	Frozen
366	02.09.	MUO-11	IW	x	x	-	x	-	-	-	Frozen
367	02.09.	MUO-12	IW	x	x	-	x	-	-	-	Frozen

Appendix 5.2-3. List of bone samples of the New Siberian Islands.

No.	samples	Taxon	Skeleton element	Preservation	Type Loc.	Locality	Remarks
		Stolbovoy Island (2 – 4 km from Stolbovaya River mouth)					
1	NS-Stl-O1	Ovibos sp.	Cranium with horn cores, female	Fragment	C	Exposure	Probably, samples 1 and 2 from one individual
2	NS-Stl-O2	Ovibos sp.	Cervical vertebra	Damaged	C	Exposure	
3	NS-Stl-O3	Equus caballus	Mandibula (right stem) with P2 - M3	Fragment	C	Exposure	Probably, samples 3, 4, 5 (C14) from one individual
4	NS-Stl-O4	Equus caballus	Thorax vertebra	Damaged, sore	C	Exposure	
5	NS-Stl-O5	Equus caballus	Tibia, left (with marrow)		C	Exposure	
6	NS-Stl-O6	Rangifer tarandus	Shed antler		B	Exposure, altitude 10-11 m	
7	NS-Stl-O7	Rangifer tarandus	Shed antler		B		Vivianit
8	NS-Stl-O8	Rangifer tarandus	Calcaneus, right		B		
9	NS-Stl-O9	Rangifer tarandus	Pelvis	Fragment	B		Trashed
10	NS-Stl-O10	Lepus sp.	Cranium	Fragment	E	Shore	
11	NS-Stl-O11	Rangifer tarandus	Sacrum	Fragment	E	Shore	Trashed
12	NS-Stl-O12	Bison priscus	Cranium with right horn	Fragment	E	Shore	
13	NS-Stl-O91	Large herbivorus mammal	Limb bone	Fragment	C	Exposure	

Appendix 5.2-3, continuation.

No.	samples	Taxon	Skeleton element	Preservation	Type Loc.	Locality	Remarks
		Kotel'ny Island (Cape Anisy area)					
14	NS-KAn-O13-a	Mammuthus primigenius	Humerus, right	Damaged	A	In situ, Baydzherakh in the tundra, altitude 10 m	Juv., trashed
15	NS-KAn-O13-b		Humerus, left	Damaged,	A		Juv., C14
16	NS-KAn-O13-c		Ulna	3 pieces, cut off	A		Juv., C14, samples 13c and 13e in natural conjunction
17	NS-KAn-O13-d		Femur, left		A		Juv., trashed
18	NS-KAn-O13-e		Radius	2 pieces, cut off	A		Juv., C14
19	NS-KAn-O13-f		Femur, right	Cut off	A		Juv., C14
20	NS-KAn-O14		Thorax vertebra	Damaged	D		Probably, samples 13, 14, 15 from one individual
21	NS-KAn-O15	Mammuthus primigenius	Cervical vertebra	Damaged	D	Baydzherakh in the tundra	
22	NS-KAn-O16	Equus caballus	Mandibula with P2-M3		D		Probably, samples 16, 17, 18, 19, 20 from one individual
23	NS-KAn-O17	Equus caballus	Pelvis	3 pieces	D		
24	NS-KAn-O18	Equus caballus	Mt III, left		D		
25	NS-KAn-O19	Equus caballus	Atlas		D		
26	NS-KAn-O20	Equus caballus	Ph I, left		D		
27	NS-KAn-O21	Ovibos sp.	Tibia, left	Distal fragment	D		
28	NS-KAn-O22	Rangifer tarandus	Shed antler	Fragment	D		
29	NS-KAn-O23	Rangifer tarandus	Mt III + IV, left		D		
30	NS-KAn-O24	Mammuthus primigenius	Tusk	Fragment	D		C14
31	NS-KAn-O25	Mammuthus primigenius	Tusk	Fragment	D		C14
32	NS-KAn-O26	? Rangifer tarandus	Thorax vertebra	2 pieces	D		

Appendix 5.2-3. continuation.

No.	samples	Taxon	Skeleton element	Preservation	Type Loc.	Locality	Remarks
33	NS-KAn-O27	Mammuthus primigenius	Tusk	Fragment	D	Baydzherakh in the tundra	C 14
34	NS-KAn-O28	Equus caballus	Humerus, left	Damaged	D		
35	NS-KAn-O29	Equus caballus	Ph I, left		D		
36	NS-KAn-O30-a	Equus caballus	Pelvis	Fragment, left part	D		Probably, samples 30b and 30c from one individual
37	NS-KAn-O30-b	Equus caballus	Humerus, left		A	In situ, baydzherakh in the tundra, altitude 10 m	Probably, samples from 30-i to 30-z from one individual, juv.
38	NS-KAn-O30-c	Equus caballus	Antebrachium, left	2 pieces	A		
39	NS-KAn-O30-d	Equus caballus	Tibia, left		A		
40	NS-KAn-O30-e	Equus caballus	Astragalus, right		A		
41	NS-KAn-O30-f	Equus caballus	Patella		A		
42	NS-KAn-O30-g	Equus caballus	Sacrum	Damaged, 2 pieces	A		
43	NS-KAn-O30-h	Equus caballus	Vertebra (8 bones)	Fragments	A		
44	NS-KAn-O30-i	Equus caballus	Epistropheus		A		
62	NS-KAn-O30-j	Equus caballus	3-rd cervical vertebra	Damaged	A		
62	NS-KAn-O30-k	Equus caballus	4-th cervical vertebra	2 pieces, damaged	A		
62	NS-KAn-O30-l	Equus caballus	5-th cervical vertebra	2 pieces, damaged	A		
62	NS-KAn-O30-m	Equus caballus	6-th cervical vertebra	2 pieces, damaged	A		
62	NS-KAn-O30-n	Equus caballus	7-th cervical vertebra	2 pieces, damaged	A		
62	NS-KAn-O30-o	Equus caballus	1-st thorax vertebra	2 pieces, damaged	A	In situ, baydzherakh in the tundra, altitude 10 m	Probably, samples 30-i to 30-z from one individual, juv.
62	NS-KAn-O30-p	Equus caballus	Thorax vertebra	2 pieces, damaged	A		
62	NS-KAn-O30-q	Equus caballus	Thorax vertebra	2 pieces, damaged	A		
62	NS-KAn-O30-r	Equus caballus	Thorax vertebra	2 pieces, damaged	A		
62	NS-KAn-O30-s	Equus caballus	Thorax vertebra	4 pieces, damaged	A		
62	NS-KAn-O30-t	Equus caballus	Thorax vertebra	Fragment	A		

Appendix 5.2-3. continuation.

No.	samples	Taxon	Skeleton element	Preservation	Type Loc.	Locality	Remarks
62	NS-KAn-O30-u	Equus caballus	Lumbar vertebra	2 fragments, damaged	A	In situ, baydzherakh in the tundra, altitude 10 m	
62	NS-KAn-O30-v	Equus caballus	Thorax vertebra	Fragment	A		
62	NS-KAn-O30-w	Equus caballus	Costa (5 bones)		A		
62	NS-KAn-O30-x	Equus caballus	Costa (35 bones)	Fragments	A		
62	NS-KAn-O30-y	Equus caballus	Vertebra, spinous process (8 bones)	Fragments	A		
62	NS-KAn-O30-z	Equus caballus	Costa (2 pieces)	Fragments, cartilage part	A		
62	NS-KAn-O31	Rangifer tarandus	Femur, left	Distal fragment	D	Baydzherakh in the tundra	Recent?
		Bel'kovsky Island (Cape Skalisty)					
63	NS-Bel-O32	Bison priscus	Radius, left	Damaged	C	Exposure	Probably, samples 32, 33, 34 (C14), 35, 36, 37 from one individual.
64	NS-Bel-O33	Bison priscus	Thorax vertebra	Damaged	C		
65	NS-Bel-O34	Bison priscus	Lumbar vertebra	Damaged	C		
66	NS-Bel-O35	Bison priscus	Humerus, right	Distal fragment	C		
67	NS-Bel-O36	Bison priscus	Pelvis (right part)	Damaged, 2 pieces	C		
68	NS-Bel-O37	Bison priscus	Thorax vertebra	Fragment, 2 pieces	C		
69	NS-Bel-O38	Mammuthus primigenius	Humerus	Fragment, cut off	D	Baydzherakh in the tundra	C 14
70	NS-Bel-O39	Equus caballus	Pelvis (left part)	Fragment	D	Baydzherakh in coastal outcrop	
71	NS-Bel-O40	Rangifer tarandus	Antler	Fragment	D		Trashed
72	NS-Bel-O41	Equus caballus	Humerus, right	Distal fragment	D	Baydzherakh in the tundra	
73	NS-Bel-O42	Equus caballus	Radius, left	Fragment	D		Trashed
74	NS-Bel-O43	Equus caballus	Mt III, right	Distal fragment	D		
75	NS-Bel-O44	Rangifer tarandus	Tibia, right	Fragment	D		Recent?
76	NS-Bel-O45	Mammuthus primigenius	Tusk	Fragment	E	Shore	C14, rounded

Appendix 5.2-3. continuation.

No.	samples	Taxon	Skeleton element	Preservation	Type Loc.	Locality	Remarks
77	NS-Bel-O46	? Rangifer tarandus	Tibia, left	Damaged	E		
78	NS-Bel-O47	Bison priscus	Horn sheet	Fragment, 2 pieces	E		
79	NS-Bel-O48	Equus caballus	Upper tooth	Fragment (6 pieces)	D	Baydzherakh in coastal outcrop	
80	NS-Bel-O92	Rangifer tarandus	Intermedium		D	Baydzherakh in the tundra	
		Kotel'ny Island (south-west coast, Khomurgannakh River mouth)					
81	NS-khom-O49	Mammuthus primigenius	Tusk	Fragment	D	Baydzherakh in the valley	C 14
82	NS-Khom-O50		Mc V, left	Damaged	D		
83	NS-Khom-O51		Tusk	Fragment	D		Probably, samples 51, 52 from one individual; trashed
84	NS-Khom-O52		Tusk	Fragment	D		
85	NS-Khom-O53	Rangifer tarandus	Shed antler	Fragment	D	Baydzherakh in the tundra	Recent?
86	NS-Khom-O54	Rangifer tarandus	Shed antler	Fragment, 2 pieces	D		Recent?
87	NS-Khom-O55	Rangifer tarandus	Antler	Fragment	D		Recent?
88	NS-Khom-O56	Rangifer tarandus	Mc III+IV, right	Damaged	D		Juv., recent?
89	NS-Khom-O57	Rangifer tarandus	Mc III+IV	Distal fragment	D		
90	NS-Khom-O58	Rangifer tarandus	Femur, right	Fragment, 2 pieces	D		Juv., sore, recent?
91	NS-Khom-O59	Mammuthus primigenius	Tusk	Fragment	C	Exposure	C 14
92	NS-Khom-O60		Upper tooth (M2 or M3)	Damaged	C		
93	NS-Khom-O61	Equus caballus	Scapula, right	Damaged	B	Exposure, altitude 15 m	Probably, samples 61, 62 from one individual
94	NS-Khom-O62		Radius, left		C		
95	NS-Khom-O63	Ovibos sp.	Humerus, left	Distal fragment	D	Baydzherakh in coastal outcrop	
96	NS-Khom-O64	Equus caballus	Mc III, right		D		Probably, samples 64, 65,

Appendix 5.2-3. continuation.

No.	samples	Taxon	Skeleton element	Preservation	Type Loc.	Locality	Remarks
97	NS-Khom-O65	Equus caballus	Ph I, right		D		66 from one individual
98	NS-Khom-O66	Equus caballus	Ph II		D	Baydzherakh in coastal outcrop	
99	NS-Khom-O67	Ovibos sp.	Mc III+IV, right	Damaged	D		
100	NS-Khom-O68	Large herbivorous mammal	Limb bone	Fragment	D	Baydzherakh in the tundra	Trashed
101	NS-Khom-O69		Limb bone	Fragment	D		Trashed
102	NS-Khom-O70		Limb bone	Fragment	D		Trashed
103	NS-Khom-O71	Rangifer tarandus	Ph I	Distal fragment	D		
104	NS-Khom-O72		Vertebra	Damaged	D		Recent?
105	NS-Khom-O73		Shed antler	Fragment	D		Trashed
106	NS-Khom-O74		Upper molar tooth		D		
107	NS-Khom-O75		Tibia, right	Distal fragment	D		
108	NS-Khom-O76		Scapula, right	Fragment	D		
109	NS-Khom-O77	Mammuthus primigenius	Vertebra	Fragment	D		C 14
110	NS-Khom-O78		Tusk	Fragment (3 pieces), cut off	D		C 14
		Novaya Sibir Island ("Derevyannye Gory)					
111	NS-Ndg-O79	Mammuthus primigenius	Tusk	Fragment	F	Near zimov'e	C 14
112	NS-Ndg-O80		Tusk	Fragment	F	Near zimov'e	C 14
113	NS-Ndg-O81	Mammuthus primigenius	Costa	Fragment	E	Shore	Trashed
114	NS-Ndg-O82	Rangifer tarandus	Scapula, left	Fragment	E	Shore	
115	NS-Ndg-O83	Equus caballus	Cervical vertebra		F	Tundra	C 14
116	NS-Ndg-O84	Large herbivorous mammal	Limb bone	Fragment	E	Shore	Heavily rounded, trashed

Appendix 5.2-3. continuation.

No.	samples	Taxon	Skeleton element	Preservation	Type Loc.	Locality	Remarks
		Novaya Sibir Island (south-east part of the location Hedenshtrom					
117	NS-Ndg-O85	Mammuthus primigenius	Limb bone	Fragment (2 pieces)	F	Tundra	C 14
118	NS-Ndg-O86		Tusk	Fragment	F	Tundra	C 14
119	NS-Ndg-O87		Tooth	Fragment	F	Tundra	
120	NS-Ndg-O88	Rangifer tarandus	Calcaneus, right		F	Tundra	
121	NS-Ndg-O89	Rangifer tarandus	Humerus, right	Distal fragment	E	Shore	
122	NS-Ndg-O90	Large herbivorous mammal	Limb bone	Fragment	E	Shore	Trashed
		Maly Lyakhovsky Island (2 - 3 km to the west of Cape Vaygach)					
123	NS-ML-O93	Mammuthus primigenius	Metacarpale		E	Shore	Heavily rounded
124	NS-ML-O94	Equus caballus	Tibia, left	Distal fragment	E	Shore	Rounded
125	NS-ML-O95	Large herbivorous mammal	Limb bone	Fragment	E	Shore	Rounded, trashed
126	NS-ML-O96	Bison priscus	Thorax vertebra	Fragment, 2 pieces	E	Shore	
127	NS-ML-O97	Bison priscus	Ulna	Fragment	E	Shore	
128	NS-ML-O98	? Ovibos sp.	Metapodium	Distal fragment	E	Shore	Rounded
129	NS-ML-O99	Ovibos sp.	Scapula, right	Fragment	E	Shore	
130	NS-ML-O100	Mammuthus primigenius	Tusk	Fragment	E	Shore	Rounded, C 14
131	NS-ML-O101		Tusk	Fragment	E	Shore	Rounded, C 14
132	NS-ML-O102		Tusk	Fragment	E	Shore	Trashed
133	NS-ML-O103	Rangifer tarandus	Tibia, left	Distal fragment	E	Shore	
134	NS-ML-O104	Bison priscus	Ph 1, left		E	Shore	
135	NS-ML-O105	Phoca sp.	Humerus	Damaged	E	Shore	Recent
136	NS-ML-O106	Rangifer tarandus	Ph 1		E	Shore	Recent

Appendix 5.2-3. continuation.

No.	samples	Taxon	Skeleton element	Preservation	Type Loc.	Locality	Remarks
137	NS-ML-O107	?Alopex sp.	Epistropheus		E	Shore	Recent
138	NS-ML-O108	Equus caballus	Cranium	Damaged	F	Tundra	
139	NS-ML-O109	Mammuthus primigenius	Tusk	Fragment	F	Tundra	
140	NS-ML-O110		Tibia	Fragment	F	Tundra	Trashed
141	NS-ML-O111		Humerus	Fragment	F	Tundra	Trashed
142	NS-ML-O112	Equus caballus	Mandibula with teeth (except I3)	Damaged (2 pieces)	F	Tundra	Very old
143	NS-ML-O113	Mammuthus primigenius	Pelvis (left part)	Fragment	D	Baydzherakh in tundra, 500 m E of the lighthouse	C 14
144	NS-ML-O114	Equus caballus	Tibia, left	Distal fragment	D	Baydzherakh near lighthouse	
145	NS-ML-O115	Equus caballus	Radius, left		D	Baydzherakh near lighthouse	
146	NS-ML-O116	Mammuthus primigenius	Scapula, left	Fragment	D	Baydzherakh in tundra, 500 m E of the lighthouse	Small, C 14
147	NS-ML-O117	Mammuthus primigenius	Vertebra	Fragment, spinous processum	D	Baydzherakh near the lighthouse	C 14
148	NS-ML-O118	Equus caballus	Mt III, left		D		
149	NS-ML-O119	Rangifer tarandus	Antler	Fragment	D		
150	NS-ML-O120	Rangifer tarandus	Femur, left	Distal fragment	D		
151	NS-ML-O121	? Rangifer tarandus	Radius, right		D		Probably, samples 121, 122, 123, 124 (trashed) from one individual, recent?
152	NS-ML-O122	Rangifer tarandus	Humerus, right	Distal fragment	D		
153	NS-ML-O123	Rangifer tarandus	Carpale II+III		D		
154	NS-ML-O124	Rangifer tarandus	Pelvis	Fragment	D	Baydzherakh near the lighthouse	
155	NS-ML-O125	Equus caballus	Mt III, right	Damaged	D		
156	NS-ML-O126	Mammuthus primigenius	Vertebra	Fragment, spinous processum	D		C 14
157	NS-ML-O127	Equus caballus	Humerus, right	Fragment	D		Trashed

Appendix 5.2-3. continuation.

No.	samples	Taxon	Skeleton element	Preservation	Type Loc.	Locality	Remarks
158	NS-ML-O128	Equus caballus	Humerus, right	Distal fragment	D		
159	NS-ML-O129	Mammuthus primigenius	Costa	Fragment	D		C 14
160	NS-ML-O130	Ovibos sp.	Mt III+IV, right		D		
161	NS-ML-O131	Rangifer tarandus	Mt III+IV, left	Proximal fragment	D		Recent ?
162	NS-ML-O132	Rangifer tarandus	Mt III+IV, right		D		Recent ?
163	NS-ML-O133	Rangifer tarandus	Ph I, left		D		Recent ?
164	NS-ML-O134	Rangifer tarandus	Radius	Fragment	D		Juv., recent?
165	NS-ML-O135	Rangifer tarandus	Shed antler	Fragment	D	Baydzherakh in tundra, 500 m from the lighthouse to the east	
166	NS-ML-O136	Mammuthus primigenius	Humerus	Fragment	D		C 14
167	NS-ML-O137		Tibia	Fragment, cut off	D		Juv., C 14
168	NS-ML-O138		Tusk	Fragment, cut off	D		C 14
169	NS-ML-O139		Femur, right	Fragment (2 pieces), cut off	D		C 14
170	NS-ML-O140		Femur, left	Fragment, cut off	D		C 14
171	NS-ML-O141		Humerus	Fragment, cut off	D		C 14
172	NS-ML-O142	Equus caballus	Mandibula (left stem) with teeth P2 - M1	Fragment	D		Trashed
173	NS-ML-O143	Mammuthus primigenius	Ulna, right	Distal fragment	F	Tundra	Juv.
174	NS-ML-O147	Mammuthus primigenius	Tooth	Fragment	D	Baydzherakh in tundra, 500 m E of the lighthouse	
175	NS-ML-O291		Pelvis	Fragment, cut off	D		C 14
176	NS-ML-O292		Limb bone	Fragment, cut off	D		C 14

Appendix 5.2-3. continuation.

No.	samples	Taxon	Skeleton element	Preservation	Type Loc.	Locality	Remarks
		Svyatoy Nos Cape (2 - 3 km from Serkin Urochichshe)					
177	NS-SN-O144	Equus caballus	Pelvis (right part)	Fragment	E	Shore	C 14
178	NS-SN-O145	Mammuthus primigenius	Tusk	Fragment	E		Trashed
179	NS-SN-O146		Tooth	Fragment	E		
		Oyogos Yar (4 km from Kondrat'eva River mouth to the west)					
180	NS-Ogk-O148	Mammuthus primigenius	Radius, right	Proximal fragment	F	Tundra	
181	NS-Ogk-O149		Tusk	Fragment	F		Trashed
182	NS-Ogk-O150	Bison priscus	Tibia, left	Fragment	C	Thermoterrace	
183	NS-Ogk-O151	Equus caballus	Femur, right	Damaged	C		
184	NS-Ogk-O152	Equus caballus	Mt III, left		C		
185	NS-Ogk-O153	Equus caballus	Mc III, right		C		
186	NS-Ogk-O154	Bison priscus	Humerus, left	Fragment	C		
187	NS-Ogk-O155	Bison priscus	Mt III+IV, left	Damaged	C		
188	NS-Ogk-O156	Equus caballus	Femur, right	Distal fragment	C	Thermoterrace	
189	NS-Ogk-O157	? Bison priscus	Mandibula (right stem) without teeth	Fragment	C		
190	NS-Ogk-O158	Bison priscus	Femur, right	Damaged	C		
191	NS-Ogk-O159	Bison priscus	Femur, left	Fragment	C		
192	NS-Ogk-O160	Equus caballus	Tibia, right		C		
193	NS-Ogk-O161	Bison priscus	Pelvis (right part)	Fragment	C		
194	NS-Ogk-O162	? Panthera spelaea	Femur	Fragment	C	Thermoterrace	
195	NS-Ogk-O163	Rangifer tarandus	Antler	Fragment	C		Trashed
196	NS-Ogk-O164	Rangifer tarandus	Scapula, right	Fragment	C		
197	NS-Ogk-O165	Rangifer tarandus	Tibia, right	Proximal fragment	C		

Appendix 5.2-3. continuation.

No.	samples	Taxon	Skeleton element	Preservation	Type Loc.	Locality	Remarks
198	NS-Ogk-O166	Bison priscus	Tibia, left	Fragment	C	Thermoterrace	Juv.
199	NS-Ogk-O167	Rangifer tarandus	Humerus, left		C		
200	NS-Ogk-O168	Rangifer tarandus	Astragalus		C		
201	NS-Ogk-O169	Rangifer tarandus	Radius, left	Proximal fragment	C		
202	NS-Ogk-O170	Rangifer tarandus	Mc III+IV	Proximal fragment, 2pieces	C		
203	NS-Ogk-O171	Mammuthus primigenius	? Ulna	Fragment	C		C 14
204	NS-Ogk-O172	Large herbivorous mammal	Limb bone	Fragment	C		Trashed
205	NS-Ogk-O173		Limb bone	Fragment	C		Trashed
206	NS-Ogk-O174		Costa	Fragment	C		
207	NS-Ogk-O175	Mammuthus primigenius	Tibia, right	Fragment	C		Juv.
208	NS-Ogk-O176		Femur, right	Fragment	C		Probably, samples 176 and 177 from one individual, juv
209	NS-Ogk-O177		Femur, left	Fragment	C		
210	NS-Ogk-O178	Equus caballus	Femur, left	Distal articulation	C		Juv.
211	NS-Ogk-O179	Bison priscus	Humerus, right	Distal fragment	C	Thermoterrace	
212	NS-Ogk-O180	Bison priscus	Femur, right	Proximal fragment	C		
213	NS-Ogk-O181	Bison priscus	Femur, left	Proximal fragment	C		
214	NS-Ogk-O182	Equus caballus	Mandibula (left stem) with teeth P2-M3 and I1 - I3	Fragment	C		
215	NS-Ogk-O183	Ovibos sp.	Horn sheet	Fragment	C		
216	NS-Ogk-O184	Rangifer tarandus	Tibia, left	Fragment	C		Juv.
217	NS-Ogk-O185	Rangifer tarandus	Tibia, left	Proximal fragment	C		
218	NS-Ogk-O186	Equus caballus	Thorax vertebra	Damaged	C		
219	NS-Ogk-O187	Rangifer tarandus	Shed antler	Fragment	C		
220	NS-Ogk-O188	Mammuthus primigenius	Femur	Fragment	C		Juv., C 14
221	NS-Ogk-O189	Mammuthus primigenius	Vertebra	Fragment, spinous processum	C	Thermoterrace	Trashed

Appendix 5.2-3. continuation.

No.	samples	Taxon	Skeleton element	Preservation	Type Loc.	Locality	Remarks
222	NS-Ogk-O190	Bison priscus	Radius, left		C		
223	NS-Ogk-O191	Bison priscus	Pelvis	Fragment	C		Juv.
224	NS-Ogk-O192	Mammuthus primigenius	Limb bone	Fragment	C		C 14
225	NS-Ogk-O193	Large herbivorous mammal	Costa	Fragment	E	Shore, near stream mouth	Trashed
226	NS-Ogk-O194	Mammuthus primigenius	Tusk	Fragment	E	Shore, near stream mouth	Trashed
227	NS-Ogk-O195		Tusk	Fragment	E		Trashed
228	NS-Ogk-O196		Tusk	Fragment	E		Trashed
229	NS-Ogk-O197		Tusk	Fragment	E		Trashed
230	NS-Ogk-O198		Tusk	Fragment	E		Trashed
231	NS-Ogk-O199		Tusk	Fragment	E	Shore, near stream mouth	Trashed
232	NS-Ogk-O200		Tusk	Fragment	E		Trashed
233	NS-Ogk-O201		Tusk	Fragment	E		Trashed
234	NS-Ogk-O202	Rangifer tarandus	Antler	Fragment	E		Trashed
235	NS-Ogk-O203	Rangifer tarandus	Antler	Fragment	E		Trashed
236	NS-Ogk-O204	Rangifer tarandus	Antler	Fragment	E		Trashed
237	NS-Ogk-O205	Large herbivorous mammal	Mandibula	Fragment	E		Trashed
238	NS-Ogk-O206	Large herbivorous mammal	Limb bone	Fragment	E		Trashed
239	NS-Ogk-O207	Equus caballus	Tooth (M)	Fragment	E		Trashed
240	NS-Ogk-O208	Equus caballus	Scapula, right	Fragment	E		
241	NS-Ogk-O209	Equus caballus	Ph I, right		E		Rounded
242	NS-Ogk-O210	Equus caballus	Antebrachium, right	With marrou	E		
243	NS-Ogk-O211	Bison priscus	Horn sheet	Fragment	E		
244	NS-Ogk-O212	Bison priscus	Horn sheet	Damaged	E		
245	NS-Ogk-O213	Equus caballus	Cranium	Occipital fragment	E		
246	NS-Ogk-O214	Mammuthus primigenius	Tusk	Fragment	E	Shore	
247	NS-Ogk-O215		Cranium	Fragment	E	Shore, near	C 14

Appendix 5.2-3. continuation.

No.	samples	Taxon	Skeleton element	Preservation	Type Loc.	Locality	Remarks
248	NS-Ogk-O216		Upper tooth (? M3)	Fragment	E	stream mouth	
249	NS-Ogk-O217		Upper tooth (M3)	Fragment	E	West shore	
250	NS-Ogk-O218		Upper tooth (M2 or M3)	Fragment	E	Shore, near stream mouth	
251	NS-Ogk-O219		Tooth	Fragment	E		
252	NS-Ogk-O220		Tusk	Fragment	E		C 14
253	NS-Ogk-O221		Costa	Fragment	E		C 14
254	NS-Ogk-O222	Bison priscus	Mc III+IV, left		E		
255	NS-Ogk-O223	Rangifer tarandus	Mandibula (left stern) with teeth dp2-dp4, M1-M2	Fragment	E		
256	NS-Ogk-O224	Bison priscus	Centrotarsale	Fragment	E		Trashed
257	NS-Ogk-O225	Mammuthus primigenius	Humerus, left	Fragment	E		C 14
258	NS-Ogk-O226	Bison priscus	Ph I, right		E		
259	NS-Ogk-O227	Mammuthus primigenius	Tooth	Fragment	E		
260	NS-Ogk-O228		Tooth	Fragment	E		
261	NS-Ogk-O229	Bison priscus	Ph II, left	Fragment	E		
262	NS-Ogk-O230	? Bison priscus	Small limb bone	Fragment	E		
263	NS-Ogk-O231	? Bison priscus	Small limb bone	Fragment	E		
264	NS-Ogk-O232	Equus caballus	Astragalus, right	Fragment	E		Rounded, trashed
265	NS-Ogk-O233	? Bison priscus	Small limb bone	Fragment	E		
266	NS-Ogk-O234	Rangifer tarandus	Calcaneus	Fragment	E		Trashed
267	NS-Ogk-O235	? Mammuthus primigenius	Costa		E		Rounded, trashed
268	NS-Ogk-O236	Mammuthus primigenius	Ph I, font 4-th, left		E	Shore, near stream mouth	
269	NS-Ogk-O237	Bison priscus	Ph I, right		E		
270	NS-Ogk-O238	Bison priscus	Mc III+IV	Fragment	E		Trashed
271	NS-Ogk-O239	Bison priscus	Astragalus, left	Damaged	E		
272	NS-Ogk-O240	Bison priscus	Tarsale II+III, right		E		
273	NS-Ogk-O241	Rangifer tarandus	Astragalus	Fragment	E		Rounded, trashed

Appendix 5.2-3. continuation.

No.	samples	Taxon	Skeleton element	Preservation	Type Loc.	Locality	Remarks
274	NS-Ogk-O242	Rangifer tarandus	Antler	Fragment	E		Trashed
275	NS-Ogk-O243	Equus caballus	Pelvis	Fragment	E		Trashed
276	NS-Ogk-O244	Rangifer tarandus	Upper tooth		E		
277	NS-Ogk-O245	Rangifer tarandus	Lower tooth (M3)	Damaged	E		
278	NS-Ogk-O246	Mammuthus primigenius	Epistropheus	Damaged	E		
279	NS-Ogk-O247	Large herbivorous mammal	Limb bone	Fragment	E		Trashed
280	NS-Ogk-O248	? Mammuthus primigenius	Costa	Fragment	E		C 14
281	NS-Ogk-O249	Mammuthus primigenius	Thorax vertebra	Fragment, spinous processum	E	West shore	C 14
282	NS-Ogk-O250	Bison priscus	Femur, right	Fragment	E		C 14
283	NS-Ogk-O251	Bison priscus	Mc III+IV, left	Fragment	E		
284	NS-Ogk-O252	Bison priscus	Radius, right	Distal fragment, with marrow	E		
285	NS-Ogk-O253	Bison priscus	Calcaneus, right	Fragment	E		
286	NS-Ogk-O254	Equus caballus	Scapula, right	Fragment	E		
287	NS-Ogk-O255	Mammuthus primigenius	Limb bone	Fragment	E		Trashed
288	NS-Ogk-O256	Equus caballus	Mt III, right	Proximal fragment	E		
289	NS-Ogk-O257	Equus caballus	Mc III, right	Distal fragment	E		Rounded
290	NS-Ogk-O258	Large herbivorous mammal	Pelvis	Fragment	E		Trashed
291	NS-Ogk-O259	? Bison priscus	Humerus	Fragment	E	West shore	Trashed
292	NS-Ogk-O260	Mammuthus primigenius	Tusk	Fragment	E		
293	NS-Ogk-O261		Tusk	Fragment	E		
294	NS-Ogk-O262	Bison priscus	Antebrachium, right	Damaged	E		
295	NS-Ogk-O263	Bison priscus	Ph I, right		E		
296	NS-Ogk-O264	Mammuthus primigenius	Tooth	Fragment	E		

Appendix 5.2-3. continuation.

No.	samples	Taxon	Skeleton element	Preservation	Type Loc.	Locality	Remarks
297	NS-Ogk-O265	Large herbivorous mammal	? Humerus	Fragment	E		Trashed
298	NS-Ogk-O266	Rangifer tarandus	Pelvis (left part)	Fragment	E		
299	NS-Ogk-o267a	Mammuthus primigenius	Pelvis (left part)	Cut off	E	East shore	Samples 267-a (C 14) and 267-b (trashed) from one individual
300	NS-Ogk-o267b		Pelvis (right part)		E		
301	NS-Ogk-O268		Femur, left	Fragment, with marrow, cut off	E		Juv., C 14
302	NS-Ogk-O269		Humerus, left	Fragment, with marrow, cut off	E		C 14
303	NS-Ogk-O270		Ulnae, left	Fragment, cut off	C	Thermoterrace	C 14
304	NS-Ogk-O271		Ulnae, left	Fragment, with marrow, cut off	E	West shore	C 14
305	NS-Ogk-O272		Femur, right	Fragment, cut off	E		C 14
306	NS-Ogk-O273		Femur	Fragment, cut off	E		C 14
307	NS-Ogk-O274		Femur, right	Fragment, cut off	E		C 14
308	NS-Ogk-O275		Tusk	Fragment, cut off	E		C 14
309	NS-Ogk-O276		Tusk	Fragment	E		Trashed
310	NS-Ogk-O277		Tusk	Fragment, cut off	E		C 14
311	NS-Ogk-O278		Antebrachium, right	Fragment, cut off	E	West shore	C 14
312	NS-Ogk-O279		Humerus	Fragment, cut off	E	West shore	C 14
313	NS-Ogk-O280		Antebrachium, right	Fragment, cut off	E	West shore	C 14
314	NS-Ogk-O281		Tusk	Fragment, cut off	E	West shore	C 14
315	NS-Ogk-O282	Mammuthus primigenius Mammuthus primigenius	Humerus, left	Fragment, cut off	E	West shore	C 14
316	NS-Ogk-O283		Tusk	Fragment, cut off	E	West shore	C 14
317	NS-Ogk-O284		Tibia, left	Fragment, cut off	E	West shore	C 14
318	NS-Ogk-O285		Humerus, left	Fragment, cut off	E	West shore	C 14

Appendix 5.2-3. continuation.

No.	samples	Taxon	Skeleton element	Preservation	Type Loc.	Locality	Remarks
319	NS-Ogk-O286		Costa	Fragment	A	In situ, costal outcrop, 100 m east of the stream mouth, altitude 1 m	Probably, samples 267-a, 267-b, 268, 269, 286 (C 14) from one individual
320	NS-Ogk-O287		Humerus, left	Fragment	E	West shore	C 14
321	NS-Ogk-O288		Scapula, right	Fragment, cut off	E	West shore	C 14
322	NS-Ogk-O289		Tusk	Fragment, cut off	F	Tundra	C 14
323	NS-Ogk-O290		Tusk	Fragment, cut off	E	West shore	C 14
324	NS-Ogk-O293		Tusk	Fragment	E	West shore	Trashed
325	NS-Ogk-O294		Tusk	Fragment	E	West shore	Trashed
326	NS-Ogk-O295		Tusk	Fragment	E	West shore	Trashed
327	NS-Ogk-O296		Tusk	Fragment	E	West shore	Trashed
328	NS-Ogk-O297		Tusk	Fragment	E	West shore	Trashed
329	NS-Ogk-O298		Tusk	Fragment	E	West shore	Trashed
330	NS-Ogk-O299		Tusk	Fragment	E	West shore	Trashed
331	NS-Ogk-O300		Tusk	Fragment	E	West shore	Trashed
332	NS-Ogk-O301		Tusk	Fragment	E	West shore	C 14
333	NS-Ogk-O302		Tusk	Fragment	E	West shore	C 14
334	NS-Ogk-O303		Tusk	Fragment	E	West shore	C 14
335	NS-Ogk-O304		Tusk	Fragment	E	West shore	C 14
336	NS-Ogk-O305		Tusk	Fragment	E	West shore	Trashed
337	NS-Ogk-O306		Tusk	Fragment	E	West shore	C 14
338	NS-Ogk-O307		Tusk	Fragment	E	West shore	Trashed
339	NS-Ogk-O308		Tusk	Fragment	E	West shore	Trashed
340	NS-Ogk-O309		Tusk	Fragment	E	West shore	Trashed
341	NS-Ogk-O310	Mammuthus primigenius	Tusk	Fragment	E	West shore	Trashed
342	NS-Ogk-O311		Tusk	Fragment	E	West shore	Trashed
343	NS-Ogk-O312		Tusk	Fragment	E	West shore	Trashed
344	NS-Ogk-O313		Tusk	Fragment	E	West shore	Trashed

Appendix 5.2-3. continuation.

No.	samples	Taxon	Skeleton element	Preservation	Type Loc.	Locality	Remarks
345	NS-Ogk-O314		Tusk	Fragment	E	West shore	Trashed
346	NS-Ogk-O315		Tusk	Fragment	E	West shore	Trashed
347	NS-Ogk-O316		Tusk	Fragment	E	West shore	C 14
348	NS-Ogk-O317		Tusk	Fragment	E	West shore	C 14
349	NS-Ogk-O318		Tusk	Fragment	E	West shore	C 14
350	NS-Ogk-O319		Tusk	Fragment	E	West shore	Trashed
351	NS-Ogk-O320		Tusk	Fragment	E	West shore	C 14
352	NS-Ogk-O321		Tooth	Fragment	E	West shore	Trashed
353	NS-Ogk-O322		Tooth	Fragment	E	West shore	Trashed
354	NS-Ogk-O323	Rangifer tarandus	Shed antler	Fragment	E	West shore	
355	NS-Ogk-O324	Mammuthus primigenius	Limb bone	Fragment	E	West shore	Trashed
356	NS-Ogk-O325	Bison priscus	Radius, right		E	West shore	
357	NS-Ogk-O326	Bison priscus	Radius, right	Distal fragment	E	West shore	
358	NS-Ogk-O327	Equus caballus	Mt III, right	Fragment	E	West shore	Rounded
359	NS-Ogk-O328	Mammuthus primigenius	Tusk	Fragment	E	West shore	C 14
360	NS-Ogk-O329		Costa	Fragment	E	West shore	C 14
361	NS-Ogk-O330	Bison priscus	Humerus, right	Distal fragment	E	West shore	
362	NS-Ogk-O331	Bison priscus	Femur, left	Fragment	E	West shore	C 14
363	NS-Ogk-O332	Mammuthus primigenius	Limb bone	Fragment	E	West shore	Trashed
364	NS-Ogk-O333		Femur, left	Distal fragment	E	West shore	C 14
365	NS-Ogk-O334	Equus caballus	Ph I, left		E	West shore	
366	NS-Ogk-O335	Equus caballus	Ph I, right		E	West shore	
367	NS-Ogk-O336	Mammuthus primigenius	Scapula	Fragment	E	West shore	C 14
368	NS-Ogk-O337		Humerus, left	Fragment	E	West shore	C 14
369	NS-Ogk-O338	Equus caballus	Mandibula (right stem) with teeth dp2-dp4	Fragment	E	West shore	
370	NS-Ogk-O339	Equus caballus	Pelvis (right part)	Fragment	E	West shore	
371	NS-Ogk-O340	Mammuthus primigenius	Femur, left	Fragment	A	West shore	C 14

Appendix 5.2-3. continuation.

No.	samples	Taxon	Skeleton element	Preservation	Type Loc.	Locality	Remarks
372	NS-Ogk-O341	Bison priscus	Scapula, left	Fragment	E	Shore, near stream mouth	
373	NS-Ogk-O342	Bison priscus	Astrogalus, left		E		
374	NS-Ogk-O343	Ovibos sp.	Cervical vertebra	Damaged	E		
375	NS-Ogk-O344	Bison priscus	Astrogalus, left	Fragment	E		
376	NS-Ogk-O345	Ovibos sp.	Thorax vertebra	Damaged	E		Trashed
377	NS-Ogk-O346	Mammuthus primigenius	Vertebra	Fragment, spinous processum	E		Trashed
378	NS-Ogk-O347	Large herbivorous mammal	Limb bone	Fragment	E		Trashed
379	NS-Ogk-O348		Limb bone	Fragment	E		Trashed
380	NS-Ogk-O349	Ovibos sp.	Astrogalus, left		E		
381	NS-Ogk-O350	Mammuthus primigenius	Mc IV	Fragment	E		Juv.
382	NS-Ogk-O351		Tusk	Fragment	E	West shore	C 14
383	NS-Ogk-O352		Tusk	Fragment	E	West shore	C 14
384	NS-Ogk-O353		Tusk	Fragment	E	West shore	C 14
385	NS-Ogk-O354		Lower tooth (?M2)	Damaged	E	West shore	
386	NS-Ogk-O355		Scapula, left	Fragment	E	West shore	C 14
387	NS-Ogk-O356	Bison priscus	Humerus, left	Distal fragment	E	West shore	
388	NS-Ogk-O357	Bison priscus	Mc III+IV, left		E	West shore	
389	NS-Ogk-O358	Bison priscus	Carpal intermedium, left		E	West shore	
390	NS-Ogk-O359	Mammuthus primigenius	Limb bone	Fragment	E	West shore	Trashed
391	NS-Ogk-O360	Equus caballus	Tibia, right	Distal fragment	E	West shore	
392	NS-Ogk-O361	Equus caballus	Astrogalus, left		E	West shore	
393	NS-Ogk-O362	? Bison priscus	Ulnae, right	Fragment	E	West shore	
394	NS-Ogk-O363	Equus caballus	Ph III	Fragment	E	West shore	
395	NS-Ogk-O364	Ovibos sp.	Astrogalus, right		E	West shore	
396	NS-Ogk-O365	Ovibos sp.	Astrogalus, left	Damaged	E	West shore	
397	NS-Ogk-O366	Ovibos sp.	Astrogalus, right		E	West shore	
398	NS-Ogk-O367	Bison priscus	Ph I		E	West shore	
399	NS-Ogk-O368	Equus caballus	?Cuneiforme III	Fragment	E	West shore	Trashed

Appendix 5.2-3. continuation.

No.	samples	Taxon	Skeleton element	Preservation	Type Loc.	Locality	Remarks
400	NS-Ogk-O369	Equus caballus	Scapula, right	Fragment	E	West shore	
401	NS-Ogk-O370	Mammuthus primigenius	Femur, left	Fragment	E	West shore	Juv.
402	NS-Ogk-O371	Rangifer tarandus	Costa	Fragment	E	West shore	
403	NS-Ogk-O372	Mammuthus primigenius	Lower tooth (M2 or M3)	Fragment	E	West shore	
404	NS-Ogk-O373		Mandibula (right stem) without teeth	Fragment (3 pieces)	E	West shore	Juv., C 14
405	NS-Ogk-O374	Equus caballus	Ulnae, right	Damaged	E	West shore	
406	NS-Ogk-O375	Bison priscus	Upper tooth	Damaged	E	West shore	
407	NS-Ogk-O376	Bison priscus	Femur, right	Fragment	E	West shore	
408	NS-Ogk-O377	Bison priscus	Lumbar vertebra	Damaged	E	West shore	
409	NS-Ogk-O378	Rangifer tarandus	Mandibula (right stem) with tooth M3	Fragment	E	West shore	
410	NS-Ogk-O379	Mammuthus primigenius	Tooth, heavily worn	Fragment	E	West shore	
411	NS-Ogk-O380		Tooth, heavily worn	Fragment	E	West shore	
412	NS-Ogk-O381	Equus caballus	Pelvis	Fragment	E	West shore	Trashed
413	NS-Ogk-O382	Bison priscus	Tibia, right	Distal fragment	E	West shore	
414	NS-Ogk-O383	Mammuthus primigenius	Limb bone	Fragment	E	West shore	Rounded, trashed
415	NS-Ogk-O384	Large herbivorous mammal	Cervical vertebra	Fragment	E	West shore	Trashed
416	NS-Ogk-O385	Bison priscus	Horn sheet	Fragment	E	West shore	
417	NS-Ogk-O386	Equus caballus	Tibia, right	Distal fragment	E	West shore	
418	NS-Ogk-O387	Bison priscus	Cranium	Fragment	E	West shore	Trashed
419	NS-Ogk-O388	Mammuthus primigenius	Tibia, left	Fragment	E	West shore	C 14
420	NS-Ogk-O389	? Mammuthus primigenius	Limb bone	Fragment	E	West shore	Trashed
421	NS-Ogk-O390	Mammuthus primigenius	Humerus, right	Fragment	E	West shore	C 14

Appendix 5.2-3. continuation.

No.	samples	Taxon	Skeleton element	Preservation	Type Loc.	Locality	Remarks
422	NS-Ogk-O391	Rangifer tarandus	Scapula, right	Fragment	E	West shore	
423	NS-Ogk-O392	Rangifer tarandus	Mt III+IV	Distal fragment	E	West shore	
424	NS-Ogk-O393	Rangifer tarandus	Calcaneus	Damaged	E	West shore	
425	NS-Ogk-O394	Large herbivorous mammal	Limb bone	Fragment	E	West shore	Trashed
426	NS-Ogk-O395	Mammuthus primigenius	Vertebra	Fragment, spinous processum	E	West shore	Trashed
427	NS-Ogk-O396	? Bison priscus	Humerus, left	Fragment	E	West shore	Trashed
428	NS-Ogk-O397	Rangifer tarandus	Shed antler	Fragment	E	West shore	Trashed
429	NS-Ogk-O398	Bison priscus	Ulnae	Fragment	E	West shore	Trashed
430	NS-Ogk-O399	Large herbivorous mammal	? Humerus	Fragment	E	West shore	Trashed
431	NS-Ogk-O400	Equus caballus	Ph I, right	Fragment	E	West shore	
432	NS-Ogk-O401	Equus caballus	Ulnae, left	Fragment	E	West shore	Trashed
433	NS-Ogk-O402	? Bison priscus	Pelvis	Fragment	E	West shore	Trashed
434	NS-Ogk-O403	Bison priscus	Ulnae	Fragment	E	West shore	Trashed
435	NS-Ogk-O404	Bison priscus	Small limb bone	Fragment	E	West shore	
436	NS-Ogk-O405	Rangifer tarandus	Metapodia	Fragment	E	West shore	Juv.
437	NS-Ogk-O406	? Equus caballus	Thorax vertebra	Fragment	E	West shore	Trashed
438	NS-Ogk-O407	Bison priscus	Ph I, left	Fragment	E	West shore	
439	NS-Ogk-O408	Large herbivorous mammal	Limb bone	Fragment	E	West shore	Trashed
440	NS-Ogk-O409		Limb bone	Fragment	E	West shore	Trashed
441	NS-Ogk-O410		Limb bone	Fragment	E	West shore	Trashed
442	NS-Ogk-O411		Limb bone	Fragment	E	West shore	Trashed
443	NS-Ogk-O412		Limb bone	Fragment	E	West shore	Trashed
444	NS-Ogk-O413	Mammuthus primigenius	Tusk	Fragment	E	West shore	C 14
445	NS-Ogk-O414	Equus caballus	Ph I	Fragment	E	West shore	Trashed
446	NS-Ogk-O415	Equus caballus	Mc III	Fragment	E	West shore	Trashed
447	NS-Ogk-O416	Equus caballus	Lower tooth	Fragment	E	West shore	Trashed

Appendix 5.2-3. continuation.

No.	samples	Taxon	Skeleton element	Preservation	Type Loc.	Locality	Remarks
448	NS-Ogk-O417	? Equus caballus	Cervical vertebra	Fragment	E	West shore	
449	NS-Ogk-O418	Equus caballus	Ph I	Fragment	E	West shore	Trashed
450	NS-Ogk-O419	Rangifer tarandus	Shed antler	Fragment	E	West shore	Trashed
451	NS-Ogk-O420	Rangifer tarandus	Shed antler	Fragment	E	West shore	Trashed
452	NS-Ogk-O421	Rangifer tarandus	Sacrum	Fragment	E	West shore	Trashed
453	NS-Ogk-O422	Large herbivorous mammal	Costa	Fragment	E	West shore	Trashed
454	NS-Ogk-O423	? Bison priscus	Tooth	Fragment	E	West shore	Trashed
455	NS-Ogk-O424	Equus caballus	Naviculare	Fragment	E	West shore	Trashed
456	NS-Ogk-O425	Mammuthus primigenius	Lower tooth (P4 or M1)		C	Thermoterrace	
457	NS-Ogk-O426	Bison priscus	Tibia, left	Distal fragment	E	West shore	
458	NS-Ogk-O427	Bison priscus	Ph I, right		E	West shore	
459	NS-Ogk-O428	Mammuthus primigenius	Femur	Fragment	E	West shore	C 14
460	NS-Ogk-O429		Limb bone	Fragment	E	West shore	C 14
461	NS-Ogk-O430		Ulnare		D	Baydzherakh in tundra, near to the theodolite	C 14
462	NS-Ogk-O431	Rangifer tarandus	Shed antler	Fragment	E	West shore	Vivianit
463	NS-Ogk-O432	Mammuthus primigenius	Atlas	Damaged	E	Shore, near stream mouth	C 14
464	NS-Ogk-O433		Mc IV, right		E		
465	NS-Ogk-O434	Bison priscus	Lumbar vertebra	Damaged	E	Shore, near stream mouth	
466	NS-Ogk-O435	Mammuthus primigenius	Humerus	Distal fragment	E	Shore, near stream mouth	Juv.
467	NS-Ogk-O436		Mandibula (right stem) without teeth	Fragment	E	West shore	C 14
468	NS-Ogk-O437		Ulnae	Fragment	E	West shore	C 14
469	NS-Ogk-O438	Bison priscus	Cervical vertebra	Damaged	E	West shore	
470	NS-Ogk-O439	Ovibos sp.	Humerus, left	Distal fragment	E	West shore	
471	NS-Ogk-O440	Large herbivorous	Cranium	Fragment	E	West shore	Trashed

Appendix 5.2-3. continuation.

No.	samples	Taxon	Skeleton element	Preservation	Type Loc.	Locality	Remarks
		mammal					
472	NS-Ogk-O441	Mammuthus primigenius	Cervical vertebra	Fragment	E	West shore	Trashed
473	NS-Ogk-O442		Radius, right	Fragment	E	West shore	C 14
474	NS-Ogk-O443	Equus caballus	Ph I, left		E	West shore	
475	NS-Ogk-O444	Mammuthus primigenius	Limb bone	Fragment (2 pieces)	E	West shore	
476	NS-Ogk-O445	Bison priscus	Pelvis (left part)	Fragment	E	West shore	C 14
477	NS-Ogk-O446	Mammuthus primigenius	Pelvis	Fragment	E	West shore	Trashed
478	NS-Ogk-O447		Tusk	Fragment	E	West shore	C 14
479	NS-Ogk-O448	Bison priscus	Epistropheus	Damaged	E	West shore	
480	NS-Ogk-O449	Rangifer tarandus	Mt III+IV	Fragment	E	West shore	
481	NS-Ogk-O450	Bison priscus	Ph II, left		E	West shore	
482	NS-Ogk-O451	Rangifer tarandus	Mandibula (left stem) with teeth P2-P3	Fragment	E	West shore	
483	NS-Ogk-O452	Mammuthus primigenius	Vertebra	Fragment, spinous processum	E	West shore	Trashed
484	NS-Ogk-O453	Large herbivorous mammal	Costa	Fragment	E	West shore	Trashed
485	NS-Ogk-O454	Bison priscus	Ph II, right	Fragment	E	West shore	Trashed
486	NS-Ogk-O455	Mammuthus primigenius	Vertebra	Fragment	E	West shore	Trashed
487	NS-Ogk-O456	Bison priscus	Pelvis, left	Fragment	E	West shore	
488	NS-Ogk-O457	Equus caballus	Astrogalus, right		E	West shore	
489	NS-Ogk-O458	Equus caballus	Ph II	Damaged	E	West shore	
490	NS-Ogk-O459	Equus caballus	Ph III		E	West shore	
491	NS-Ogk-O460	Equus caballus	Astrogalus, right	Fragment	E	West shore	Trashed
492	NS-Ogk-O461	Ovibos sp.	Vertebra	Fragment	E	West shore	
493	NS-Ogk-O462	Bison priscus	Cervical vertebra		E	West shore	
494	NS-Ogk-O463	Bison priscus	Ph III, right		E	West shore	
495	NS-Ogk-O464	Bison priscus	Ph II, left		E	West shore	

Appendix 5.2-3. continuation.

No.	samples	Taxon	Skeleton element	Preservation	Type Loc.	Locality	Remarks
496	NS-Ogk-O465	? Rangifer tarandus	Sacrum	Fragment	E	West shore	
497	NS-Ogk-O466	? Ovibos sp.	Ph II, left		E	West shore	
498	NS-Ogk-O467	Equus caballus	Ph II	Damaged	E	West shore	Juv.
499	NS-Ogk-O468	Bison priscus	Ulnare	Fragment	E	West shore	
500	NS-Ogk-O469	Bison priscus	Calcaneus, left	Fragment	E	West shore	Trashed
501	NS-Ogk-O470	Ovibos sp.	Astrogalus, right	Damaged	E	West shore	
502	NS-Ogk-O471	Bison priscus	Cervical vertebra	Fragment	E	West shore	
503	NS-Ogk-O472	Bison priscus	Sacrum	Damaged	E	West shore	
504	NS-Ogk-O473	Bison priscus	? Thorax vertebra	Fragment	E	West shore	
505	NS-Ogk-O474	Mammuthus primigenius	Mt V, left	Fragment	E	West shore	Trashed
506	NS-Ogk-O475	? Bison priscus	? Cervical vertebra	Fragment	E	West shore	
507	NS-Ogk-O476	Mammuthus primigenius	Mc III, left	Damaged	E	West shore	
508	NS-Ogk-O477		Centrale		E	West shore	
509	NS-Ogk-O478		Epistropheus	Damaged	E	West shore	
510	NS-Ogk-O479		Tibia, right	Proximal fragment	E	West shore	Juv., C 14
511	NS-Ogk-O480	Equus caballus	Ph I	Distal fragment	E	West shore	
512	NS-Ogk-O481	Mammuthus primigenius	Tooth	Fragment	E	West shore	Trashed
513	NS-Ogk-O482		Tooth, heavily worn	Fragment	E	West shore	Trashed
514	NS-Ogk-O483		Tooth, heavily worn	Fragment	E	West shore	Trashed
515	NS-Ogk-O484	Equus caballus	Ph II	Fragment	E	West shore	
516	NS-Ogk-O485	Equus caballus	Magnum, right		E	West shore	
517	NS-Ogk-O486	? Ovibos sp.	Ph I, right	Fragment	E	West shore	
518	NS-Ogk-O487	Equus caballus	Ph I	Fragment	E	West shore	Trashed
519	NS-Ogk-O488	Equus caballus	Upper tooth	Fragment	E	West shore	
520	NS-Ogk-O489	Mammuthus primigenius	Tooth	Fragment	E	West shore	Trashed
521	NS-Ogk-O490	Rangifer tarandus	Ph II, right	Fragment	E	West shore	
522	NS-Ogk-O491	Mammuthus primigenius	Tusk	Fragment	E	West shore	

Appendix 5.2-3. continuation.

No.	samples	Taxon	Skeleton element	Preservation	Type Loc.	Locality	Remarks
523	NS-Ogk-O492	Lepus sp.	Tibia	Fragment	E	West shore	
524	NS-Ogk-O493	Mammuthus primigenius	Tooth	Fragment	C	Thermoterrace	
525	NS-Ogk-O494		Tooth		C	Thermoterrace	Trashed
526	NS-Ogk-O495	Mammal	? Lumbar vertebra	Fragment	E	West shore	Trashed
527	NS-Ogk-O496	Large herbivorus mammal	Palanx	Fragment	E	West shore	Trashed
528	NS-Ogk-O497	Equus caballus	Ph I	Distal fragment	E	West shore	Rounded, trashed
529	NS-Ogk-O498	Equus caballus	Tibia, left	Distal fragment	E	West shore	Trashed
530	NS-Ogk-O499	Rangifer tarandus	Metapodium	Fragment	E	West shore	Trashed
531	NS-Ogk-O500	Rangifer tarandus	Mt III+IV	Fragment	E	West shore	Trashed
532	NS-Ogk-O501	Equus caballus	Humerus	Fragment	E	West shore	Trashed
533	NS-Ogk-O502	Bison priscus	?	Fragment	E	West shore	
534	NS-Ogk-O503	Equus caballus or Bison priscus	Intermedium	Fragment	E	West shore	
535	NS-Ogk-O504	? Equus caballus	Incisor, heavily worn		E	West shore	
536	NS-Ogk-O505	Bison priscus	Lower tooth	Damaged	E	West shore	
537	NS-Ogk-O506	Bison priscus	Upper premolare tooth	Damaged	E	West shore	
538	NS-Ogk-O507	Bison priscus	Lower tooth	Fragment	E	West shore	Trashed
539	NS-Ogk-O508	Bison priscus	Upper tooth	Fragment	E	West shore	Trashed
540	NS-Ogk-O509	Rangifer tarandus	Ph I, left	Distal fragment	E	West shore	Rounded
541	NS-Ogk-O510	Rangifer tarandus	Carpale II+III		E	West shore	
542	NS-Ogk-O511	Rangifer tarandus	Ph II, left	Proximal fragment	E	West shore	
543	NS-Ogk-O512	Equus caballus	Cuneiforme III	Fragment	E	West shore	Trashed
544	NS-Ogk-O513	Rangifer tarandus or Ovibos sp.	Astragalus	Fragment	E	West shore	Rounded, trashed
545	NS-Ogk-O514	? Rangifer tarandus	Pelvis	Fragment	E	West shore	Rounded, trashed
546	NS-Ogk-O515	Large herbivorus mammal	Metapodium	Distal fragment	E	West shore	Rounded, trashed
547	NS-Ogk-O516	Large herbivorus mammal	Costa	Fragment	E	West shore	Rounded, trashed

Appendix 5.2-3. continuation.

No.	samples	Taxon	Skeleton element	Preservation	Type Loc.	Locality	Remarks
548	NS-Ogk-O517	Equus caballus	Radius	Proximal fragment	E	West shore	Trashed
		Muostakh Island (north part)					
549	NS-Mst-O532	Mammuthus primigenius	Scapula	Fragment	E	Shore	C 14
550	NS-Mst-O533		Costa	Fragment	E	Shore	C 14
551	NS-Mst-O534	Bison priscus	Astrogalus		E	Shore	
552	NS-Mst-O535	Large herbivorus mammal	Pelvis	Fragment	B	Exposure, altitude 3 - 6 m	Juv., from Lutz, AMS
553	NS-Mst-O536	Mammuthus primigenius	Mt III, left		E	Shore	Rounded
554	NS-Mst-O537	Equus caballus	Ph III	Damaged	E	Shore	Small
555	NS-Mst-O538	Large herbivorus mammal	Vertebra	Fragment	E	Shore	Trashed
		Bykovsky Peninsula, Mamontovy Khayata					
556	Mkh-02-O539	Rangifer tarandus	Shed antler	Fragment	A	In situ, exposure, altitude 35.6m	From Hanno, AMS

Appendix 5.2-4. Measuring sites for soil temperature and soil moisture; Measurement interval as well as average, minimum and maximum values are given.

Location	Descriptive text in Chapter	Lat	Long	Measuring time (5 min interval)		Temperature (°C)			Volumetric moisture for organic soils ($m^3 \times m^{-3}$)		
				start - end	data points	Average	Min	Max	Average	Min	Max
Kotel'ny south coast, Komurganakh R.- mouth	5.2.5	74°44.317'	138°24.219'	10:59 – 16:39	69	5.3	4.5	5.8	0.519	0.518	0.521
Bunge-Land, high terrace	5.2.6	74°52.849'	142°06.277'	10:37 – 18:17	93	6.5	5.4	7.0	0.210	0.208	0.213
Island Novaya Sibir	5.2.7	75°07.183'	146°38.843'	13:12 – 18:17	62	1.9	1.5	2.4	0.420	0.416	0.421
Bunge-Land, low terace	5.2.6	74°50.662'	140°29.007'	15:33 – 18:26	37	-	-	-	0.301	0.298	0.310
Maly Lyakhovsky Island	5.2.8	74°14.576'	140°19.167'	17:17 – 21:27	52	4.3	3.4	5.6	0.384	0.383	0.384
Cape Svyatoy Nos	5.2.9	72°53.188'	140°48.237'	19:10 – 21:30	29	5.2	4.9	5.9	0.255	0.252	0.257
Oyogos Yar coast	5.2.10	72°40.525'	143°35.925'	13:03 – 21:03	97	3.8	2.5	5.3	0.380	0.366	0.381
Muostakh Island	5.2.11	71°36.801'	129°56.175'	09:56 – 12:51	36	6.2	4.3	7.6	0.169	0.166	0.170
Mamontovy Bysagassa	4.5.2	71°47.236'	129°24.260'	13:13 – 22:23	111	2.8	2.2	3.3	0.583	0.563	0.600
Polar Fox Lake	4.5.3	71°44.099'	129°20.775'	10:29 – 17:09	81		-	-	0.543	0.540	0.546